THESE

présentée pour obtenir le grade de

**Docteur de l'Ecole Nationale Supérieure
des Télécommunications**

Spécialité: Communication et Electronique

Issam TOUFIK

**Allocation Dynamique des Ressources pour les Systèmes
Cellulaires Futurs à Bande Large.**

La Thèse sera soutenue le 27 Octobre 2006, devant le jury composé de :

David Gesbert	Président
Ana Pérez-Neira	Rapporteurs
Ralf Muller	
Kari Kalliojarvi	Examinateurs
Raymond KNOPP	Directeur de thèse

THESIS

In Partial Fulfillment of the Requirements for the

Degree of Doctor of Philosophy
from Ecole Nationale Supérieure des Télécommunications

Specializing: Communication and Electronics

Issam TOUFIK

Wideband Dynamic Resource Allocation for Future Cellular Networks

Will be defended on October 27, 2006, before the committee composed by:

David Gesbert	President
Ana Pérez-Neira	Readers
Ralf Muller	
Kari Kalliojarvi	Examiners
Raymond KNOPP	Thesis supervisor

To My parents

Contents

List of Figures

List of Tables

Acronyms

Here are the main acronyms used in this document.

1G	First Generation
2G	Second Generation
⋮	⋮
4G	Fourth Generation
AWGN	Additive White Gaussian Noise
BS	Base Station
CDF	Cumulative Distribution Function
CDMA	Code Division Multiple Access
CSI	Channel State Information
CSIT	Channel State Information at the Transmitter
DFT	Discrete Fourier Transform
DPC	Dirty Paper Coding
DSP	Digital Signal Processing
FDMA	Frequency Division Multiple Access
FEC	Forward Error Correction
FFT	Fast Fourier Transform
HDR	High Data Rate
iff	if and only if
IFFT	Inverse Fast Fourier Transform
i.i.d.	independent and identically distributed
ISI	Inter-Symbol Interference
LTE	Long Term Evolution
MAC	Multiple-Access Channel

MMSE   Minimum Mean-Square Error

MIMO   Multiple-Input Multiple-Output

MRC   Maximum Ratio Combining

OFDM   Orthogonal Frequency Division Multiplexing

OFDMA   Orthogonal Frequency Division Multiple Access

PAPR   Peak-to-Average Power Ratio

PDP   Power Delay Profile

PDF   Probability Distribution Function

QoS   Quality of Service

Rx   Receiver

SC-FDMA   Single Carrier FDMA

SDMA   Space Division Multiple Access

SINR   Signal-to-Interference plus Noise Ratio

SNR   Signal-to-Noise Ratio

SM   Spatial Multiplexing

S/P   Serial-to-Parallel Conversion

STC   Space-Time Code

TDD   Time Division Duplexing

TDMA   Time Division Multiple Access

Tx   Transmitter

US   Uncorrelated Scattering

UMTS   Universal Mobile Telecommunications Services

ZF   Zero Forcing

Notations

A note on notation: We use boldface and underlined letters to denote matrices (e.g. $\underline{\mathbf{a}}$ or $\underline{\mathbf{A}}$), boldface letters to denote vectors (e.g. $\mathbf{a}$ or $\mathbf{A}$) and capital letters for scalars (e.g. a or A).

$\mathbf{A}^i$ is the i-th vector of matrix $\underline{\mathbf{A}}$.

A_k^i is the k-th element of the i-th vector of matrix $\underline{\mathbf{A}}$.

Chapter 1

Introduction and Motivation

One of the most attractive and hottest topics in communication research during the recent years has been the wireless technology. This attention is the consequence of the big success of cellular phones and the growing demand on new wireless services. Having a permanent connectivity offers people flexibility, feeling of security and makes theme more productive. Internet as well as corporate intranets are becoming increasingly wireless and it is inevitable that the demand for high wireless data rates, reliability and Quality of Service (QoS) is also growing. Along the history, cellular systems has been constantly accompanying these changes in market requirements and evolve to satisfy customers demand. First-generation wireless networks were targeted at voice and data communications at very low rate using analog modulation techniques. Recently, we have seen the evolution of second and third-generation systems offering more data rates and thus a wider range of wireless services based on digital technologies. The evolution continues toward a system eliminating incompatibilities between previous technologies and becoming a truly global system.

Evolution of mobile cellular systems

The history of cellular system began during the 1980s with the appearance of the First-generation of mobile devices, also referred to as 1G, which were basic analogue systems. The first standardized cellular service is the *Advanced Mobile Phone System* (AMPS) which was made available in 1983. In Europe, the first 1G standard is the *Nordic Mobile Telephony* (NMT), operating in whole Scandinavia. It has two variants based on the

operating frequency bands. Both AMPS and NMT use the frequency modulation (FM) technique for radio transmission.

The main problem of 1G mobile systems is their capability to handle a large number of users due to insufficient channel capacity. 1G also suffers from poor voice quality, no security, very limited battery life and poor handover reliability. The will to overcome these limitations and the development of digital technology led to the emergence of the second-generation (2G) of cellular wireless systems offering an increase on capacity and an improvement of security and hand-over. A better recovery of radio signal is also possible using digital vocoders and Forward Error Correction (FEC). To enhance the spectral efficiency and to support multiple users, 2G systems use new multiple-access techniques: Time Division Multiple-access (TDMA) and Code Division Multiple-Access (CDMA) techniques.

The first European 2G system is the *Global System for Mobile communications* (GSM) and it is commercialized since 1992 where the narrowband TDMA solution was chosen for the air interface. In North America two standards have emerged. TDMA IS-136 was first specified in 1994 and is an evolution of AMPS using the same frequency band but it offers enhanced capacity and improved performance. The second standard is CDMAone which is also known as IS-95. First designed for voice, it was improved in IS-95A to support data transmission at rate up to 14.4Kbps. CDMAone is the first generation of CDMA technology based systems. Developed originally by Qualcomm, CDMA is characterized by high capacity and small cell radius, employing spread-spectrum technology and a special coding scheme. 2G systems are in current use around the world and are offering voice service and low rate data communications such as fax and short message service (SMS) based on circuit switched connection.

Second-plus generation (also known as 2.5G) is an intermediate solution between 2G with their low transmission rate and systems that will offer sufficient rate for the transmission of application such as video and real time application (3G and beyond). 2.5G offers data transmission rates up to 144Kbps. General Packet Radio Services (GPRS) is the 2.5G system derived from GSM. It allows users to be allocated up to 8 time slots in the TDMA air interface. GPRS then evolved to the development of Enhanced Data for Global Evolution (EDGE) system. It is similar to GPRS, but uses more advanced modulation techniques to support multimedia IP based services at a maximum rate of 384Kbps. This system allows mobile operators to provide 3G services with only small changes on the existent

GSM infrastructure since it uses the same TDMA frame structure, same logic channel and the same carrier bandwidth. In north America, an enhancement of CDMAone system toward the 3G resulted on the emergence of 1xRTT standard as a first step of CDMA2000. 1xRTT is also deployed in existent CDMAone spectrum and thus also requires a modest investment in infrastructure. It provides IP-based services at a data rate up to 144Kbps. During the 1990s, two organizations worked jointly to define the third-generation of mobile systems (3G). Their objective was to come with a global system eliminating the incompatibilities of previous systems allowing users to have a full inter-operability and global roaming between different 3G networks. Unfortunately the two groups could not come over their differences and this results on the development of three different standards. Wideband CDMA (W-CDMA) is backed by the GSM operators in Europe and the European Telecommunications Standards Institute (ETSI). The second standard called CDMA2000 is supported by the north American CDMA community while the third one, Time Division-Synchronous CDMA (TD-SCDMA), has won the support of China. The three standards uses an air interface based on CDMA technology. 3G promises increased data rates up to 128 Kbps when a user is in a moving vehicle, 384 Kbps when stationary or moving at pedestrian speed and 2 Mbps for fixed applications. Such capacities will allow service providers to offer faster and more complex data transmission such as video conferencing and wireless gaming.

While 2G systems support only circuit switched connections to insure voice and short data transmission, successor systems (2.5G and 3G) integrated packet based services. This transmission scheme is used for non real-time applications while circuit switched connection still adopted for service with QoS requirements as for voice and video.This convergence toward packet based transmissions will be confirmed on beyond 3G systems which will be fully packet based for both real and non-real time applications. This will be possible through IP packets scheduling over "shared channels". The spectral and spatial dimensions of future wireless systems will offer an increase in the granularity of physical resources allowing thus a finer allocation of the available resources and on users scheduling. The evolution of the connection nature of cellular systems is summarized in figure 1.1

From Third generation to 4G and beyond: Even before 3G systems were deployed, some research groups and companies have already started working on 4G mobile communications. In their way toward 4G, working groups defined several intermediate improvement
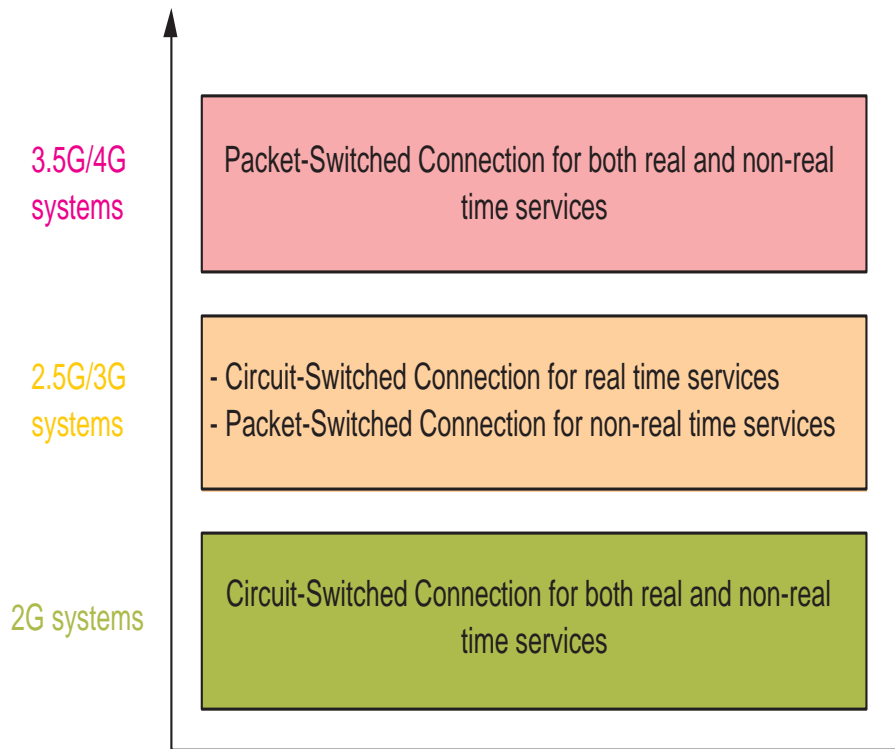
Figure 1.1: Connection evolution in cellular system

of 3G standards. High-Speed Downlink Packet Access (HSDPA) is a new technology sometimes referred to as a 3.5G as it is an extension to WCDMA in the same way that EV-DO extends CDMA2000. HSDPA provides high rates up to 14.4 Mbit/s using Adaptive Modulation and Coding (AMC), fast packet scheduling at the base station and fast retransmissions from base station known as Hybrid Automatic Repeat Request (HARQ). High-Speed Uplink Packet Access (HSUPA) is the dual of HSDPA for uplink transmissions. It offers extremely high upload rates up to 5.76 Mbit/s and is referred to as a 3.75G. Similarly to HSDPA there will be a packet scheduler, but it will operate on a request-grant principle. The user send a permission request to send data and the scheduler in the base station decides depending in the information fed-back by users on when and which users will be allowed to transmit. A request for transmission will contain information about the transmission buffer state and user's available power margin.

The Third Generation Partnership Project (3GPP) has began also considering the next major step in the evolution of the 3G, the Long-Term Evolution (LTE). The objective is to maintain a highly competitive position in wireless service world market during the

next 10 years and even in the 4G era. The main aims of this evolution is significant enhancement on data rates and supporting higher QoS requirement compared to HS-DPA with significant reduction in latency and delay. To achieve these objectives, it is inevitable to choose new access technologies. The 3GPP recently launched a Study entitled Evolved UTRA and UTRAN. It is anticipated that Orthogonal Frequency Division Multiple-Access (OFDMA) and Multiple Input Multiple Output (MIMO) will be adopted to fulfill the requirements.

The term 4G is broadly used to include several broadband wireless access communication systems, not only cellular systems. 4G mobile communication systems are expected to solve still-remaining limitation of 3G systems. They will provide a wide variety of more demanding new services and finally offer a global standard. To offer high rate requirements, 4G may use OFDM (Orthogonal Frequency Division Multiplexing), and also OFDMA combined with multiple antenna solutions to better allocate radio resources to users. 4G devices may also use Software-Defined Radio (SDR) receivers which allows better use of available bandwidth as well as making use of multiple channels simultaneously.

The evolution of cellular mobile systems from very basic services (audio for 1G) to more demanding and complex services as high quality video conferencing and music download in future systems, shows how wireless systems are in a permanent development and constantly looking for new efficient technologies in order to always offer better services and satisfy customer requirements. Recent researches show that one of the keys to success for future systems comes from a finer allocation of the available resources with inevitably a cross-layer approach.

Cross Layer design

A fundamental problem in wireless systems is the allocation of limited resources among active users. Traditional layered networking approaches optimize each layer independently of the others. This may lead to largely suboptimal network designs. Traditionally in multiuser wireless communications, when designing the physical layer, users are considered symmetrical and having the same data buffer length and the same delay and latency constraints. The objective function is to maximize channel capacity which may result in a highly unfair system. In the other hand the resource allocation at higher layers (multiple access control and network layers) considers the communication links as fixed rate bit pipes. There is a growing awareness that this simple bit-pipe view is inadequate,

particularly for wireless systems. Recently several studies has considered cross-layer approach and showed that this can substantially improve the overall system performance.

1.1   Thesis Outline

The convergence of broadband cellular systems to a wideband (OFDMA/ MIMO-OFDMA) solution and the growing interest on cross layered resource allocation approaches motivated the work in this thesis. We consider the interesting problem of channel allocation on multiuser wideband systems with *Hard Fairness* constraints.

In order to better understand the physical nature of the medium we begin in chapter 2 with a brief introductory presentation of basic radio propagation characteristics and OFDM modulation principles. The various forms of diversity offered by the wireless medium are presented as well. Chapter 3 addresses the problem of resource allocation on wideband Multiple Access Channels (MAC) under hard fairness constraints. It is widely believed that guaranteeing QoS for a set of users is accompanied with a huge system performance degradation. We show in this chapter that this belief is not true in wideband systems with intelligently allocated resources. After reviewing the ergodic channel capacity region and the corresponding optimal resource allocation for wideband MAC, we define the Delay-Limited capacity of these channels with a Lagrangian characterization of its boundary surface. An iterative algorithm for resource allocation to achieve a rate vector target with minimum power is proposed. We also propose different algorithms for resource allocation when orthogonal signaling is adopted with different hard fairness constraints. It is shown through numerical results that these orthogonal signaling fair algorithms achieve performances approaching that of the optimal delay limited strategy. This result may encourage the use and research on applicable delay limited rate algorithms for real systems.

In Chapter 4, we consider the downlink of multiple antenna multi-cellular wideband systems with hard fairness scheduling. We show how the additional spatial dimension effects the system performance in terms of spectral efficiency and minimum allocated channel gain. We propose different allocation and transmission techniques based on Space Time Coding (STC) and Spacial Multiplexing (SM). The presented schemes requires the knowl-

edge of only the channel gain amplitudes. We first consider the case of symmetric users (i.e. only fast fading is considered so that users are experiencing the average SNR) in a single cell system. We show through numerical results that a simple SM system where no channel gain phase estimation is needed and subject to hard fairness constraints can provide system capacity approaching that of Zero-Forcing Dirty Paper Coding (ZF-DPC) scheme. We then extend our study to multi-cellular systems and show the benefit from using distributed antennas in terms of both system throughput and fairness.

Chapter 5 addresses another important issue of future wireless systems: Feed-back load. We propose different feed-back schemes, for MIMO-OFDMA systems with opportunistic beamforming. The proposed schemes are designed, for different ranges of number of users, to considerably reduce the feed-back load while preserving channel information allowing an efficient scheduling and thus high system performance. We also provide different power allocation algorithms for MIMO-OFDMA systems. A part of this work was achieved during my summer internship in Samsung Advanced Institute of technology in South Korea.

We present our conclusions and perspectives in chapter 6.

In the following the list of publications related to this thesis

- Issam TOUFIK and Raymond KNOPP, "Channel Allocation Algorithms For Multi-Carrier Multiple-antenna Systems," EURASIPs Signal Processing Journal, Volume 86 N8, August 2006 , pp 1864-1878.

- Issam TOUFIK and Raymond KNOPP, "Multiuser Channel Allocation Algorithms Achieving Hard Fairness," Globecom 2004, 47th annual IEEE Global Telecommunications Conference, November 29th-December 3rd, 2004, Dallas, USA.

- Issam TOUFIK and Raymond KNOPP, "Channel Allocation Algorithms For Multi-carrier Systems," VTC Fall 2004, IEEE Vehicular Technology Conference, September 26-29, 2004, Los Angeles, USA.

- Issam TOUFIK and Hojin KIM, "MIMO-OFDMA Opportunistic Beamforming with Partial Channel State Information," IEEE Intern. Conf. on Communications (ICC), 2006.

- Issam TOUFIK and Marios Kountouris, "Power Allocation and Feedback Reduction for MIMO-OFDMA Opportunistic Beamforming," IEEE Vehicular Technology Conference, (VTC Spring) 2006.

- Issam TOUFIK and Raymond KNOPP, "Wideband Channel Allocation In Distributed Antenna Systems" VTC Fall 2006, IEEE 64th Vehicular Technology Conference, 25-28 September 2006, Montreal, Canada.

Chapter 2

Digital Communications Over Frequency Selective Channels

This chapter introduces the propagation characteristics of typical mobile radio channels and the basic background on transmission schemes used in this thesis. In our treatment, we first explain the three scale models for the propagation-attenuation phenomena on typical landmobile radio channels. Fast fading is the most widely studied effect in the literature, but since in this thesis we are also considering multi-cellular systems, characterizing the large scale fading effects (path-loss and shadowing) becomes primordial. We also review OFDM and its multiuser variant (OFDMA) principles, since these techniques are the basic foundation of future cellular systems and for the algorithms proposed in this material. We finally present the different diversity techniques used to combat deep fading effect and thus to improve the channel reliability.

2.1 Fading Channel

Designers of wireless communication systems face an important challenge due to the varying nature of the wireless radio channel. Characterizing this medium becomes then an inescapable task. The exact mathematical channel model is very complicated to derive,
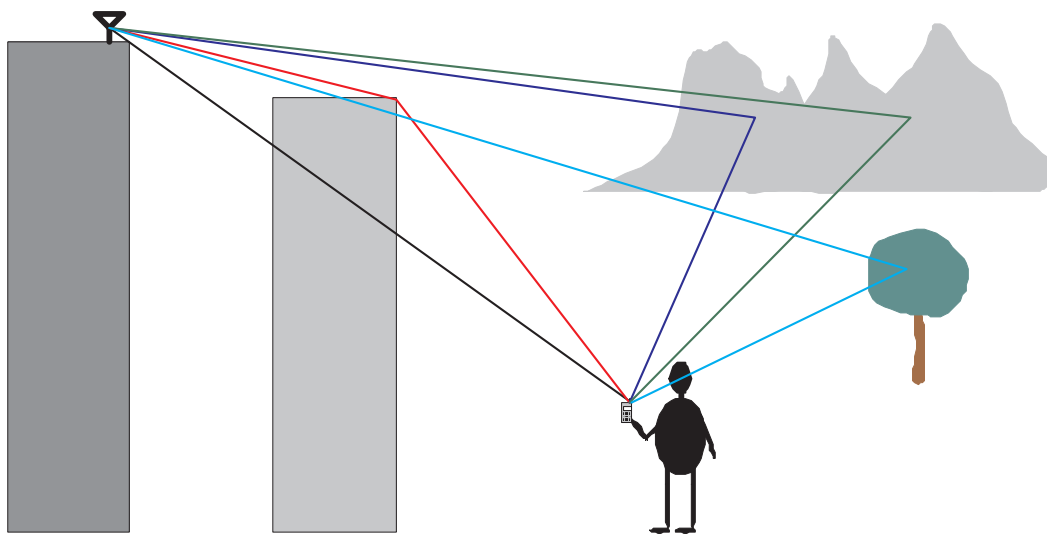
Figure 2.1: Signal Propagation Example

however there exist a range of relatively accurate and simple empirical models of the channel depending in the propagation environment.

The signal at a receiver at any given location and time instant is the result of superposition of corrupted duplicates of the transmitted signal resulting from reflections, refractions and diffractions on surrounding objects referred to as scatterers (figure 2.1). Scatterers may be buildings, trees, mountains or mobile objects such as cars or trains. The changes in the environment and the movement of the transmitting and/or the receiving terminals induces a fluctuations of the received signal on time. Because of the presence of multiple time delayed replicas of the transmitted signal, fading also occurs in the frequency domain (there are some frequencies where the signal at the receiver is higher than others). These fluctuations take place for signal with a bandwidth greater than the channel coherence bandwidth (see section 2.1.3 for a definition coherence bandwidth). We talk then of a *Frequency Selective Channel*.

When talking about fading , one should consider whether the observation is made over long distances or short distances. We distinguish two levels of signal fading (Figure 2.2)

- *Small-scale fading*, is due to the constructive and destructive combination of the multiple replicas of the signal arriving from different directions. The randomness
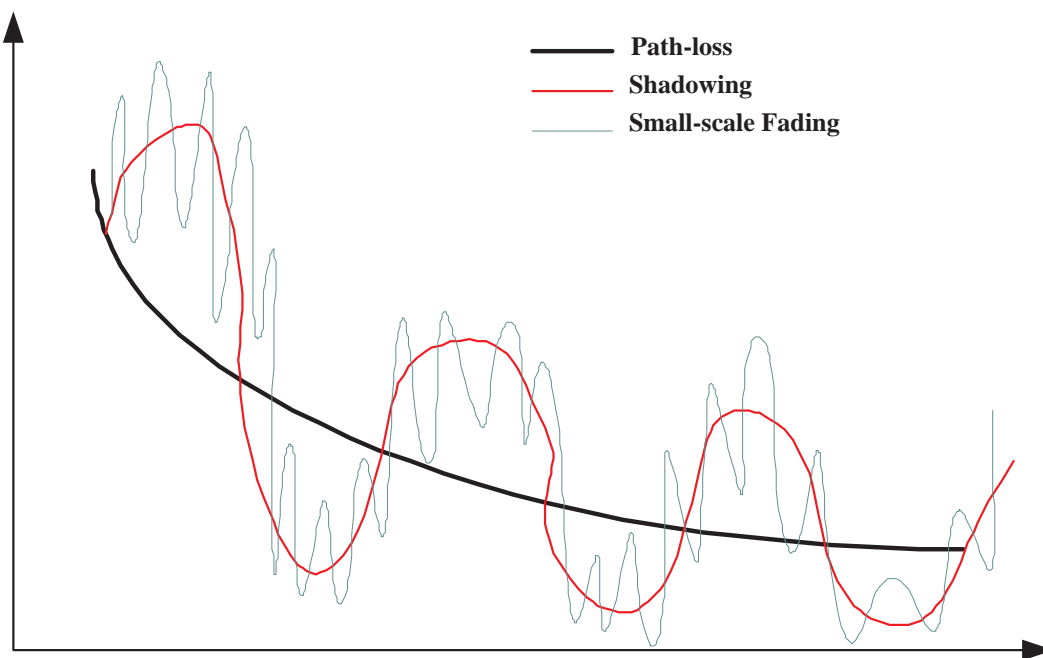
Figure 2.2: Characteristics of signal propagation

of the phases induces a wide variation of the sum of contributions. In small-scale fading, fast fluctuations on the received signal power may occur as the transmit or the receive station moves, even over very short distances (of the order of the carrier wavelength) or also by the movement of surrounding objects. For this reason, it is called small-scale or fast fading. Since these fluctuations are heavily frequency dependent, the bandwidth of the transmitted signal is critical in describing the effects of multi-path.

- *Large-scale fading*, is due to two phenomena: path loss and shadowing. Propagation path loss depends on the distance covered by the signal from the transmitter to the receiver and is random only due to the position of the mobile station. Shadowing is due to the peculiarities of the environment surrounding the transmitter and the receiver (Building, trees, mountains, cars, ...). Shadowing happens at a faster time-scale when compared to path loss, but slower compared to small-scale fading. Shadowing and path loss are virtually frequency invariant.

2.1.1   Path Loss Modeling

The most widely employed mathematical models for path loss and shadowing results from numerous experimental studies in a wide range of environments. During the deployment of a cellular network these models play an and extremely important role in the planning phase. The more accurate the model, the less we need on site measurements when defining base station placement.

Free space path loss

This model considers the region between the transmitter and receiver as perfectly uniform, non-absorbing and free from all objects that might reflect or absorb the signal. Path loss in free space is analytically described by

$$\frac{P_R}{P_T} = \left(\frac{\lambda}{4d\pi}\right)^2 G_L \tag{2.1}$$

where P_R and P_T are respectively the received and transmitted powers, λ is the signal wavelength, d the distance between the transmitter and the receiver in meters, and G_L is the product of the transmit and receive antenna gains.

For isotropic antennas $G_L = 1$, the path loss can be expressed in decibels as

$$L_{FS} = 32.4 + 20\log_{10}(d) + 20\log_{10}(f) \quad dB \tag{2.2}$$

where d is now in kilometers and f is the frequency in MHz. The power decays with 20 dB/decade in both frequency and distance which means, that path loss is a virtually distance (for practical mobile speeds) and frequency invariant.

This model is useful in providing a rough idea of the true path loss in an outdoor environment. We now briefly describe a few classic models for the path loss which are based on measurements.

Okumura's Tokyo Model

This model is based on measurements made in Tokyo, one of the most widely used in urban areas, and is valid for distances from 1 to 100 Km and frequencies range of 150-1920 MHz. It adjusts the free space path loss equation with empirical constants depending on the heights of the transmit and receive antennas and characteristics of the terrain (hilly, sloping, land-sea, foliage, ...). The empirical path loss formula of Okumura at distance d and carrier frequency f is given by

$$L_{Okumura} = L_{FS} + A_m(f,d) - H_B(h_B,d) - H_M(h_M,f) - K_U(f) - K \quad dB \quad (2.3)$$

where L_{FS} is the free space path loss given in 2.2, $A_M(f,d)$ is a factor, dependent of the frequency and the distance, indicating the median attenuation with respect to free space loss in an urban area over quasi smooth terrain. Its measurements assumed a fixed terminal antenna height of $h_B = 200m$ and mobile terminal antenna height of $h_M = 3m$. $H_B(h_B,d)$ and $H_M(h_M,f)$ are the distance and frequency dependent height gain factors, $K_U(f)$ is the so called urbanization factor (depending on whether the environment is urban, suburban or an open area). K is an additional term taking into account the terrain characteristics. These adjustment factors are all tabulated in curves for different environmental parameters [2].

Hata's Model

The main problem with Okumura's model is determining the different adjustment factors from tabulated data. Hata solved this problem by an empirical formulation of the graphical path loss data provided by Okumura. This model is valid in the 150-1000MHz frequency range and for distances of 1-20km. The fixed transmit antenna height range is 30-200m and for the receive mobile antenna 1-10m. The path loss formula of Hata model is given by

$$\begin{aligned} L_{Hata} &= 69.55 + 26.16 \log_{10} f - 13.82 \log_{10} h_B - A_m(h_M,f) + \\ &\quad (44.9 - 6.55 \log_{10} h_M) \log_{10} d + K_U(f) \quad dB \end{aligned} \quad (2.4)$$

where $A_m(h_M, f)$ is the correction factor for the mobile terminal's antenna height and is a function of the size of the city. This factor is given by

$$A_m(h_M, f) = (1.1 \log_{10} f - 0.7)h_M - (1.56 \log_{10} f - 0.8) \quad dB \tag{2.5}$$

for small or medium sized city and

$$A_m(h_M, f) = \begin{cases} 8.29(\log 1.54 h_M)^2 - 1.1 & f \le 200MHz \\ 3.2(\log 11.75 h_M)^2 - 4.97 & f \ge 200MHz. \end{cases} \tag{2.6}$$

for a large sized city. The urbanization correction factor, $K_U(f)$ is given by

$$K_U(f) = -2(\log_{10}(f/28))^2 - 5.4 \quad dB \tag{2.7}$$

for suburban area and

$$K_U(f) = -4.78(\log_{10} f)^2 + 18.33 \log_{10} f - 40.94 \quad dB \tag{2.8}$$

for open area. This factor is equal to zero in urban area.

COST 231 Refinements of Hata's Model

The Hata model was extended within the COST 231 project for the 1500-2000MHz frequency range. The path loss formula becomes

$$L_{COST231} = 46.3 + 33.9 \log_{10}(f) - 13.82 \log_{10}(h_B) A_m(h_M, f)$$
$$+ (44.9 - 6.55 \log_{10}(h_B)) \log_{10}(d) + K_M, \tag{2.9}$$

where $A_m(h_M, f)$ is the same as in Hata's model and K_M is 0 dB for medium sized cities and suburbs, and 3 dB for metropolitan areas.

Simplified Path Loss Model

There are situations where an accurate path loss model is required, for example when a base station location has to be determined during deployment of cellular networks. However, for general analysis it is sometimes more useful to have a simple and more general

model that captures main characteristics of empirical path loss models without going into the details of these. The following is the most widely used simple model

$$L_{simple} = L_0 \left(\frac{d}{d_0} \right)^{-\gamma} \tag{2.10}$$

where d_0 is a reference distance, L_0 is a unitless constant representing the attenuation at distance d_0, and γ is the path loss exponent. The values for L_0, d_0, and γ can be obtained to approximate either an analytical or empirical model.

2.1.2   Log Normal Shadowing Model

The other long term fading effect, called shadowing, is a result of attenuation or blockage of the signal due to the presence of large objects. Shadowing is usually characterized statistically as the short term fading component described in the following sections. It was shown that the channel fluctuation due to the shadowing on a dB scale is approximately Gaussian with standard deviation, σ_s, from 6-10 dB. The amplitude factor due to shadowing is therefore a log-normal random variable given by

$$A_{sh} = 10^{\sigma_s \zeta} \tag{2.11}$$

where ζ is a zero mean Gaussian random variable with variance 1.

2.1.3   Small-scale fading Modeling

Let us first consider the simple situation illustrated in figure 2.3 where there exists a line-of-sight (LOS) propagation path between the transmitter and the receiver and a second propagation path due to a reflecting object (i.e. building or a hill). The receiving antenna is moving at speed v_0 toward the transmit antenna. The path lengths are given by

$$d_i(t) = -v_i t + d_i \quad i = 0, 1 \tag{2.12}$$

where v_0 and v_1 denote the relative speed with respect to the transmitter and the reflector respectively (in this case $v_1 = -v_0 \cos(\alpha)$).

Let the transmitted (bandpass) signal be

$$s(t) = Re\{x(t)\exp(j2\pi f_c t)\} \tag{2.13}$$

where $x(t)$ is the complex envelop and f_c is the carrier frequency. The received signal is
the sum of two delayed version of the transmitted signal where the propagation delays are
given by

$$\tau_i = d_i(t)/c = -(v_i/c)t + d_i/c \tag{2.14}$$

where $c = 3 \times 10^8$m/s, denotes the speed of light. The received signal is the given by

$$
\begin{aligned}
r(t) &= Re\{x(t - \tau_0)\exp(j2\pi f_c(t - \tau_0)) + ax(t - \tau_1)\exp(j2\pi f_c(t - \tau_1))\} \\
&\approx Re\{x(t - \tau_0)\exp(\phi_0)\exp(j2\pi(f_c + \xi_0)t) + ax(t - \tau_1)\exp(\phi_1)\exp(j2\pi(f_c + \xi_0)t)\} \\
&= Re\left\{\left(\sum_{i=0}^{1}\rho_i x(t - \tau_i)\exp(j2\pi\xi_i t)\right)\exp(j2\pi(f_c + \xi_0)t)\right\}
\end{aligned} \tag{2.15}
$$

where a is a complex attenuation due to reflection, $\xi_i = f_c v_i/c$ and $\phi_i = -2\pi f_c d_i/c$. In
the second equation, we used the fact that for terrestrial wireless applications, v_i/c is very
small but the term $\xi_i = f_c v_i/c$ can be non-negligible. In the last equation $\rho_0 = \exp(j\phi_0)$
and $\rho_1 = a\exp(j\phi_1)$. Note that the time varying propagation delays causes shifts of the
carrier frequency by ξ_i (called *Doppler effect*) and shift in phase by ϕ_i.

The complex envelop of the received signal (2.15) is

$$y(t) = \sum_{i=0}^{1}\rho_i x(t - \tau_i)\exp(j2\pi\xi_i t) \tag{2.16}$$

Assume that $x(t)$ varies slowly, so that $x(t) \approx x$, constant over the observation interval.
Nevertheless the envelope of the received signal may be subject to time-variation. In fact,
we have

$$
\begin{aligned}
|y(t)| &= |x\rho_0|\left|1 + \frac{\rho_1}{\rho_0}\exp(j2\pi(\xi_1 - \xi0)t)\right| \\
&= A\sqrt{1 + b^2 + 2b\cos(2\pi\Delta\xi t + \Delta\phi)}
\end{aligned} \tag{2.17}
$$

where we let $A = |x\rho_0|$, $\Delta\xi = \xi_1 - \xi0$ and $\frac{\rho_1}{\rho_0} = b\exp(j\Delta\phi)$, with $b \in \mathbb{R}_+$. We can
observe from 2.17 that when the observation interval is larger than $\Delta\xi$, then the received
signal envelope varies between a maximum value $A|1 + b|$ and a minimum value $A|1 - b|$.
The rate of variation is given by *Doppler frequency spread* $\Delta\xi$ (given by the difference
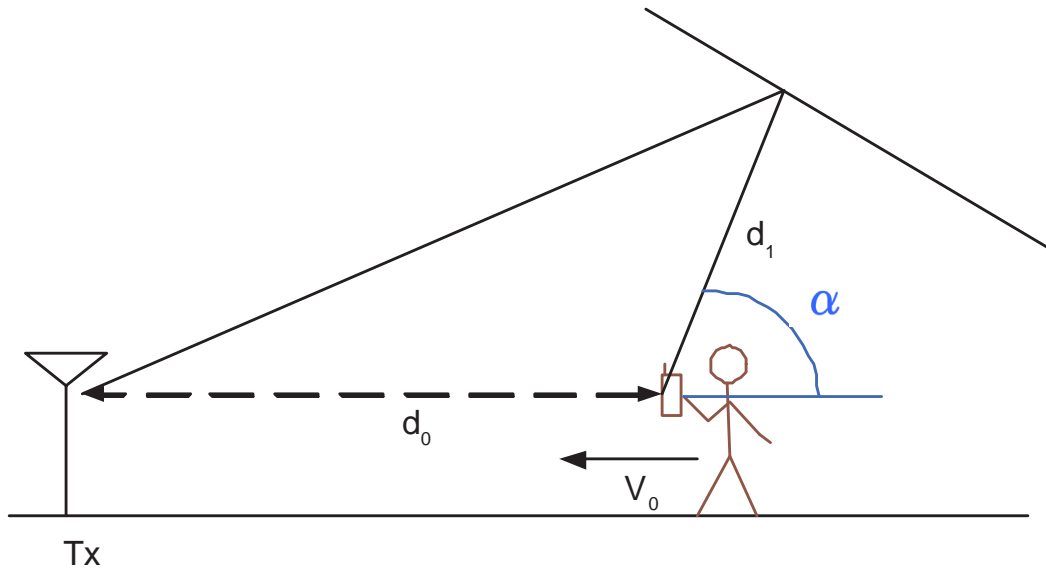
Figure 2.3: Two-ray propagation with a mobile terminal

between the maximum and the minimum Doppler shifts).

This simple example illustrates how, in the presence of more than one propagation path, the received signal envelope changes even if the transmit signal envelope is constant. This effect is called fast fading. In this example, we considered the movement of the received antenna, but the fast effect can also result from the movement of the transmit antenna or the reflecting objects.

The Gaussian Fading Model

The channel response in the two path situation is perfectly characterized and thus the time varying channel is deterministic. However in real situations where the transmitted signal goes usually through a large unknown number of paths with different characteristics. It is not possible to perfectly characterize the channel and it is convenient to describe the resulting fading channel by a statistical model depending on the underlying physical environment. The statistical description of multi-path propagation was first given by Clarke [3] and further refinements were done by Jakes [4]. Consider now the situation of Figure
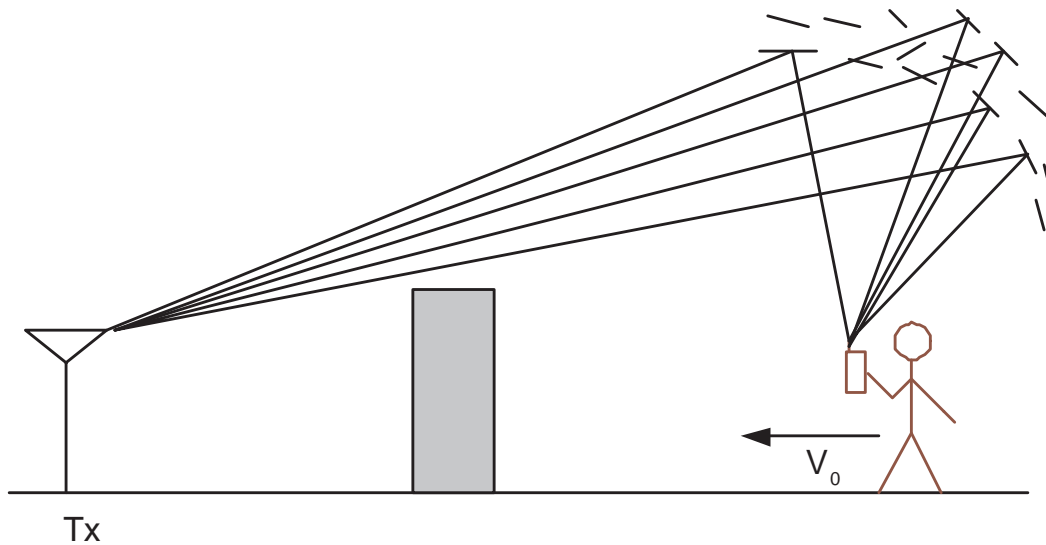
Figure 2.4: Scattering from several elements

2.1.3, where the propagation goes through a large number of paths. We can generalize the equation 2.16 and write the received signal envelope as

$$y(t) = \sum_i \rho_i x(t - \tau_i) \exp(j2\pi\xi_i t) \tag{2.18}$$

where the index i runs over the scattering elements and where the scattering element i is characterized by the complex coefficient ρ_i, modeled as random variables with some joint distribution, and the Doppler shift ξ_i. A common simplifying assumption, followed in most literature on the field and supported by physical arguments and experimental evidence [3, 5], is that the scattering coefficients ρ_i are zero-mean pairwise uncorrelated, i.e. $\mathbb{E}\{\rho_i\rho_j^*\} = 0$ for all $i \neq j$. This is known as the *Uncorrelated Scattering* (US) assumption.

Discrete multi-path channel

One important case in applications is the "Discrete multi-path channel" considered for example in all specifications of ETSI.

Assume that the scattering elements are clustered, so that there exist P clusters. The path in the same cluster have similar propagation delay. Let τ_p and $\mathcal{S}_p$ be respectively the delay

and set of indices of scattering elements of the p-th cluster. Then equation 2.18 can be written as

$$y(t) = \sum_{p=0}^{P} \left(\sum_{i \in S_p} \rho_i \exp(j2\pi\xi_i t) \right) x(t - \tau_p) \qquad (2.19)$$

$$= \sum_{p=0}^{P} \alpha_p(t) x(t - \tau_p) \qquad (2.20)$$

where $\alpha_p(t) = \sum_{i \in S_p} \rho_i \exp(j2\pi\xi_i t)$. This can be interpreted as the output of the complex baseband equivalent time-varying linear channel with impulse response

$$h(t, \tau) = \sum_{p=0}^{P} \alpha_p(t) x(\tau - \tau_p) \qquad (2.21)$$

The above channel can be represented as a tapped delay-line with time-varying coefficients $\alpha_p(t)$ and a non-uniformly spaced delays τ_p. Each process $\alpha_p(t)$ is given by the superposition of several complex sinusoids at different frequencies $\{\xi_i : i \in S_p\}$, with different amplitudes and uniformly distributed phases, due to the random coefficients $\{\rho_i : i \in S_p\}$. If each cluster is made of a very large number of scattering elements, each giving a very small contribution to the received signal, we can safely use the Central Limit Theorem [6] and conclude that the $\alpha_p(t)$'s are jointly circular symmetric complex Gaussian processes with zero mean. Since the clusters $S_p\}$ are disjoint, because of the US assamption, we have $\mathbb{E}\{\alpha_p(t)\alpha_q(t')^*\} = 0$ for all $p \neq q$ and t,t'. Therefore, the path gains $\alpha_p(t)$ are statistically independent.

The channel frequency response of discrete multi-path channel is given by

$$H(f, t) = \sum_{p=0}^{P-1} \alpha_p(t) e^{-j2\pi f_c \tau_p} \qquad (2.22)$$

The contribution due to p-th path has a phase linear in f_c. For multiple paths, there is a a differential phase $2\pi f_c (\tau_p - \tau_{p'})$ which causes selective fading in frequency.

Delay Spread and Coherence Bandwidth

An important parameter of multi-path channels is the delay spread which is simply given by $T_d = \tau_{P-1} - \tau_0$. It heavily depends on the environment and the antenna types. The

delay spread is normally much smaller in open rural areas than in urban and suburban areas due to the lack of distant objects at which the signal can be reflected. The delay spread governs its frequency *coherence bandwidth* (range of frequencies over which the channel can be considered "flat"). The coherence bandwidth is given by [7]

$$W_c = \frac{1}{2T_d} \tag{2.23}$$

Power Delay Profile

Let Ω_p denotes the means square of the random variable α_p. The sets $\{\tau_p\}_{p=0,...,P-1}$ and $\{\Omega_p\}_{p=0,...,P-1}$ define the channel's *Power Delay Profile* (PDP). In order to predict the effect of multi-path and to design systems to work well in a target environment, there have been a wide range of models proposed for DPD. Since describing a given multi-path environment perfectly is an impossible task, these models attempt to capture the key features from a series of measurements in the desired system setting (i.e. frequency band and environment nature). At the same time as being representative of a typical channel, they should be mathematically suitable for performing an analytical/simulation system performance analysis. One simple example of PDP is the exponentially decaying model. In this profile the tap's average fading power is given by:

$$\Omega_p = \Omega_1 e^{-\frac{\tau_p}{T_d}} \tag{2.24}$$

where Ω_1 is the average fading power of the first path. This PDP model is shown to be suitable for indoor office building and congested urban areas [8, 9].

We also find other PDP models in project or standard specifications. One of the most known is the ITU channel model. Tables 2.1 to 2.3 describe the tapped delay parameters for each of the terrestrial test environments according to ITU. Each table contains two different channels in order to cover a large range of delay spreads. Root-mean-squared delay spreads are majority of the time relatively small, but occasionally, there are "worst cases" which lead to much larger delay spreads. As this delay spread variability cannot be captured using a single model, up to two multi-path channels are presented for each test environment. Channel A and channel B represent respectively low and median delay spread cases that occurs frequently. Each of these two channels is expected to be encoun-

tered for some percentage of time in a given test environment. These percentages are summarized in Table 2.4.

2.2   Orthogonal Frequency Division Multiplexing (OFDM)

OFDM is a multi-carrier transmission technique that has been recognized as an excellent method for high speed wireless data communications due to its high spectral efficiency and its ability on combating Inter-Symbol Interferences (ISI).

Let $x(t)$ be the signal symbol transmitted a time t. The received signal in multi-path environment is then given by

$$y(t) = x(t) * h(t) + z(t) \tag{2.25}$$

We consider that $x(t)$ is band-limited to $[-W/2, W/2]$ and we work directly with the samples at sampling rate T

$$y[nT] = x[nT] * h'[n] + z(nT) \tag{2.26}$$

where $h'[n]$ is the channel response given by equation(2.21) sampled at rate T. we have

$$h'(n) = \int_{-\infty}^{\infty} h(t)\text{sinc}\,(t - nT)\,dt \tag{2.27}$$

 The difficulty of the equalization is mostly due to the memory of the channel (frequency selectivity) with a complexity of equalizers growing with the size of channel memory. In order to insure quasi-memoryless behavior, OFDM systems insert at the beginning of each symbol period in a clever manner a cyclic prefix with length equal to the worst case channel duration . The added data are then removed at the receiver since they contain the interference from the previous symbol. Using the fact that FFT can diagonalize circular convolution, the frequency-selective fading channel (multi-path-channel) is converted into several parallel flat-fading sub-channels.

Figure 2.5 illustrates a conventional OFDM transceiver. Let $\mathbf{s} = [s(0), ..., s(N-1)]$ be

	Channel A		Channel B	
Tap	Relative delay (ns)	Average Power (dB)	Relative delay (ns)	Average Power (dB)
1	0	0	0	0
2	50	-3.0	100	-3.6
3	110	-10.0	200	-7.2
4	170	-18.0	300	-10.8
5	290	-26.0	500	-18.0
6	310	-32.0	700	-25.2

Table 2.1: Indoor office test environment tapped-delay-line parameters.

	Channel A		Channel B	
Tap	Relative delay (ns)	Average Power (dB)	Relative delay (ns)	Average Power (dB)
1	0	0	0	0
2	110	-9.7	200	-0.9
3	190	-19.2	800	-4.9
4	410	-22.8	1200	-8.0
5	-	-	2300	-7.8
6	-	-	3700	-23.9

Table 2.2: Outdoor to indoor and pedestrian test environment tapped-delay-line parameters.

	Channel A		Channel B	
Tap	Relative delay (ns)	Average Power (dB)	Relative delay (ns)	Average Power (dB)
1	0	0	0	2.5
2	310	-1.0	300	0
3	710	-9.0	8900	-12.8
4	1090	-10.0	12000	-10.0
5	1730	-15.0	17100	-25.2
6	2510	-20.0	20000	-16.0

Table 2.3: Vehicular test environment, high antenna, tapped-delay-line parameters.

Test environment	Channel A	Channel B
Indoor office	50	45
Outdoor office and pedestrian	40	55
Vehicular	40	55

Table 2.4: Expected percentage of each of the two channels in different test environments.
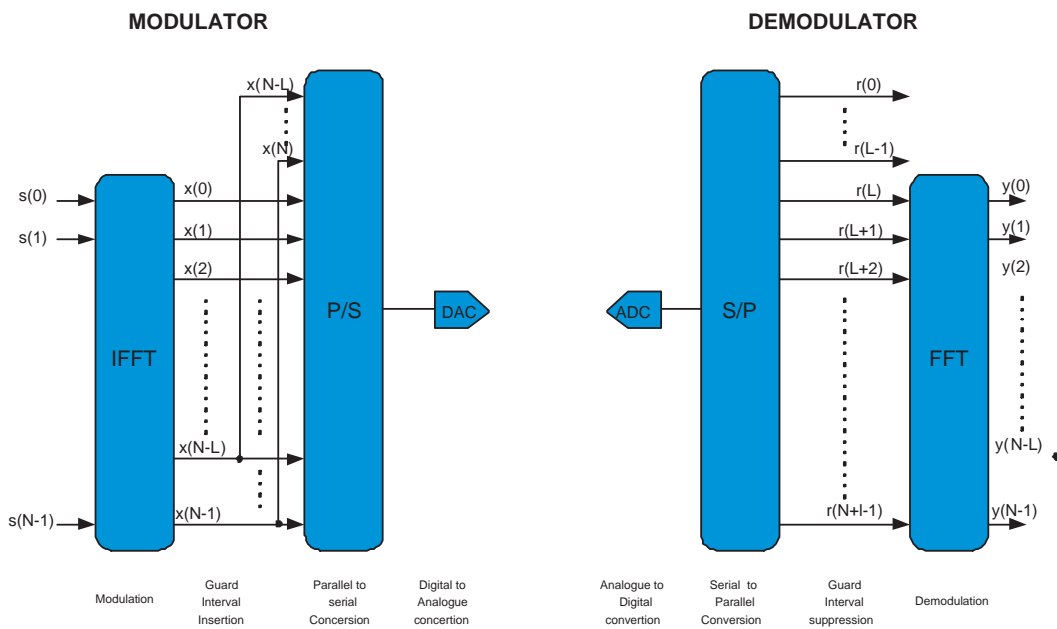
Figure 2.5: OFDM System Model

the N samples symbol to be transmitted. This symbol is precoded using an IFFT and the last L samples of the output $\mathbf{x} = [x(0), ..., x(N-1)]$ are duplicated at the beginning of $\mathbf{x}$ yielding to the time domain OFDM symbol $[x(N-L), ..., x(N-1), x(0), ..., x(N-1)]$ to be transmitted. L is chosen such that it is greater then the worst case channel duration. The received signal in a particular symbol can be written in a matrix form as

$$
\begin{bmatrix} r(0) \\ r(1) \\ \vdots \\ r(N-L+1) \\ r(N-L) \\ \vdots \\ r(N+L-1) \end{bmatrix} = \begin{bmatrix} x(L) & x(L-1) & \cdots & x(1) \\ x(L+1) & x(L) & \cdots & x(2) \\ \vdots & \ddots & \ddots & \vdots \\ x(N-1) & x(N-2) & \cdots & x(N-L) \\ x(0) & x(N-1) & \cdots & x(N-L+1) \\ \vdots & \ddots & \ddots & \vdots \\ x(L-1) & x(L-2) & \cdots & x(0) \end{bmatrix} \begin{bmatrix} h'(0) \\ h'(1) \\ \vdots \\ h'(L-1) \end{bmatrix} + \begin{bmatrix} z(0) \\ z(1) \\ \vdots \\ z(N-L+1) \\ z(N-L) \\ \vdots \\ z(N+L-1) \end{bmatrix}
$$

Adding zeros to the channel vector can extend the signal matrix without changing the output vector

$$
\begin{bmatrix} r(0) \\ r(1) \\ \vdots \\ r(N-L+1) \\ r(N-L) \\ \vdots \\ r(N+L-1) \end{bmatrix} = \underline{\mathbf{X}} \begin{bmatrix} h'(0) \\ h'(1) \\ \vdots \\ h'(L-1) \\ 0 \\ \vdots \\ 0 \end{bmatrix} + \begin{bmatrix} z(0) \\ z(1) \\ \vdots \\ z(N-L+1) \\ z(N-L) \\ \vdots \\ z(N+L-1) \end{bmatrix}
$$

where

$$
\underline{\mathbf{X}} = \begin{bmatrix} x(L) & x(L-1) & \cdots & x(1) & x(0) & x(N-1) & \cdots & x(L+1) \\ x(L+1) & x(L) & \cdots & x(2) & x(1) & x(0) & \cdots & x(L+2) \\ \vdots & \ddots & \ddots & \ddots & \ddots & \ddots & & \vdots \\ x(N-1) & x(N-2) & \cdots & x(N-L) & x(N-L-1) & x(N-L-2) & \cdots & x(0) \\ x(0) & x(N-1) & \cdots & x(N-L+1) & x(N-L) & x(N-L-1) & \cdots & x(1) \\ \vdots & \ddots & \ddots & \ddots & \ddots & \ddots & & \vdots \\ x(L-1) & x(L-2) & \cdots & x(0) & x(N-1) & x(N-2) & \cdots & x(L) \end{bmatrix}
$$

We can write the equivalent channel as

$$
\mathbf{r} = \underline{\mathbf{X}}\mathbf{h}' + \mathbf{z}
$$

The matrix $\underline{\mathbf{X}}$ is circular and since any circular matrix is diagonal in the Fourier basis with its eigenvalues given by the FFT of its first row. The equivalent received signal can then be written as

$$
\mathbf{r} = \underline{\mathbf{F}}\,\underline{\mathbf{\Lambda}}\,\underline{\mathbf{F}}^H\mathbf{h}' + \mathbf{z}
$$

and in the transform domain

$$
\mathbf{R} = \underline{\mathbf{F}}^H\mathbf{r} = \underline{\mathbf{\Lambda}}\mathbf{H}' + \mathbf{Z}
$$

with $\underline{\Lambda} = \mathrm{diag}(\lambda_i)$, and where $\{\lambda_i\}$ are the eigenvalues of $\underline{\mathbf{X}}$.

This shows how a signal transmitted over a multi-path channel can be converted in the frequency domain into a transmission over N parallel flat fading channels.

2.2.1   Orthogonal Frequency Division Multiple Access (OFDMA)

OFDMA is the multiuser version of OFDM. In classical OFDM systems, only a single user can transmit on all sub-carriers at any given time. To support multiple users, time division or frequency division multiple access is employed. OFDMA distributes sub-carriers among users so all users could be scheduled at the same time each one in one of the different sub-channels. A sub-channel is a set of adjacent sub-carriers. Since different users see the wireless channel differently, the probability that all users experience a deep fade in the same sub-channel is very low. Allocating sub-carriers to different users depending on their channel quality can enhance considerably the system performances. LTE is expected to use OFDMA in the downlink, and single-carrier FDMA (SC-FDMA) would be employed in the uplink.

2.2.2   Single Carrier FDMA (SC-FDMA)

The basic LTE uplink transmission scheme is based on SC-FDMA, a low Peak-to-Average Power Ration (PAPR) single-carrier transmission. Cyclic prefix is also used to achieve uplink inter-user orthogonality and to enable efficient frequency-domain equalization at the receiver side.

  SC-FDMA model is illustrated in figure 2.6. First, a packet (bit stream) is generated. The bit stream is converted to symbol stream through symbol mapping. After the Serial to Parallel mapping of symbols, "DFT Spread OFDM" operation is carried out. The DFT-spread OFDM operation consists of DFT, symbol to sub-carrier mapping, IFFT and cyclic prefix insertion. The data symbols are spread by performing a DFT before being mapped to the sub carriers. This means that each sub carrier carries a portion of superposed DFT spread data symbols. Various mappings are possible, which is illustrated in figure 2.7.
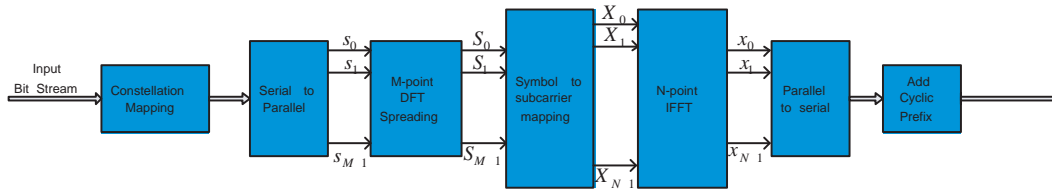
Figure 2.6: SC-FDMA transmission scheme

2.3 Diversity

Performance and reliability of a wireless communication system depend on the strength
of the received signal paths and can be strongly degraded by fading. A natural solution
to improve the system performance in fading channels is to use the so called *Diversity*
techniques: Instead of transmitting and receiving the desired signal through one channel,
several copies of the same signal are transmitted over independent fading paths. The idea
is that while some copies may undergo deep fades, others may not. We might still be
able to obtain enough energy to retrieve the sent message. There are many ways to obtain
diversity. The replicate can be sent in different time instant, different frequencies or from
different antennas. In the following we summarize the various diversity techniques and
give simple examples for a better understanding.

2.3.1 Time Diversity

In this Diversity scheme, signals representing the same information are sent at differ-
ent times. This can be achieved by using an interleaver. Interleaving split up the data
over time in different coherence periods thus different parts of the codewords experience
independent fades. Figure 2.8 represents an example of transmission with and without
interleaving. While in the first case an entire codeword is experiencing deep fading and
thus is received with a poor reliability, in the latter only one coded symbol from each
codeword is lost.

For interleaving based schemes, the time intervals between transmissions of successive
parts of the same codeword should be longer than the channel coherence. Typically a
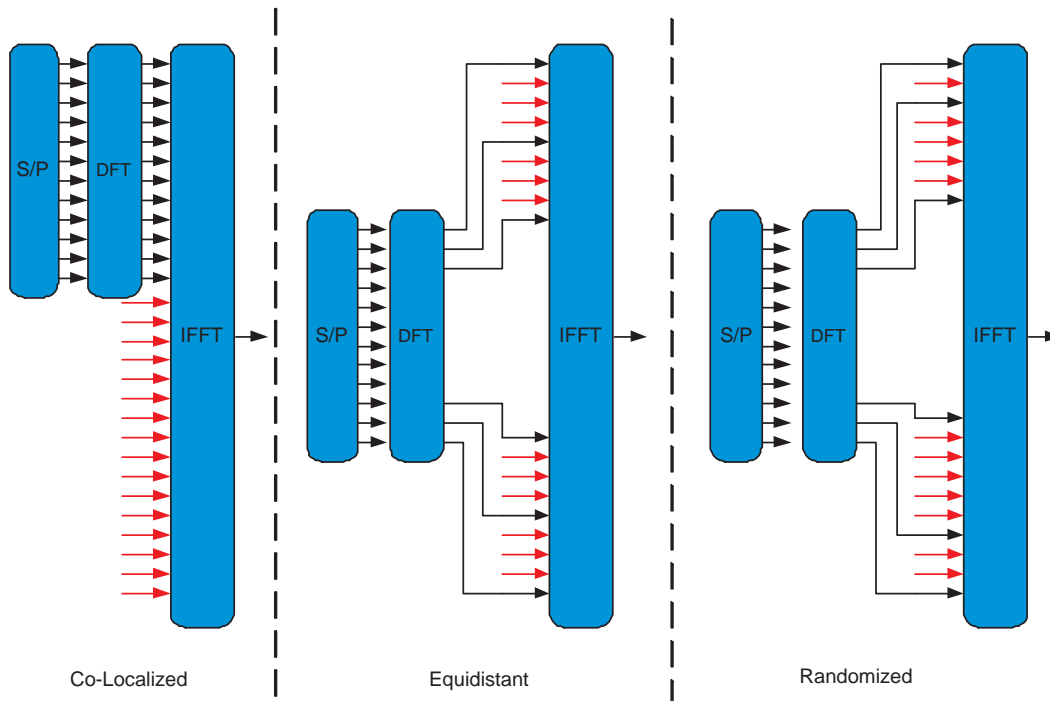
Figure 2.7: Mappings schemes in SC-FDMA transmission

symbol duration is much shorter than the channel coherence time, thus the interleaving should be done over a large number of symbols to avoid the high correlation of channel across consecutive symbols. When there is a strict delay constraint this may not be feasible. In this case other forms of diversity have to be used.

2.3.2 Frequency Diversity

For wideband systems, because of multi-path, different replicas of the transmit signal arrive at different symbol times and can be resolved at the receiver. The channel bandwidth is larger then the channel coherence bandwidth and the channel gain is varying also in the frequency domain. Those variations of the channel amplitude in different parts of the spectrum can be exploited as an other form of diversity: Frequency diversity.
In multi-path environment the received signal can be expressed as

$$y[n] = \sum_{p=0}^{P-1} h_p[n]x[n-p] + z[n] \tag{2.28}$$
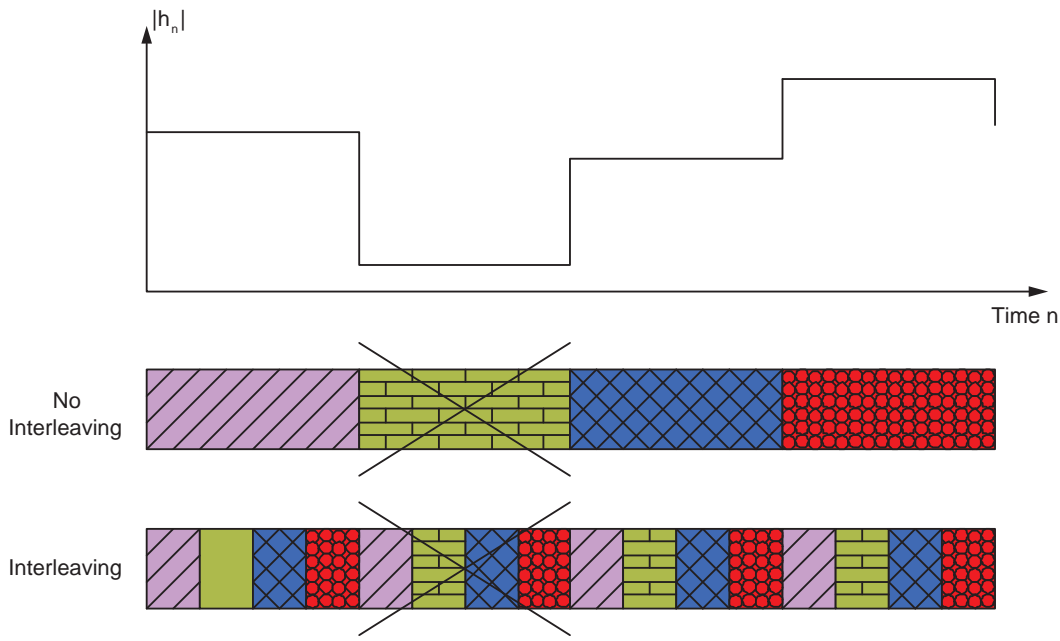
Figure 2.8: Example of transmission with and without interleaving

Here $h_p[n]$ denotes the p-th channel filter tap at time n. A very simple scheme is to transmit a symbol $x[0]$ at time 0, and no symbols at the $L-1$ following symbols. The receiver will get L replicates of the transmitted symbol $x[0]$ which is similar to the repetition codes in the narrowband case. This scheme achieves frequency diversity but it is not exploiting all degrees of freedom since only one symbol is transmitted each delay spread period. In the other hand, transmitting symbols each time symbol results on ISI. Different techniques where designed in order to combat the ISI and thus sufficiently profit from frequency diversity. OFDM is one of these techniques (cf. section 2.2).

2.3.3   Antenna Diversity

Antenna diversity, also known as space diversity, consists of placing multiple antennas at the transmitter and/or the receiver. The distance between antennas should be large enough so that the channel gains between different antenna pairs has independent fading (distance of half of the wavelength is sufficient to obtain two uncorrelated signals). Depending on whether the antennas are placed at the receiver or at the transmitter, we talk about receiver
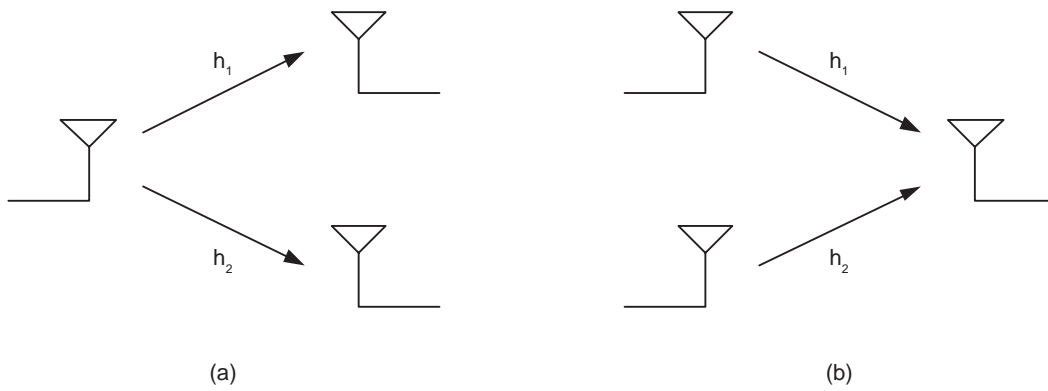
Figure 2.9: Antenna diversity example: (a) Receive diversity. (b) Transmit diversity.

diversity or transmit diversity. Note that with antenna diversity, independent fading paths are realized without an increase in transmit signal power or bandwidth.

2.3.4 Receive Diversity

In this case the antenna array is placed in the receiver side. Figure 2.9(a) represents such a scheme with one transmitting and two receiving antennas. At the receiver, the signals on the various antennas are multiplied with a complex coefficient to extract the original message. Let $y_i = \sqrt{P} h_i x + z_i$ be the signal received at i-th antenna. In the following we enumerate two simple ways to extract the sent signal.

Maximum Ratio Combining (MRC)

The received signal at the different receiving antennas is totally analogue to the observations obtained from the fingers of a rake receiver. The optimal receiver consists of a Maximum Ratio Combining (MRC). The output of the MRC is given by

$$y = \sqrt{P} \sqrt{\sum_{i=1}^{N_r} |h_i|^2} x + z \qquad (2.29)$$
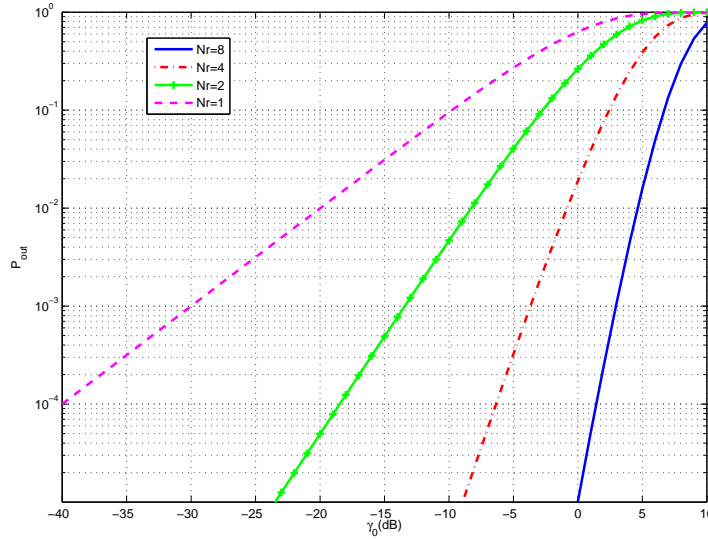
Figure 2.10: Outage probability of MRC for different numbers of receive antennas ($\gamma = 0$dB)

The SNR is then given by

$$SNR_{mrc} = \frac{P}{N_0} \sum_{i=1}^{N_r} |h_i|^2 \tag{2.30}$$

where N_r is the number of receiving antennas. The outage probability associated with a given threshold γ_0 for independent and identically distributed Rayleigh fading is given by [10]

$$P_{out}(\gamma_0) = \Pr\left(SNR_{mrc} < \gamma_0\right) = 1 - e^{-\gamma_0/\gamma} \sum_{n_r=1}^{N_r} \frac{(\gamma_0/\gamma)^{n_r-1}}{(n_r-1)!} \tag{2.31}$$

where $\gamma = \frac{P}{N_0}$. Figure 2.10 plots this probability indexed by the number of receive antennas.

Selection Combining

A sub-optimal but simpler combining scheme consists of selecting the output of the antenna with the largest instantaneous SNR. This method is called Selection Combining.
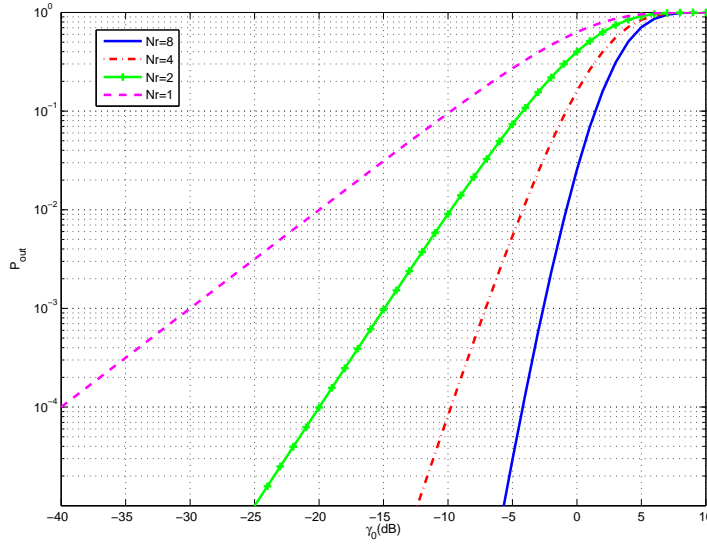
Figure 2.11: Outage probability of selection combining for different numbers of receive antennas ($\gamma = 0$dB)

The combiner output is given by

$$y = \sqrt{P}h_{\max}x + z \tag{2.32}$$

The SNR is given by

$$SNR_{sel} = \frac{P}{N_0}|h_{\max}|^2 \tag{2.33}$$

If the fading coefficients of all antennas are i.i.d., we can write the SNR outage probability as

$$P_{out}(\alpha) = (F_g(\alpha/\gamma))^{N_r} \tag{2.34}$$

where g denotes the power gain of any of the channels (they are i.i.d.) and $F_g(\alpha)$ is its cumulative density function (cdf). In case of i.i.d. Rayleigh fading, we have that

$$P_{out}(\gamma_0) = \left(1 - \exp\left(-\frac{\gamma_0}{\gamma}\right)\right)^{N_r} \tag{2.35}$$

This outage probability is plotted for different values of N_r in Figure 2.11.

2.3.5   Transmit Diversity: Space Time Coding

The antenna array is placed at the transmitter side (figure 2.9(b)). This scheme consists of a transmitter coding over both the time and spatial dimensions. A very simple example is a variant of the repetition code where the same symbol is transmitted from the N_t different transmit antennas during N_t symbol times. At any one time, only one antenna is transmitting and the rest are turned off. Repetition codes are shown to be wasteful of degrees of freedom. Several works dealing with STC were conducted. One of the most famous codes is the Alamouti Code.

Alamouti Code

This scheme considers the use of two transmitting and one receiving antennas. With flat fading, the received signal at time n is written as

$$y[n] = h_1[n]x_1[n] + h_2[n]x_2[n] + z[n] \tag{2.36}$$

where x_i and h_i are respectively the transmitted symbol and the channel gain from transmit antenna i. The Alamouti scheme transmits two complex symbols u_1 and u_2 over two symbol times: at time 1, $x_1[1] = u_1$; $x_2[1] = u_2$; at time 2, $x_1[2] = -u_2^*$; $x_2[2] = u_1^*$. If we assume that the channel remains constant over the two symbol times and set $h_1 = h_1[1] = h_1[2]$; $h_2 = h_2[1] = h_2[2]$, then we can write in matrix form:

$$[y[1] \quad y[2]] = [h_1 \quad h_2] \begin{bmatrix} u_1 & -u_2^* \\ u_2 & u_1^* \end{bmatrix} + [z[1] \quad z[2]] \tag{2.37}$$

This equation can also be writing as

$$\begin{bmatrix} y[1] \\ y^*[2] \end{bmatrix} = \begin{bmatrix} h_1 & h_2 \\ h_2^* & -h_1^* \end{bmatrix} \begin{bmatrix} u_1 \\ u_2 \end{bmatrix} + \begin{bmatrix} z[1] \\ z^*[2] \end{bmatrix} \tag{2.38}$$

We observe that the detection problem of u_1; u_2 decomposes into two separate, orthogonal problems. We project y onto each of the two columns to obtain the sufficient statistics

$$r_i = \|\mathbf{h}\|u_i + z_i; \quad i = 1; 2 \tag{2.39}$$

where $\mathbf{h} = [h_1 \quad h_2]^t$ and $z_i \sim \mathcal{CN}(0; N_0)$ and z_1, z_2 are independent. Thus, we have a diversity gain of 2 for the detection of each symbol.
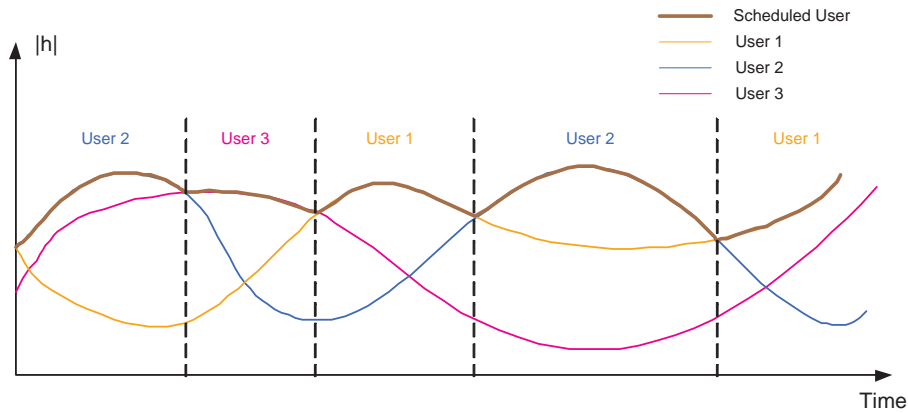
Figure 2.12: Opportunistic scheduling example

2.3.6 Multiuser Diversity

This form of diversity is different from those presented previously since it does not consist of sending the same copy of the same signal at independent channels. It instead benefits, when many users are present in the system, from the fact that they experience independent channel gains. The system performance is enhanced by allocating each system resource (Time, Frequency, Antenna) to the user which make the better use of it i.e. the user with the best channel conditions. Figure 2.12 illustrates an example of opportunistic scheduler. By opportunistic we mean the scheduling, at each time and frequency, the user with the best channel conditions. This form of diversity is similar to selection combining receive diversity. By allocating the channel gain at each time to the strongest user, the effective channel gain at time n is improved from $|h_1[n]|^2$ to $\max_{k}|h_k[n]|^2$. The more users that are present, the more likely it is that one user has a very good channel at any time. This form of diversity was first introduced in [11, 12].

2.4 Conclusion

In this chapter, we reviewed some important fading channel characteristics used in the thesis. We also give an introductory background on OFDM and OFDMA which are important schemes used in the future broadband cellular systems and are the direct ap-

plication basis for the algorithm presented in the thesis. We also explained the different diversity techniques used to combat the deep fading effects on wireless communication systems.

Chapter 3

Dynamic Channel Allocation in Wideband Systems

3.1 Introduction

Dynamic Channel Allocation (DCA) can provide data transmission with very high spectral efficiency. Channel State Information available at the Transmitter (CSIT) can be used to schedule users across the available system bandwidth by employing the concept of Multiuser Diversity introduced in [11, 13] and extended in [14]. The most remarkable result in these works is that for multiuser systems significantly more information can be transmitted across a fading AWGN channel than a non-fading AWGN channel for the same average signal power at the receiver. This is due to the fact that at a given time and frequency, the channel gain is random and can be significantly higher than its average level. One can take advantage of this by using proper dynamic time-frequency resource allocation based on the time/frequency varying characteristics of the channel. Allowing at each given time instant only the user with the best channel condition to access the medium yields a considerable increase of the total throughput as a function of the number of users. The success key of DCA is the use of CSIT, but one may question the practicality of assuming that quasi-perfect CSI can be made available at the transmission end. This strongly depends on the considered system architecture. In systems such as HDR (also

known as IS-865) the receiver estimates the CSI based on a common channel pilot and feeds the information back to the transmitter [20]. If we employ the same antenna array for transmission and reception in a time-division duplexing (TDD) system then channel reciprocity allows us to use our channel estimates obtained during reception for transmission, which is for instance the case of the DECT cordless telephone system or power control in UMTS-TDD. In practical TDD systems, amplitude information is reasonably simple to estimate from the opposite link. However, this is not the case for accurate phase information, mainly due to the difficulty of calibrating the difference in phase response between transmitter and receiver chains.

The main issue arising from channel-dependent resource allocation schemes is fairness. Users (or the base station) cannot always wait until their channel conditions are most favorable for transmission specially in slowly varying channels. For instance, in real-time applications like video-conferencing, users subscribe to services with a certain rate that should be achieved independently of the channel state. The set of these achievable rates is called *Delay Limited Capacity*. Strategies allowing to achieve these rates are the most fair since they guarantee to each user his request rate. Authors in [15] propose a comprehensive and complete study of delay limited capacity for flat fading (narrowband) MAC. Using the polymatroid structure of this capacity, an explicit characterization is derived and optimal power allocation to achieve a target rate is given. MAC ergodic capacity is treated in [14]. Ergodic and delay limited capacities for broadcast flat fading channel are studied in [16] and [17], respectively. For Wideband channels, the problem of power and rate allocation in delay limited systems is addressed in [18, 19] with more attention to the asymptotic case (very large number of users). It is shown that, both for optimal and orthogonal signaling, the delay limited throughput is achieved by letting each user transmit through his best channel irrespectively of other users. With the objective of achieving a target rate for multi-cell systems, [22]-[24] study combined power control and base station assignment in multi-cell systems. Similar opportunistic techniques for multi-cell systems are briefly discussed in [21]. In [21], the authors treat the fairness problem between users in slow fading environments, discuss the implementation in the IS-865 system and propose methods to enhance fairness. Their approach consists of using multiple antennas to induce fast channel fluctuations combined with the Proportionally Fair Scheduling (PFS) policy. This approach is suited for fairness enhancement in non real-time applications. In [27], a fair allocation criterion with deterministic channel access in a K-user system

with K parallel sub-channels is proposed. The criterion maximizes the minimum allocated channel gain and thus tends to harmonize the users' channel quality. It is shown in this work that, even under these hard fairness constraints, high multiuser diversity gain can still be achieved. Several other works adopted a cross-layer approach for resource allocation in wideband systems. We cite [25] among others. The authors of this work studied the relationship between ergodic information rates, stability and delay in multiuser wideband communication systems. They showed that exploiting multiple channels can considerably decrease the average packet delay. In [26], the authors consider the sub-carrier assignment problem in OFDMA systems and compare the simplicity and fairness properties of different allocation algorithms.

The work in this chapter is in the same spirit as in [19] since we also study the delay limited capacity for wideband cellular systems with a focus on practical scenarios (limited number of users) and we only consider the effect of fast fading while in [19] large-scale fading is also considered. It is commonly considered that fairness comes at the cost of a significant capacity penalty and system performance degradation. In this work, we show that for wideband systems, large multiuser diversity gains can be successfully achieved even under hard fairness constraints, and thus also high aggregate data rates can be provided. We also show that the spectral efficiency of delay limited systems approaches that of unfair strategies, in which the objective is to maximize the total sum rate. These results are in accordance with those in [19], where the authors show that delay limited wideband systems with optimal signaling do not suffer from significant throughput loss with respect to PFS in high SNR regime.

In this chapter, we also explore practical algorithms for orthogonal multiple-access (OFDMA-like systems). We show that the use of such a sub-optimal signaling scheme does not cause an important decrease in system total sum-rate when the number of users is less then the number of uncorrelated sub-channels.

This chapter is organized as follows: Section 3.2 presents MAC system and channel models. In Section 3.3, we recall the MAC wideband ergodic capacity and review the optimal strategy achieving the maximum sum rate. The delay limited capacity is presented in Section 3.4 and an iterative algorithm for resource allocation to achieve a rate vector target is proposed. In Section 3.6, two different channel allocation strategies for orthogonal signaling are presented and numerical results are given. Finally, in Section 3.7 we present our conclusions.

Contributions

- Lagrangian characterization of the rate vectors on the boundary surface of the MAC delay limited capacity.

- Optimal power and rate allocation algorithm achieving a target delay limited rate vector.

- Power and channel allocation algorithm for delay limited orthogonal signaling systems.

- Channel allocation algorithm achieving hard fairness when no power control is allowed. The algorithm maximizes the minimum allocated rate.

3.2   Channel Model

We consider the uplink (MAC) of a single-cell multiuser system where K single antenna users are transmitting to one receiver at the base station over a total fixed bandwidth W. Let $\mathcal{K}$ denote the set of users. The total bandwidth W is divided into M equal bandwidth parallel sub-channels. We assume that data are coded and split into signal blocks of duration T seconds, and that T is shorter than the coherence time of the channel so that the channel can be assumed stationary for the duration of coded transmission blocks, but may vary from block to block. We also assume that the channel is constant on one sub-channel but channel gain of a user may change from one sub-channel to another (i.e. $\frac{W}{M}$ is smaller than the channel coherence bandwidth). Let $\mathcal{H}$ be the set of possible joint fading states and assume that $\mathcal{H}$ is bounded. The channel state at block fading n can be represented by the channel gain matrix

$$
\underline{\mathbf{H}}(n) = \begin{bmatrix} H_1^1(n) & H_1^2(n) & \cdots & H_1^M(n) \\ H_2^1(n) & \ddots & & \vdots \\ \vdots & & \ddots & \vdots \\ H_K^1(n) & \cdots & \cdots & H_K^M(n) \end{bmatrix}
\tag{3.1}
$$

where $H_k^m(n)$ is the channel gain of user k on sub-channel m. The n-th block received signal on sub-channel m is given by

$$Y^m(n) = \sum_{k=1}^{K} \sqrt{P_k^m(n)} H_k^m(n) X_k^m(n) + Z^m(n) \tag{3.2}$$

where $X_k^m(n)$ and $P_k^m(n)$ are respectively the signal and the transmit power of user k on sub-channel m and $Z^m(n)$ is the Gaussian noise. We assume that the channel gains are perfectly known to users and the base station thus the power can be adapted to channel variations. We call power allocation the mapping from channel fading state $\underline{\mathbf{H}}$ to a power matrix $\underline{\mathcal{P}}(\underline{\mathbf{H}})$, where

$$\underline{\mathcal{P}}(\underline{\mathbf{H}}) = \begin{bmatrix} \mathcal{P}_1^1(\underline{\mathbf{H}}) & \mathcal{P}_1^2(\underline{\mathbf{H}}) & \cdots & \mathcal{P}_1^M(\underline{\mathbf{H}}) \\ \mathcal{P}_2^1(\underline{\mathbf{H}})_2^1 & \ddots & & \vdots \\ \vdots & & \ddots & \vdots \\ \mathcal{P}_K^1(\underline{\mathbf{H}}) & \cdots & \cdots & \mathcal{P}_K^M(\underline{\mathbf{H}}) \end{bmatrix} \tag{3.3}$$

$\mathcal{P}_k^m(\underline{\mathbf{H}})$ is the power allocated to user k on sub-channel m at fading state $\underline{\mathbf{H}}$. For notation simplicity we will use the notation $\underline{\mathcal{P}}(n)$ instead of $\underline{\mathcal{P}}(\underline{\mathbf{H}}(n))$ to denote the power allocation matrix corresponding to the fading state at block n. For a power allocation to be feasible, it must satisfy the per-user imposed power constraint, namely $\mathbb{E}\left[\sum_{m=1}^{M} \mathcal{P}_k^m(n)\right] \leq \overline{P}_k$.

In the following section, we review the ergodic capacity for wideband channel systems.

3.3 MAC Ergodic Capacity

The Ergodic Capacity (Also known as Shannon capacity) is defined as the maximum data rate that can be sent over the channel with asymptotically small error probability averaged over the fading process. Under the assumption of Gaussian signals, the time invariant achievable capacity for a power matrix $\underline{\mathbf{P}}$ and a given fading state $\underline{\mathbf{H}} \in \mathcal{H}$ is given by

$$\mathcal{C}_g(\underline{\mathbf{P}}, \underline{\mathbf{H}}) = \left\{ \mathbf{R} : \sum_{m=1}^{M} \sum_{k \in S} R_k^m \leq \sum_{m=1}^{M} \log\left(1 + \frac{\sum_{k \in S} P_k^m |H_k^m|^2}{N_0}\right), \quad \forall S \subset \mathcal{K} \right\} \tag{3.4}$$

we obtain the ergodic capacity by averaging the set of achievable rates over all fading states. Hence, the MAC capacity for a fixed power allocation matrix $\underline{\mathbf{P}}$ is given by

$$\mathcal{C}_{MAC}(\underline{\mathbf{P}}) \equiv \left\{ \mathbf{R} : \sum_{k \in S} R_k \leq \mathbb{E}\left[\sum_{m=1}^{M} \log\left(1 + \frac{\sum_{k \in S} P_k^m |H_k^m(n)|^2}{N_0}\right)\right], \quad \forall S \subset \mathcal{K} \right\}$$

With CSI available at the transmitter, the transmit power can be adapted to the channel quality in order to enhance the system rate. The ergodic capacity is then expressed as

$$\mathcal{C}_{ERG} \equiv \bigcup_{\substack{\mathbb{E}[\sum_m \mathcal{P}_k^m] \leq \overline{P}_k \\ k=1,\dots,K}} \left\{ \mathbf{R} : \sum_{k \in S} R_k \leq \mathbb{E}\left[\sum_{m=1}^{M} \log\left(1 + \frac{\sum_{k \in S} \mathcal{P}_k^m(n)|H_k^m(n)|^2}{N_0}\right)\right], \quad \forall S \subset \mathcal{K} \right\}$$

The set of rates in the boundary region of this capacity can be parameterized as given in the following theorem stated without proof.

Theorem 1 *[37, 14]*

For an ergodic block-fading multiuser system with CSIT, the set of maximum rates and corresponding powers are parametrically described by the solution, for each block n and for each sub-channel m, of the maximization problem

$$\arg\max_{\mathbf{R},\mathbf{P}} \sum_{k=1}^{K} \alpha_k R_k^m - \lambda_k \mathbb{E}\left[\sum_{m=1}^{M} P_k^m \right]$$

$$\text{subject to} \quad \sum_{k \in S} R_k^m \leq \log\left(1 + \frac{\sum_{k \in S} P_k^m |H_k^m(n)|^2}{N_0}\right), \quad \forall S \subset \mathcal{K}$$

where α_k are parameters defining the maximum rates and λ_k are Lagrange multipliers satisfying the power constraints.

It has been shown in [36, 14], that the point on the ergodic capacity region corresponding to the maximum total ergodic sum rate $\sum_{k=1}^{K} R_k$ (the point of capacity boundary corresponding to $\alpha_k = 1, \forall k$) is achieved with input power

$$\mathcal{P}_k^m(n) = \begin{cases} \left[\frac{1}{\lambda_k} - \frac{N_0}{|H_k^m(n)|^2} \right]^+ & \text{if } |H_k^m(n)|^2 \geq \frac{\lambda_k}{\lambda_{k'}} |H_{k'}^m(n)|^2 \\ 0 & \text{otherwise} \end{cases}$$

where $[x]^+ = \max(0, x)$

This result is an extension of the multiuser diversity and opportunistic scheduling concept

Figure 3.1: Opportunistic scheduling example
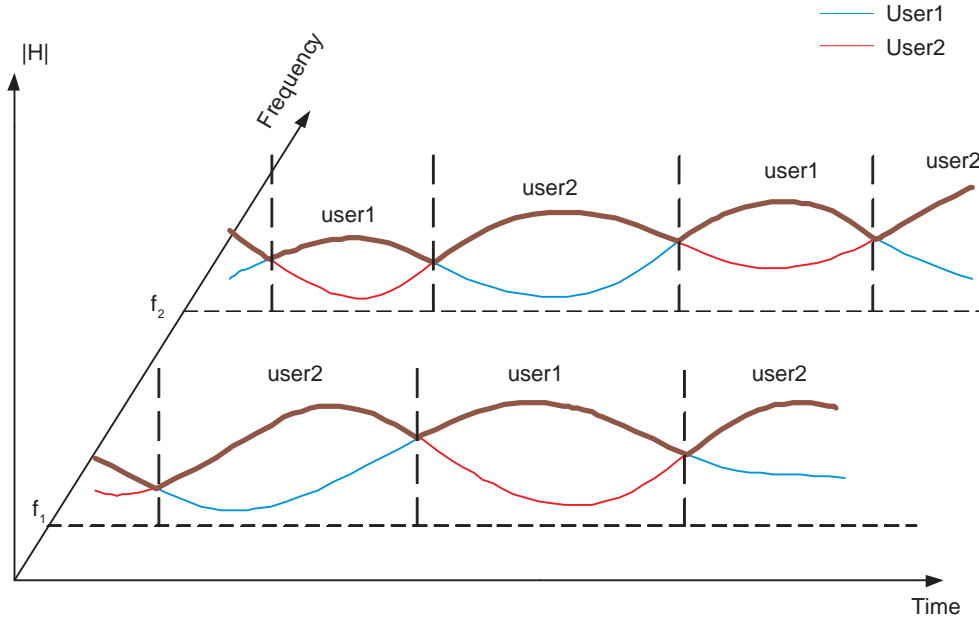
to the case of wideband systems. It shows that the maximum sum rate is only achieved by orthogonal multiplexing where in each channel we only schedule the user with the best channel gain and thus no joint decoding is required. In this case, the ergodic achievable total rate is given by

$$R = \sum_{m=1}^{M} \mathbb{E} \left[\log \left(\frac{2}{\lambda_{k_m^{(n)}} N_0} |H_{k_m^{(n)}}^m(n)|^2 \right) \right] \tag{3.5}$$

where for each fading block n and sub-channel m, the user $k_m^{(n)}$ is given by

$$k_m^{(n)} = \arg\max_k \frac{H_k^m(n)}{\lambda_k}$$

Figure 3.1 illustrates a full opportunistic scheduling example for a 2-user, 2 sub-channel system. At each time instant and in each sub-channel the user with the best channel gain is chosen. In each sub-channel, this is similar to selection combining in multiple antenna receive diversity (Chapter 2, section 2.3.4). At each time instant, the SNR is given by

$$SNR_{MUD} = \frac{P}{N_0} |h_{\max}^m|^2 \tag{3.6}$$

For independent and identically distributed Rayleigh fading gains, the cdf of the SNR is given by [10]

$$F_{MUD}(\alpha) = \left(1 - \exp\left(-\frac{\alpha}{\bar{\gamma}} \right) \right)^K \tag{3.7}$$

Figure 3.2: Per channel SNR's CDF for different number of users
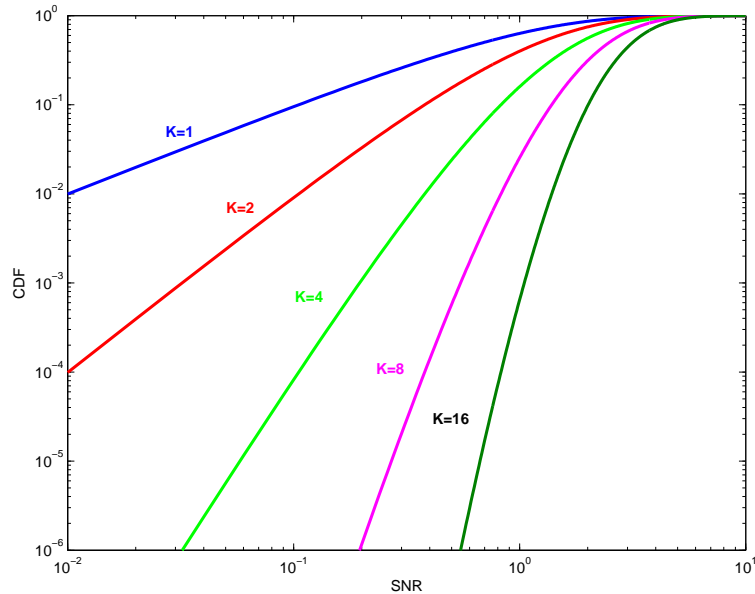
where $\overline{\gamma}$ is the average SNR. Figure 3.2 plots this cdf for different number of users. It shows the effect of multiuser diversity when increasing the average SNR and decrease its variance.

Ergodic sum rate corresponds to the optimal rate for non real-time traffic. When the users application cannot allow any delay on the transmission, this rate is no longer optimal and another notion of capacity is defined referred to as Delay Limited Capacity studied in the next section.

3.4   MAC Delay Limited Capacity

The delay-limited capacity (also known as Zero-Outage Capacity) is defined as the transmission rates that can be guaranteed in all fading states under finite long-term power constraints. In contrast with ergodic capacity, where power and mutual information between the transmitter and the receiver can vary depending on the fading state in order to maximize the average rates, the powers in delay limited capacity are coordinated between users and sub-channels with the objective of maintaining a constant mutual information vector over all fading states. Delay limited capacity for flat fading MAC channel is ele-

gantly studied in [15] and explicitly characterized exploiting the polymatroid structure of the capacity region. This structure is not valid for wideband systems and only an implicit Lagrangian characterization is possible. Zero-outage capacity for wideband systems is also studied in [19] where they considered asymmetric users case. The authors show that for large number of users, guaranteeing delay limited rate results only on small through-put decrease.

Wideband delay limited capacity is defined as

$$
\mathcal{C}_d(\overline{\mathbf{P}}) \quad \equiv \quad \bigcup_{\substack{\mathcal{P}:\mathbb{E}\left[\sum_m \mathcal{P}_k^m\right] \leq \overline{P}_k \\ k=1,\ldots,K}} \bigcap_{\underline{\mathbf{H}} \in \mathcal{H}} \mathcal{C}_g(\mathcal{P}, \underline{\mathbf{H}})
$$

$$
\equiv \quad \bigcup_{\substack{\mathcal{P}:\mathbb{E}\left[\sum_m \mathcal{P}_k^m\right] \leq \overline{P}_k \\ k=1,\ldots,K}} \bigcap_{\underline{\mathbf{H}} \in \mathcal{H}} \left\{ \mathbf{R} : \sum_{k \in S} R_k \leq \sum_{m=1}^{M} \log\left(1 + \frac{\sum_{k \in S} \mathcal{P}_k^m |H_k^m|^2}{N_0} \right), \quad \forall S \subset \mathcal{K} \right\}
$$

where $\mathcal{C}_g(\mathcal{P}, \underline{\mathbf{H}})$ is the time invariant Gaussian capacity for power matrix $\mathcal{P}$ and channel fading state $\underline{\mathbf{H}}$ as defined in (3.4).

The following theorem gives a Lagrangian characterization of the zero-outage capacity boundary. The proof of the theorem is given in Appendix A. This proof is inspired by the reasoning in [14, 15]. We first follow the method used, for delay limited narrowband channels, in [15] until bringing the problem to an optimization for each channel state. We then use a similar reasoning as used, for ergodic capacity, for a [14] for the optimization over sub-channels in given channel state.

Theorem 2 *For a given power constraint vector $\overline{\mathbf{P}}$, the boundary surface of $\mathcal{C}_d(\overline{\mathbf{P}})$ is the set of rate vectors $\mathbf{R}^*$ such that there exist $\lambda \in \mathbb{R}_+^K$ and for each block time n, there exist a power allocation matrix $\underline{\mathcal{P}}(.)$, a rate allocation matrix $\underline{\mathcal{R}}(.)$ and a rate reward vector $\alpha(n) \in \mathbb{R}_+^K$, where for each sub-channel m, $(\mathcal{R}^m(n), \mathcal{P}^m(n))$ is a solution to the optimization problem*

$$
\max_{\mathbf{r},\mathbf{p}} \sum_{k=1}^{K} \alpha_k(n) r_k - \lambda_k p_k
$$

$$
\text{subject to} \quad \sum_{k \in S} r_k \leq \log\left(1 + \frac{\sum_{k \in S} p_k |H_k^m(n)|^2}{\sigma^2} \right)
$$

and

$$\sum_{m=1}^{M} \mathcal{R}_k^m(n) = R_k^* \quad , \quad \mathbb{E}\left[\sum_{m=1}^{M} \mathcal{P}_k^m(n)\right] = \overline{P}_k \quad \forall k \in \mathcal{K}$$

$\mathcal{R}^m(n)$ and $\mathcal{P}^m(n)$ are the rate vector and power vector allocated to users in sub-channel m at time n. $\{\lambda_k\}$ are Lagrangian multipliers satisfying the power constraints and $\{\alpha_k(n)\}$ are rate rewards permitting to achieve the target rates at fading block n.

Let $\mathbf{q}^m = \{p_1^m|H_1^m(n)|^2, ..., p_K^m|H_K^m(n)|^2\}$ and $g(z) = \log\left(1 + \frac{z}{N_0}\right)$. We can then reformulate our maximization problem for each sub-channel m as follows,

$$\max_{\mathbf{r},\mathbf{p}} \sum_{k=1}^{K} \alpha_k r_k - \frac{\lambda_k}{|H_k^m(n)|^2} q_k^m \quad \text{subject to} \quad \sum_{k \in S} r_k \leq g\left(\sum_{k \in S} q_k^m\right)$$

This optimization problem can be solved using a greedy algorithm [14]. For each fading block n and for each sub-channel m, let us define the marginal *utility functions* for user k as

$$u_k^m(z) \equiv \frac{\alpha_k(n)}{z + N_0} - \frac{\lambda_k}{H_k^m(n)}, \quad k = 1, ..., K$$

$$u_m^*(z) \equiv \left[\max_k u_k^m(z)\right]^+$$

If $u_m^*(0) > 0$, then let $0 = z_0 < z_1 < ... < z_L$ where z_L is the smallest z for which $u_m^*(0) = 0$, and such that z_l is the point where $u_{i_l}^m(z)$ intersects $u_{i_{l+1}}^m(z)$ (i.e. in the interval $[z_l, z_{l+1}]$, $u_m^*(z) = u_{i_l}^m(z)$) for some i_l, $l = 1, ..., K$. Then $u_m^*(z)$ can be expressed as

$$u_m^*(z) = \begin{cases} z_l - z_{l-1} & \text{If} \quad z_l \leq z \leq z_{l-1}, l = 1, ..., L \\ 0 & \text{if} \quad z \geq z_L \end{cases}$$

which gives the optimal rate allocation solution expressed as

$$\mathcal{R}_k^m(n) = \begin{cases} g(z_l) - g(z_{l-1}) & \text{if} \quad k = i_l \text{ for some} \quad l = 1, ..., L \\ 0 & \text{otherwise} \end{cases}$$

and the optimal power allocation

$$\mathcal{P}_k^m(n) = \begin{cases} z_l - z_{l-1} & \text{if} \quad k = i_l \text{ for some} \quad l = 1, ..., L \\ 0 & \text{otherwise} \end{cases}$$

which is equivalent to

$$\mathcal{R}_k^m(n) = \int_{A_k^m} \frac{1}{N_0 + z} dz \tag{3.8}$$

$$= \int_0^\infty \frac{1}{N_0 + z} \mathcal{I}\{u_k^m(z) > u_{k'}^m(z), \forall k' \neq k \quad \text{and} \quad u_k^m(z) > 0\} dz$$

and

$$\mathcal{P}_k^m(n) = \frac{1}{|H_k^m(n)|^2}|A_k^m| \tag{3.9}$$

$$= \frac{1}{|H_k^m(n)|^2}\int_0^\infty \mathfrak{I}\left\{u_k^m(z) > u_{k'}^m(z), \forall k' \neq k \quad \text{and} \quad u_k^m(z) > 0\right\} dz$$

where $\mathfrak{I}\{.\}$ is the indicator function and $A_k^m \equiv \{z \in [0, \infty[: u_k^m(z) > u_{k'}^m(z), \quad \forall k' \neq k \text{ and } u_k^m(z) > 0\}$.
The solution to this optimization problem is given by successive decoding in each sub-channel in the order given by the permutation π satisfying [14, 19]

$$\frac{\alpha_{\pi_1}(n)}{|H_{\pi_1}^m(n)|} \geq \frac{\alpha_{\pi_2}(n)}{|H_{\pi_2}^m(n)|} \geq \ldots \geq \frac{\alpha_{\pi_K}(n)}{|H_{\pi_K}^m(n)|}$$

The decoding order can be different from one sub-channel to another.

The set $\{\alpha_k(n)\}_{k=1,\ldots,K}$ satisfy the equations

$$\sum_{m=1}^M \mathcal{R}_k^{m*}(n) = R_k^* \tag{3.10}$$

and $\{\lambda\}_{k=1,\ldots,K}$ are solutions to

$$\sum_{m=1}^M \mathbb{E}\left\{\mathcal{P}_k^{m*}(n)\right\} = \overline{P}_k \tag{3.11}$$

Equation 3.10 guarantees that each user is achieving its desired rate while equation 3.11 preserves the individual power constraints.

3.4.1 Single User case

Let us consider the case of one user transmitting over $M \geq 2$ symmetric and independent sub-channels. Let $f(h) = \frac{1}{a}\exp(-\frac{h}{a})$ and $F(h) = \left(1 - \exp\left(-\frac{h}{a}\right)\right)$ denote respectively the pdf and cdf of the fading process in each sub-channel. It has been shown in [15] that in the case of narrowband Rayleigh fading channel, the delay limited rate for a single user system is equal to zero. We show in this section that this result does not hold for a number of sub-channels $M \geq 2$.

For a single user, the set A_k^m is simplified to

$$A_1^m \equiv \{z \in [0, \infty[: u_1^m(z) > 0\} = \left\{z \in [0, \infty[: z < \frac{\alpha_1(n)}{\lambda_1} - N_0\right\}.$$

From equation(3.9), the optimal power allocation can then be expressed as

$$\mathcal{P}_1^m(n) = \left(\frac{\mu}{\lambda} - \frac{N_0}{H_1^m(n)} \right)^+ \tag{3.12}$$

We can notice that $\mathcal{P}_1^m(n)$ is an increasing function of $H_1^m(n)$. Let m^* be the sub-channel with the highest channel gain. We have then

$$
\begin{aligned}
\overline{P}_1 &\leq M\mathbb{E}\left[\mathcal{P}_1^{m^*}(n)\right] \\
&= M\mathbb{E}\left[\frac{N_0\left(\exp\left(\mathcal{R}_1^{m^*}(n)\right) - 1\right)}{H_1^{m^*}(n)} \right] \\
&\leq MN_0\left(\exp\left(R_1\right) - 1\right)\mathbb{E}\left[\frac{1}{H_1^{m^*}(n)} \right] \\
&= MN_0\left(\exp\left(R_1\right) - 1\right)\int_0^\infty \frac{1}{h}\left(F\left(h\right)\right)^{M-1} f(h)dh \\
&= MN_0\left(\exp\left(R_1\right) - 1\right)\int_0^\infty \frac{1}{ah}\left(1 - \exp\left(-\frac{h}{a}\right)\right)^{M-1}\exp\left(-\frac{h}{a}\right)dh \\
&= \frac{MN_0}{a}\left(\exp\left(R_1\right) - 1\right)\sum_{l=0}^{M-1}(-1)^{M-l}\binom{M-1}{l}\log\left(M - l\right)
\end{aligned}
$$

From the second to the third inequality we used the fact that the allocated channel at channel m^* is smaller or equal the delay limited rate R_1. From the last inequality we have

$$R_1 \geq \log\left(1 + \frac{a\overline{P}_1}{MN_0\sum_{l=0}^{M-1}(-1)^{M-l}\binom{M-1}{l}\log\left(M - l\right)} \right) \tag{3.13}$$

The right hand side of this inequality is greater than zero for $M = 2$ and is also an increasing function of M. This shows that for multi-channel systems, the delay limited capacity is not null.

This problem has been also considered in [28] and an explicit formula for the delay limited achievable rate for $M = 2$ is derived.

3.4.2   Achieving a target rate vector $\mathbf{R}^*$ with minimum power

The focus of this section is to find, for each block fading state $\underline{\mathbf{H}}(n)$, the optimal power and rate allocations $\underline{\mathcal{P}}(n)$ and $\underline{\mathcal{R}}(n)$ minimizing the total transmit power while achieving

a given target rate vector.

Let $\mathbf{R}^*$ be the target rate to be achieved. The announced objective can be expressed mathematically as follows

$$\min_{\mathbf{p}} \sum_{k=1}^{K} p_k$$

$$\text{subject to} \quad \mathbf{R}^* \in \mathcal{C}_d(\mathbf{p})$$

A power vector $\mathbf{P}^*$ is solution to the above problem if and only if for each block fading n there exists a rate allocation $\underline{\mathcal{R}}(n)$, a power policy $\underline{\mathcal{P}}(n)$ and a vector $\alpha(n) \in \mathbb{R}^K$, such that for each sub-channel m, $(\mathcal{R}^m(n), \mathcal{P}^m(n))$ is a solution to

$$\max_{\mathbf{r},\mathbf{p}} \sum_{k} \alpha_k(n) r_k - p_k$$

$$\text{subject to} \quad \sum_{k \in S} r_k \leq \log_2(1 + \frac{\sum_{k \in S} p_k |H_k^m(n)|^2}{N_0}) \quad \forall S \subset \mathcal{K})$$

and $\sum_{m=1}^{M} \mathcal{R}_k^m(n) = R_k^*, \qquad \mathbb{E}\left\{\sum_{m=1}^{M} \mathcal{P}_k^m(n)\right\} = P_k^*, \quad \forall k \in \mathcal{K}.$

For a given vector $\alpha(n)$, the optimal rate and power allocations are given by equations 3.8 and 3.9 respectively, with $\lambda_k = 1 \ \forall k$. To find the vector $\alpha(n)$ achieving the target rates, an iterative algorithm can be used. Let $\alpha^{(0)}(n)$ be any arbitrary starting point. At each iteration i and for each user k, compute $\alpha_k^{(i)}(n)$ as the unique solution of equation 3.10 assuming other users' rate rewards as fixed at the previous iteration $\{\alpha_{k'}^{(i-1)}\}_{k' \neq k}$. This algorithm converges to the optimal solution $\alpha(n)$.

A similar algorithm is proposed in [19].

3.5   Multiple-Access & Broadcast Channels Duality

There is an interesting duality between Multiple-Access and Broadcast Gaussian channels that has been showed in [29]. It can be demonstrated that for a given $\overline{P}_{total}$ and a given channel state matrix $\underline{\mathbf{H}}$ both uplink and downlink have the same achievable total-capacity

$$C_{BC}(\overline{P}_{total}, \underline{\mathbf{H}}) = \bigcup_{\substack{\mathbf{P}: \sum_k \sum_m P_k^m \leq \overline{P}_{total} \\ k=1,\dots,K}} C_{MAC}(\underline{\mathbf{P}}, \underline{\mathbf{H}}) \tag{3.14}$$

Any point in the boundary surface of C_{BC} is a vertex of a the MAC capacity region for a given power allocation matrix $\underline{\mathbf{P}}$.

This duality results also on the similarity of the transmission on reception schemes of the uplink and downlink. In both cases, the receiver gets a sum of K coded signal and uses successive cancellation to extract each user's signal.

For orthogonal signaling systems the duality between MAC and BC is the direct consequence of the reciprocity of the channel gains.

3.6   Orthogonal Multiple Access

For delay limited capacity, it has been shown that the optimal strategies to achieve delay limited rates is the transmission to multiple users in each sub-channel. The emergence of OFDM like system motivates the search for orthogonal access sub-optimal strategies. An other advantage of orthogonal signaling is the simplicity of receiver implementation and the reciprocity of the algorithms for both up and down links.

It has been shown in [19] that for delay limited capacity, the asymptotically optimal solution (for $K \to \infty$) in the case of orthogonal signaling is achieved by letting each user transmit on its best channel and using optimized fractions on each sub-channel. In our case we are interested in practical scenarios with limited number of users. We also impose in our system that there is only one user occupying each sub-channel (no partitioning of sub-channels in time or frequency). Each user is guaranteed one sub-channel at any given time instant to transmit. Under these assumptions we can accommodate up to $K = M$ users, and we consider this case in the following sections. For a fixed number of sub-channels M and under the constraint $K \leq M$, it is worth reminding that imposing $K = M$ offers maximum diversity for ergodic rate maximization, while zero-outage capacity suffers since there is an increased number of rate constraints to satisfy.

The K-user system with K parallel sub-channels can be represented by a weighted bipartite graph $G = (X, Y, E)$ where the left hand side set of vertices X represents users and the right hand side set Y represents sub-channels (Figure 3.3). E is the set of edges between X and Y. For notational simplicity, we denote the edge between vertex $x \in X$ and vertex $y \in Y$ by the tuple (x, y). Each edge (x, y) in the graph is weighted by $w(x, y)$

Users Sub-Channels
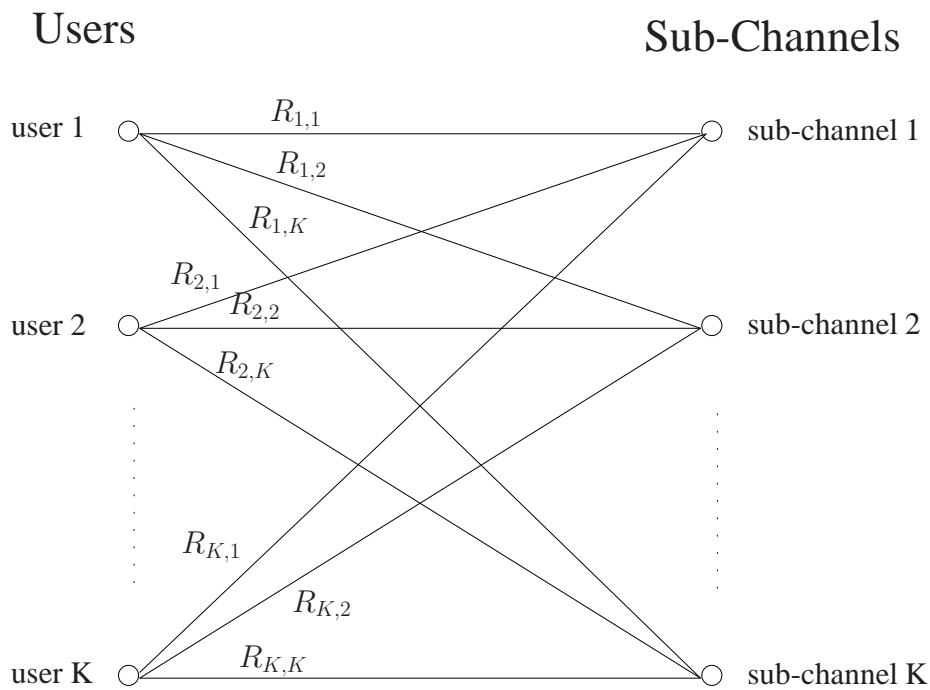
Figure 3.3: Graph representation of the system.

which will be defined as a function of the optimization criterion.

Definition 3 *A matching Mat in G is a subset of E such that no two edges in Mat have a vertex in common. Intuitively we can say that no vertex in $X \bigcup Y$ is incident to more than one edge in Mat.*

Definition 4 *A matching Mat is said to be Maximum if for any other matching Mat', $card(\mathrm{Mat}) \geq card(\mathrm{Mat}')$.*

where $card(\mathrm{Mat})$ is the number of edges in the matching Mat.

Definition 5 *A perfect matching is a maximum matching Mat such that $card(\mathrm{Mat}) = |X| = |Y|$. In other words, Mat is a perfect matching if every vertex is incident to an edge in Mat.*

Using this definition, an allocation of users over sub-channels under our assumptions is equivalent to find a perfect matching in the system corresponding graph.

In the considered system all users can transmit on all sub-channels, thus the graph G is complete $(card\,(E) = K^2)$. There exists $K!$ possible allocations of sub-channels to users each one represented by a perfect matching $\mathcal{M}at_i$ with $i = 1, ..., K!$. Let the vector $\mathbf{C_i} = \{C_i(1), C_i(2), ..., C_i(K)\}$ represent the matching $\mathcal{M}at_i$ such that $C_i(k)$ is the sub-channel assigned to user k when matching $\mathcal{M}at_i$ is applied.

In the following we propose two scheduling schemes achieving hard fairness for the considered orthogonal signaling system. Description of sub-optimal algorithms of the following allocation strategies for a more general case $(K \leq M)$ are given in Appendix B and C.

3.6.1   Orthogonal-Delay Limited Rates Allocation (ODLRA)

The objective here, as in the previous section for delay limited capacity, is to find the allocation of users to sub-channels minimizing the total transmit power while achieving some required rate-tuple $\mathbf{R}^* = (R_1^*, R_2^*, ..., R_K^*)$, or equivalently the SNR tuple $(\gamma_1^*, \gamma_2^*, ..., \gamma_K^*)$, where R_k^* is the rate of user k. This problem can be formulated mathematically as

$$\min_{\beta_k^m, P_k^m} \sum_{k=1}^{K} \sum_{m=1}^{M} \beta_k^m P_k^m \tag{3.15}$$

$$\text{subject to} \quad \beta_k^m \in \{0,1\}, \quad \text{for all } k, m$$

$$\sum_{k=1}^{k} \beta_k^m = 1, \quad \text{for all } m$$

$$\sum_{m=1}^{M} \beta_k^m \log\left(1 + \frac{P_k^m \cdot |H_k^m|^2}{N_0}\right) = R_k^*, \quad \text{for all } k$$

$$\tag{3.16}$$

The two first constraints ensure the orthogonal multiple-access while the third constraint guarantees the achievability of the rate target vector.

We represent our system by a weighted bipartite graph $G = (X, Y, E)$ as described previously with the weight of each edge (x, y) set to be the power needed for user x to achieve its target rate R_x^* (or equivalently the desired SNR γ_x^*) if it is assigned to sub-channel y, that is

$$w(x, y) = \frac{N_0\,(\exp\,(R_x^*) - 1)}{|H_x^y|^2} = \frac{\gamma_k^* N_0}{|H_x^y|^2} \tag{3.17}$$

Finding the matching that minimizes the sum of weights permits us to find the desired allocation of users to sub-channels.

Authors in [32] describe an algorithm that permits to find this optimal matching in $O(K^3)$ time based in the well-known Hungarian method.

3.6.2   Max-Min Allocation (MMA) policy

Allocation Criterion

This policy consists of finding the matching $\mathcal{M}at_{i^*}$ such that

$$i^* = \arg\max_{i=1,\dots,K!} \min_{k=1,\dots,K} \left| H_k^{C_i(k)} \right| \tag{3.18}$$

This policy guarantees that at any given time instant the minimum channel gain allocated is the best possible among all allocations and thus maximizes the minimum of all user rates when all users have equal and fixed power. This is particularly relevant for systems where no power control is allowed with the purpose of achieving maximum fairness between users. This criterion was introduced in [27] and it was shown that this scheme can still achieve multiuser diversity and provides a non-negligible gain even with respect to a non-fading channel. In what follows we give a description of an algorithm achieving this allocation criterion in polynomial time with K. In practice this policy allows the user's instantaneous information rate to vary but is strictly non-zero.

Allocation Algorithm description

We first construct the bipartite graph G corresponding to the system with the weight of edge (x, y) set to be the channel gain of user x on sub-channel y. Using the following lemma, we initialize the graph by removing the $K-1$ edges with minimum channel gains.

Lemma 6 *If we consider the K^2 order statistics of users' channel gains, we have that*

$$ord\left(\min_{k=0,\dots,K-1} \left| H_k^{C_{i^*}(k)} \right| \right) \geq K \tag{3.19}$$

The operator $\mathrm{ord}\,(H_k^m)$ *gives the rank of the channel gain between the user* k *on sub-channel* m *withing the* K^2 *channel gains arranged in ascending order.*

The idea in the algorithm is to remove at each iteration the edge with the minimum weight (i.e eliminate the link with minimum channel gain) until no perfect matching could be found in the bipartite graph. The last removed edge then corresponds to the link with the minimum allocated channel gain under Max-Min allocation policy, since we can not find a perfect matching with better minimum rate. Once the first user is assigned a sub-channel, we remove the two nodes from the graph, we set its dimension to $(K-1)$ and operate in the same way to allocate a sub-channel to the second user and so on until all users are assigned one sub-channel. Before giving the details of the allocation algorithm let us first point out some general definitions that will help in the algorithm's description.

Definition 7 *Given a matching* Mat *in a bipartite graph* G, *an augmenting path for* Mat *is a path that comprises edges in* Mat *and edges not in* Mat *alternatively and which starts and ends at exposed vertexes. An exposed vertex is a vertex not connected to any edge.*

Theorem 8 (Berge's theorem) *[31]): A matching* Mat *is maximum if and only if it has no augmenting path.*

This theorem will be of great help in our algorithm. In fact, in some cases we will have to check the existence of perfect matching in a graph having a matching of cardinality equal to the graph dimension minus one. Thus, if no augmenting path can be found for this matching this shows that the graph does not have any perfect matching. In Appendix D, we review an algorithm to search an augmenting path of a given matching Mat. We also describe how to augment a matching along an augmenting path.

The Max-Min allocation algorithm can be described as follows.

Algorithm 1 Max-Min allocation algorithm

---

1. *Initialization*

   - Construct the system corresponding graph $G = (X, Y, E)$ as previously described.

   - Remove the $K - 1$ edges with the minimum weights from E,

   $$E = E - \{(x, y)/\text{ord}(w(x, y)) < K - 1\}$$

   - Construct an arbitrary perfect matching Mat_p corresponding to an arbitrary allocation.

2. *Iteration*

   (a) Find, in graph G, the edge (x^*, y^*) with the minimum weight (i.e. the link with minimum channel gain)

   $$(x^*, y^*) = \underset{(x,y) \in X \times Y}{\arg\min} \ \{w(x, y)\}$$

   (b) - If $(x^*, y^*) \notin \text{Mat}_p$, then remove the edge (x^*, y^*) from the graph (i.e. $E = E - (x^*, y^*)$) and go to (a).
        - If $(x^*, y^*) \in \text{Mat}_p$, then let $\text{Mat}'_p = \text{Mat}_p - (x^*, y^*)$ and
          – If Mat'_p admits an augmenting path P, then set Mat_p to the result of augmenting Mat'_p along P, and go to (a).
          – If Mat'_p admits no augmenting path, then we allocate sub-channel y^* to user x^*, remove vertices x^* and y^* and all edges connected to them (after this the dimension of the graph is reduced by 1 and Mat'_p is a perfect matching in the new graph), set $\text{Mat}_p = \text{Mat}'_p$ and go to (a)

   (c) Stop the algorithm when all user are assigned one sub-channel

---

Figures 3.4 and 3.5 represent respectively the pdf and cdf of the worst allocated channel gain using Max-Min allocation strategy for different values of the number of sub-channels M. This figures highlight the impact of multiuser diversity characterized by the

considerable enhancement of the min-allocated channel gain average and its diminished variance. Multiuser Diversity can still be achieved even under hard fairness constraints. Furthermore, for a large user population the CDF of the worst case received power is extremely sleep (i.e. close to the mean). This suggests that power control (as in ODLRA) should not bring much benefit. From the point of view of the system architecture this is a very appealing feature of the max-min policy.   This is confirmed by figure 3.6, which
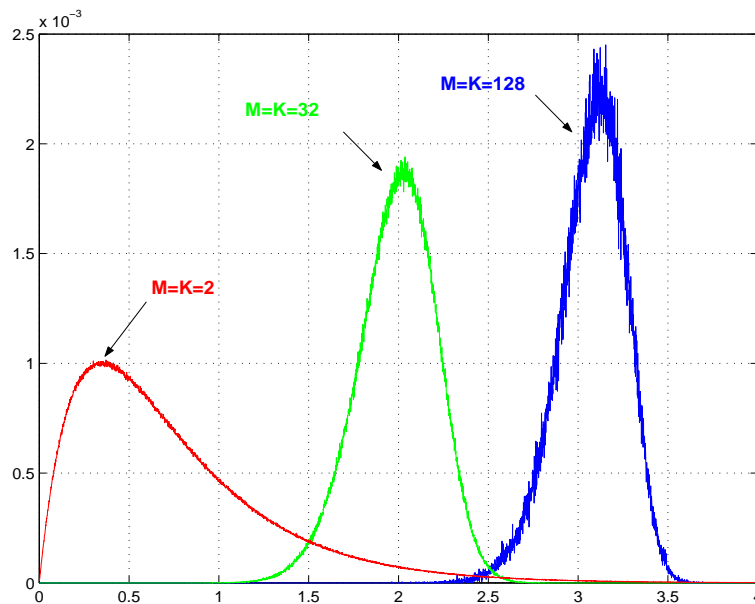
Figure 3.4: PDF of the minimum allocated channel gain using Max-Min Allocation for different values of M.

represents the system spectral efficiency as a function of the number of users (which in our assumptions is equal to the number of sub-channels) with the different allocation strategies presented previously. The "Ergodic sum-rates" curve represents the averaged per sub-channel rate under the strategy maximizing the total sum-rate with power allocation given by equation (3.5). Curves "Optimal delay limited rates" and "orthogonal delay limited rates" represent the common rate (equal rate for all user) under optimal and orthogonal multiple access, respectively. This rate is not the optimal one in terms of spectral efficiency for delay limited capacity since the common rate point is not necessarily the point of zero-outage capacity boundary corresponding to the maximum total sum-rate. We assume Rayleigh fading with uncorrelated frequency channel gains. Although unrealistic, this provides an idea of the achievable rates as a function of the number of
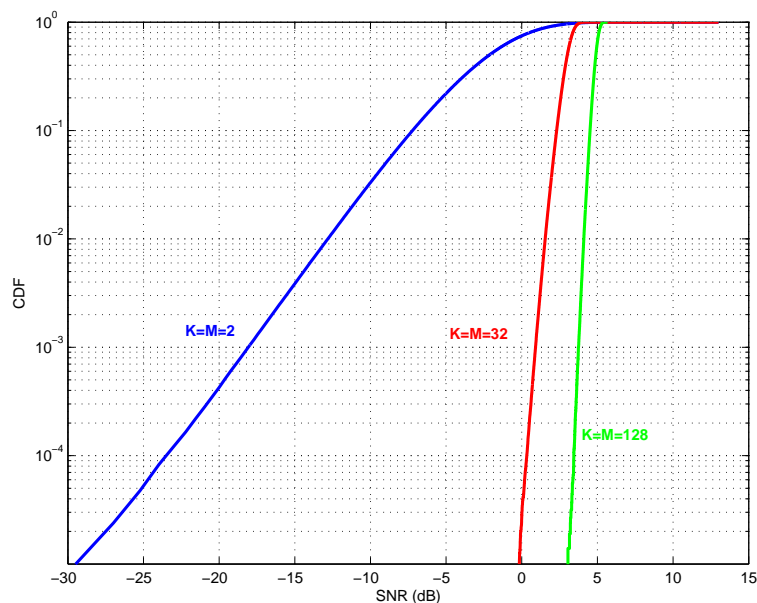
Figure 3.5: CDF of the minimum allocated channel gain using Max-Min Allocation for different values of M.

uncorrelated channels (or the approximate number of degrees of freedom) of the propagation environment in the system's available bandwidth. These curves have been computed for the same per channel average SNR (0dB). We first note in figure 3.6 that the per-user average throughput increases with the number of users, in all cases, which proves that even under delay limited requirements high multiuser diversity can still be achieved. We can also see that even under hard fairness constraints we can achieve performances which are very close to the optimal unfair policy, thus hard fairness constraints do not introduce a significant throughput degradation and this is also valid for orthogonal signaling.

Figure 3.7 shows the spectral efficiency as a function of the number of accommodated users, for different values of the system bandwidth, using the proposed max-min allocation algorithm on a frequency selective channel with correlated frequency channel gains. The number of sub-carrier is kept fixed (equal to 64) and only the sub-channels spacing changes to evaluate the effect of sub-channels' correlation. Here the number of sub-carriers per user is M/N. For the correlated channel results, we assumed a maximum path delay $\tau_{max} = 2\mu s$ and an exponentially-decaying multi-path intensity profile. The algorithm performance for independent frequency channel gains is also given for comparison. As expected, bandwidth plays an important role in how much scheduling users on
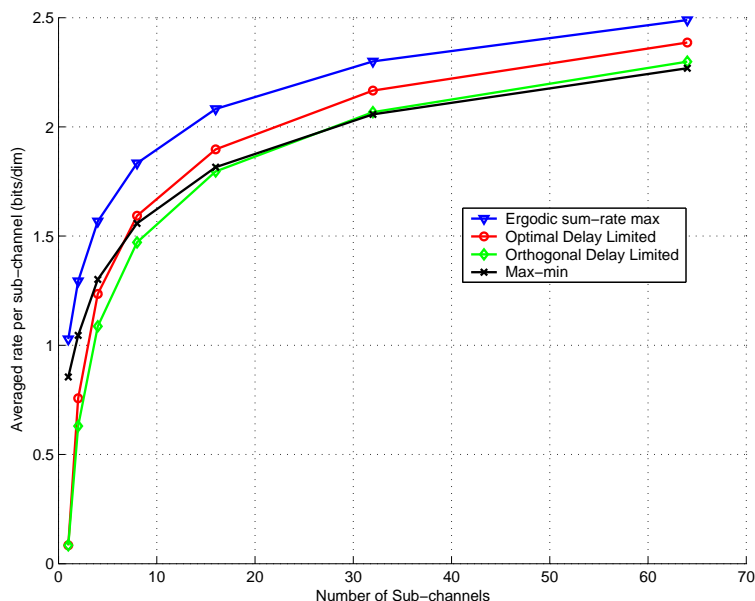
Figure 3.6: Averaged throughput over Rayleigh fading at 0-dB with fair and unfair allocations

sub-channels can increase spectral efficiency. We see that when the system bandwidth is appropriately chosen spectral efficiency can be increased by more than a factor of 2 for moderate user populations even with hard fairness constraints.

We also note that for sufficiently large bandwidth (here $B = 50$MHz) we approach the performance of a system with independent frequency channel gains. Another interesting result, given by the lower curve ($B = 5$MHz), is that for a number of users greater than the number of uncorrelated sub-channels, an increase in the number of users induces only a very slight improvement of the system's spectral efficiency. This result is confirmed by figure 3.8 which shows the SE as a function of the system bandwidth for a fixed number of users ($N = 8$) and a fixed number of sub-carriers ($M = 64$). This curve shows that an increase in the system bandwidth yields a rapid improvement of the system SE and slowly approaches the performance of the system with independent frequency channel gains for bandwidth greater than 50 MHz. This result is due to the increase in sub-carrier spacing, which becomes greater than the coherence bandwidth for $B > 50$MHz and thus the frequency correlation of the channel becomes small. The value of 50MHz is also the system bandwidth for which the number of uncorrelated sub-channels is almost equal to the number of users accommodated in the system.
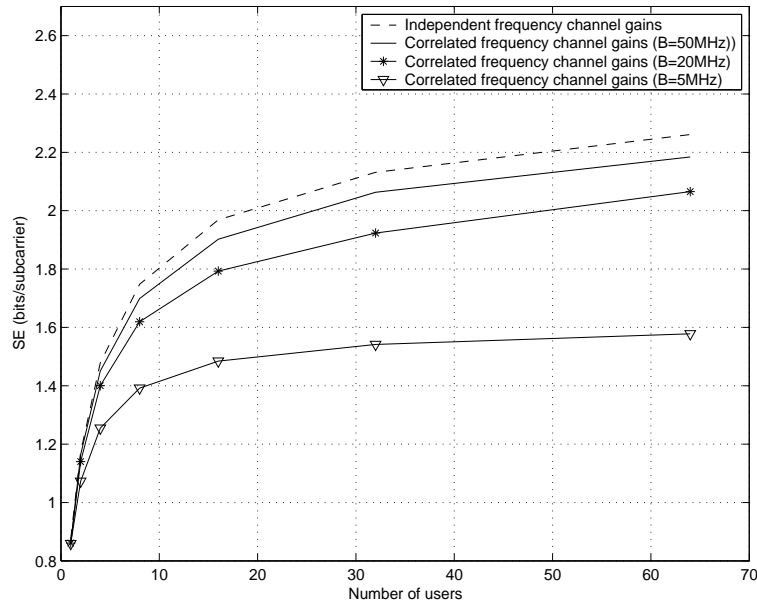
Figure 3.7: Spectral Efficiency variation with user population for a fixed number of sub-carriers and variable system bandwidth ($\tau_{max} = 2\mu s$).

3.7 Conclusion

In this chapter, we studied resource allocation for delay limited wideband systems. We showed that with optimal signaling such systems do not suffer from an important decrease of system spectral efficiency. We also proposed different low complexity allocation algorithm for delay limited orthogonal signaling systems. We showed that orthogonal access introduces only a slight degradation on system performance compared to optimal signaling. This result may encourages research on applicable algorithms achieving hard fairness for future wideband systems.
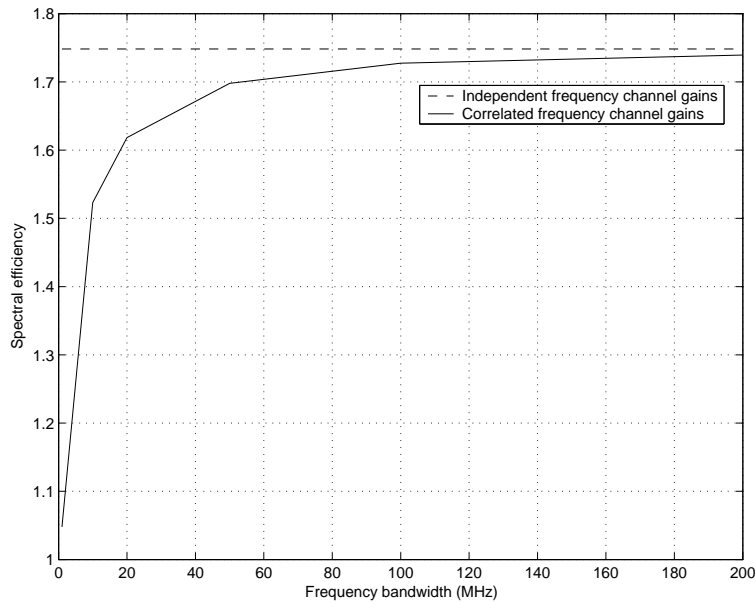
Figure 3.8: Spectral efficiency variation with system bandwidth for fixed number of users and sub-carriers with the max-min allocation policy

Appendix A

The delay limited capacity region $\mathcal{C}_d(\overline{\mathbf{P}})$ is convex. Thus the vector $\mathbf{R}^*$ is in the boundary surface of $\mathcal{C}_d(\overline{\mathbf{P}})$ if and only if there exists a vector $\mu \in \mathbb{R}_+^K$ such that $\mathbf{R}^*$ is a solution to the optimization problem

$$\max_{\mathbf{R}} \sum_{k=1}^{K} \mu_k R_k \quad \text{subject to} \quad \mathbf{R} \in \mathcal{C}_d(\overline{\mathbf{P}}) \tag{3.20}$$

Let $\mathbf{S} \equiv \left\{ (\mathbf{R}, \mathbf{P}) : \mathbf{P} \in \mathbb{R}_+^K, \mathbf{R} \in \mathcal{C}_d(\mathbf{P}) \right\}$.

The set $\mathbf{S}$ is concave, thus $\mathbf{R}^*$ is solution to 3.20 if and only if there exists $\lambda \in \mathbb{R}_+^K$ such that $(\mathbf{R}^*, \overline{\mathbf{P}})$ is solution to

$$\max_{(\mathbf{R},\mathbf{P}) \in \mathbf{S}} \sum_{k=1}^{K} \left(\mu_k R_k - \lambda_k P_k \right) \tag{3.21}$$

$\mathbf{R}^*$ is in the boundary surface of $\mathcal{C}_d(\overline{\mathbf{P}})$ if and only if $\overline{\mathbf{P}}$ is solution to

$$\min_{\mathbf{P}} \sum_{k=1}^{k} \lambda_k P_k \quad \text{subject to} \quad \mathbf{R}^* \in \mathcal{C}_d(\mathbf{P}). \tag{3.22}$$

if and only if there exists a power allocation $\underline{\mathcal{P}}(.)$ solution to

$$\min_{\underline{\mathbf{P}}} \sum_{k=1}^{K} \lambda_k \mathbb{E} \left\{ \sum_{m=1}^{M} P_k^m \right\} \quad \text{subject to} \quad \mathbf{R}^* \in \bigcap_{\underline{\mathbf{H}} \in \mathcal{H}} \mathcal{C}_g \left(\underline{\mathbf{P}}, \underline{\mathbf{H}} \right) \quad (3.23)$$

and

$$\mathbb{E} \left\{ \sum_{m=1}^{M} P_k^m \right\} = \overline{P}_k$$

which is equivalent to the existence of a power allocation $\underline{\mathcal{P}}(.)$ such that, for each channel fading state $\underline{\mathbf{H}}$, $\underline{\mathcal{P}}(\underline{\mathbf{H}})$ is a solution to

$$\min_{\underline{\mathbf{P}}} \sum_{k=1}^{K} \lambda_k \left(\sum_{m=1}^{M} P_k^m \right) \quad \text{subject to} \quad \mathbf{R}^* \in \mathcal{C}_g \left(\underline{\mathbf{P}}, \underline{\mathbf{H}} \right) \quad (3.24)$$

and

$$\mathbb{E} \left\{ \sum_{m=1}^{M} P_k^m \right\} = \overline{P}_k$$

Let us define for each channel fading block n,

$$\mathbf{S}_n \equiv \left\{ (\mathbf{R}, \mathbf{P}) : \mathbf{P} \in \mathbb{R}_+^K, \mathbf{R} \in \mathcal{C}_g \left(\mathbf{P}, \underline{\mathbf{H}}(n) \right) \right\} \quad (3.25)$$

$\mathbf{S}_n$ is concave, thus a power allocation is solution to eq (3.24) if and only if for each block fading n, there exist Lagrange multipliers $\alpha(\mathbf{n}) \in \mathbb{R}^K$ for which $(\mathbf{R}^*, \underline{\mathcal{P}}(n))$ is a solution to

$$\max_{\mathbf{R}, \underline{\mathbf{P}}} \sum_{k=1}^{K} \left(\alpha_k(n) R_k - \lambda_k \sum_{m=1}^{M} P_k^m \right)$$

$$\text{subject to} \quad \sum_{k \in S} R_k \leq \sum_{m=1}^{M} \log \left(1 + \frac{\sum_{k \in S} P_k^m |H_k^m(n)|^2}{\sigma^2} \right)$$

if and only if there exist a power allocation $\underline{\mathcal{P}}(.)$ and a rate allocation $\underline{\mathcal{R}}(.)$ such that for each channel block fading n, $\underline{\mathcal{R}}(n), \underline{\mathcal{P}}(n)$ is solution to

$$\max_{\underline{\mathbf{R}}, \underline{\mathbf{P}}} \sum_{k=1}^{K} \left(\alpha_k(n) \sum_{m=1}^{M} R_k^m - \lambda_k \sum_{m=1}^{M} P_k^m \right)$$

$$\text{subject to} \quad \sum_{k \in S} \sum_{m=1}^{M} R_k^m \leq \sum_{m=1}^{M} \log \left(1 + \frac{\sum_{k \in S} P_k^m |H_k^m(n)|^2}{\sigma^2} \right)$$

and

$$\sum_{m=1}^{M} R_k^m = R_k^* \quad , \quad \mathbb{E} \left[\sum_{m=1}^{M} P_k^m \right] = \overline{P}_k \quad \forall k \in \mathcal{K}$$

The last optimization is equivalent to, $(\underline{\mathcal{R}}^m(n), \underline{\mathcal{P}}^m(n))$ is solution to

$$\max_{\mathbf{R},\mathbf{P}} \sum_{k=1}^{K} (\alpha_k(n) R_k^m - \lambda_k P_k^m)$$

$$\text{subject to} \quad \sum_{k \in S} R_k^m \leq \log\left(1 + \frac{\sum_{k \in S} P_k^m(n) |H_k^m(n)|^2}{\sigma^2}\right)$$

and

$$\sum_{m=1}^{M} R_k^m = R_k^* \quad , \quad \mathbb{E}\left[\sum_{m=1}^{M} P_k^m(n)\right] = \overline{P}_k \quad \forall i \in 1, ..., K$$

where $\underline{\mathcal{R}}^m(n)$ and $\underline{\mathcal{P}}^m(n)$ are the rate vector and power vector allocated at sub-channel m.

Appendix B

In this section we present an extension, to the general case of an arbitrary number of users, of the ODLRA algorithm proposed in section 3.6.1. Under our assumption, the number of users can not be greater than M since we do not consider sub-channel fractioning. Let us consider a system with K users sharing M parallel sub-channels and $K < M$. This is typically the case for OFDMA-like systems.

As in section III-A, we begin by constructing the graph $G = (X, Y, E)$ corresponding to the system. We have now $|X| \leq |Y|$, so we call a perfect matching each maximum matching $\mathcal{M}at$ s.t. $card(\mathcal{M}at) = |X|$. Not all vertices of Y are incident to an edge of a perfect matching anymore.

The algorithm proceeds in two steps. It first allocates one sub-channel to each user and then uses the remaining sub-channels to improve the power allocation. It works as follows.

Algorithm 2 ODLRA extension

- Use the Hungarian algorithm to find a perfect matching in G, minimizing the total transmitted power. Each user is then allocated one sub-channel.

- *Improvement:*

  Let A be the set of remaining sub-channels.

  While $A \neq \emptyset$

      - For each sub-channel $m \in A$ and each user k, we compute Δp_k^m, the power reduction on the total transmit power if m joins the set of sub-channels allocated to k and where the power is optimally split on sub-channels of this set in order to achieve the desired rate.

          - Find $(k^*, m^*) = \arg\max\limits_{k,m} \Delta p_k^m$

          - We allocate m^* to k^*.

          - $A = A - m^*$

  end while

- Stop the algorithm

Appendix C

In this section we present the extension of the Max-Min allocation algorithm to the general case of an arbitrary number of users. Consider a system with K users sharing M parallel sub-channels. The Max-Min assignment problem can be formulated as

$$\max_{S_k} \min_k \sum_{m \in S_k} \log\left(1 + \frac{P.|H_k^m|^2}{N_0}\right) \tag{3.26}$$

$$\text{subject to} \quad S_0 S_2, ..., S_{K-1} \quad \text{are disjoint}$$

$$S_0 \cup S_2 \cup ... \cup S_{K-1} = \{1, 2, ..., M\}$$

where S_k is the set of indices of sub-channels assigned to user k. Regarding the complexity of searching the optimal solution to equation (3.26), we present in the following a sub-optimal solution which has performance close to those of the optimal one obtained by an exhaustive search.

In this allocation, we proceed in two steps. We first allocate one sub-channel to each user and then use the remaining sub-channels to improve the amount of rate allocated to the users with the worst channel gains. We again begin by constructing the graph

$G = (X, Y, E)$ corresponding to the system.

The sub-optimal algorithm works as follows

Algorithm 3 Max-Min Allocation extension

1. *Initialization*: Use the Max-Min allocation algorithm proposed in 3.6.2 to allocate one sub-channel to each user.

2. *Improvement*

   Let A be the set of remaining sub-channels.

   While $A \neq \emptyset$

         - Find k^* satisfying $R_{k^*} \leq R_k$ for all $k \in 0, ..., K-1$

         - Find m^* satisfying $|H_{k^*,m^*}| \geq |H_{k^*,m}|$ for all $m \in A$

         - set $R_{k^*} = R_{k^*} + \log\left(1 + \frac{P.|H_{k^*,m^*}|^2}{N_0}\right)$ and $A = A - m^*$

3. Stop the algorithm

Figure 3.9 shows the minimum allocated rate of all users as a function of the SNR for a system with 5 users and 8 sub-channels. This choice of parameters is completely arbitrary. This figure shows that our proposed algorithm performs almost as well as the exhaustive search based allocation.

Appendix D

Search for an augmenting path

The following is a pseudo-code for searching an augmenting path:
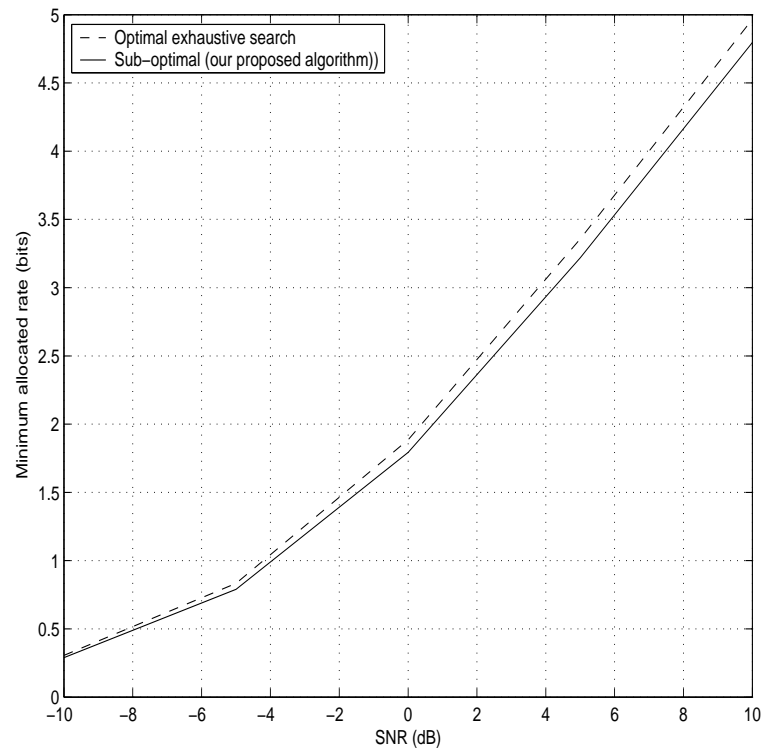
Figure 3.9: The minimum of all user rates vs SNR with the optimal exhaustive search and our sub-optimal proposed allocation for a system with 5 users and 8 sub-channels

---

Algorithm 4 Search for an augmenting path

---

assign all vertices as unvisited;

create an empty vertex queue Q;

AP_found := false;

while an exposed u in U is unvisited

and not AP_found loop

add u to Q;

visit u and record u as start vertex;

while Q not empty loop

remove v from (front of) Q;

for each w adjacent to v loop

if w unvisited then

predecessor(w) := v;

if w is exposed then

record w as end vertex;

AP_found := true;

exit;

else

visit w;

add w's mate to (rear of) Q;

end if;

end if;

end loop;

end loop;

end loop;

Augmenting the matching along an augmenting path

Let $G = (X, Y, E)$ be a bipartite graph and $\mathcal{M}at$ is a matching (not maximum) in G. Consider $\mathcal{P}at$ to be an augmenting path for $\mathcal{M}at$. The augmenting path must have $2k + 1$ edges for some k. We can form a matching $\mathcal{M}at'$ of size $card(\mathcal{M}at) + 1$ by augmenting

along $\mathcal{P}at$ as follows

Algorithm 5 Augmenting a matching

- Initially let $\mathcal{M}at' = \mathcal{M}at$

- Remove from $\mathcal{M}at'$ the k edges on the augmenting path $\mathcal{P}at$ belonging to $\mathcal{M}at$

- Add to $\mathcal{M}at'$ the $k + 1$ edges on the augmenting path $\mathcal{P}at$ not belonging to $\mathcal{M}at$.

Chapter 4

Fair Channel Allocation Strategies for Wideband Multiple Antenna Systems

4.1 Introduction

Mmultiple antenna systems have emerged as one of the most promising technical advancements in modern wireless communications. The pioneering work by Telatar [38] and Foschini [39] predicted remarkable spectral efficiency for wireless systems using multiple antennas to increase data rates through multiplexing or to improve performance through diversity. For a detailed study of multiple antenna systems, one can refer to [33] where different classes of techniques and algorithms which attempt to realize the various benefits of multiple antennas are surveyed. Multiple antenna techniques can be divided into two groups

- *Diversity techniques*, which are an efficient way of mitigating fading an thus increase the reliability of communication links. By using multiple antennas at the transmitter and/or the receiver, multiple and independent paths are created and thus by coding the data over different transmitter branches and/or combining the received signal at the receiver, the transmitter-receiver link reliability can be significantly improved. The literature on spatial diversity and STC is huge, we cite

[39]-[41] among others.

- *Multiplexing techniques*, where independent data streams are sent simultaneously each one from a different antenna. At the receiver, signal processing techniques are applied to separate the signals and recover the original streams [42]-[45]. It was shown that SM offers a considerable enhancement of the system spectral efficiency. In the multiuser context, the different streams can be allocated to different user.

Several works have studied the trade-off between diversity and spatial multiplexing (see for instance [46], [47] among others).

For multiuser environment, there have also been many other studies of MIMO systems including proposals for scheduling algorithms for both the downlink [48]-[53] and the up-link [54]-[56]. It has been shown in [48] that the sum-rate capacity is achieved by dirty paper coding (DPC). Authors of [53] propose a scheduling scheme with a throughput scaling law the same as that of DPC but, with considerably decreased complexity and with only partial channel state information at the transmitter. This scheme is an extension to space division multiple access of the opportunistic beamforming and scheduling proposed in [49]. In [54], authors study the optimal strategy for MAC with multiple antennas at the base station. The proposed scheduling algorithm straddles both the physical and low level protocol layers.

In this chapter, we consider the downlink of a multiuser wideband system. We propose a simple system scheme based on the knowledge of only channel gain amplitudes. Actually, to optimally design the transmission scheme for systems based on MIMO, an accurate estimate of the phases should be available at the transmitter in addition to the channel amplitudes. However such an estimate is not simple to obtain mainly due to the difficulty of calibrating the difference in phase response between the transmitter and the receiver chains. We show through numerical results that even with such a simple system and under hard fairness constraints between users, high multiuser diversity gain can still be achieved and system performance approaches that of the optimal DPC scheme in the scenario where only fast fading is considered. In the case of multi-cell systems, and when both large scale fading (path loss and shadowing) and fast fading are considered, our system still offers the possibility to attain high throughput. This work also highlights the importance of distributed antennas on cellular systems not only in the improvement

of the system spectral efficiency but also on the enhancement of fairness between users. Fairness is measured by the minimum allocated rate.

The chapter is organized as follows: Section 4.2 presents the channel and system model. In Section 4.3 we review some interesting results of BC MIMO transmission techniques. We then propose in Sections 4.4,4.5, 4.6 , three channel allocation schemes achieving hard fairness. Numerical results for single cell system are presented in Section 4.7 and in section 4.8 we study multi-cell systems with distributed antennas. Finally, in Section 4.9 we present our conclusions and outline future extensions and perspectives.

Contributions

- Max-Min allocation algorithm extension for multiple antenna systems. Both spatial multiplexing and diversity variants are presented.

- Resource allocation algorithm for delay limited rates constrained systems.

- Comparison of hard fairness algorithms to Zero-Forcing-DPC.

- Study of distributed antenna performance on multi-cellular systems.

4.2   Channel Model

We consider the downlink of a multi-cell system involving C cells with frequency reuse factor F. We consider that cell $c = 1$ is the cell of interest and cells from $c = 2$ to $c = C$ are interfering cells. Each cell is equipped with N_t antennas transmitting over M parallel channels each of bandwidth W. Let K denote the number of users, each having a single receive antenna. The channel between the N_t transmit antennas of cell c and user k on channel m is giving by the $1 \times N_t$ row

$$\mathbf{G}_{k,m}^c = \left[G_{k,m}^c[1], G_{k,m}^c[2], ..., G_{k,m}^c[N_t] \right] \tag{4.1}$$

where $G_{k,m}^c[i]$ is given by

$$G_{k,m}^c[i] = \sqrt{L_k^c[i]} H_{k,m}^c[i] \tag{4.2}$$

$H_{k,m}^c[n_t]$ is the channel gain between the n_t-th antenna of cell c and user k on channel m. The channel is assumed stationary for the duration of coded transmission block but may vary from block to block. $\sqrt{L_k^c[n_t]}$ corresponds to the large scale fading from the n_t-th transmit antenna of cell c which includes path loss and shadowing. The path loss is modeled as $(\frac{d_{t,r}}{d_0})^{-\alpha}$, where $d_{t,r}$ is the distance between the transmitter and the receiver, and d_0 is used as a reference point in measurements. α is the path loss exponent which depends on the environment and terrain structure and can vary between 2 in free space and 4.5 in heavily built urban areas. The shadow fading for each user is modeled as an independent log-normal random variable with standard deviation σ_s. The combined large scale fading between user k and antennas n_t of cell c is given by

$$L_k^c[n_t] = \left(\frac{d_{n_t,k}}{d_0}\right)^{-\alpha} 10^{\frac{\chi n_t}{10}} \tag{4.3}$$

where χ_{n_t} is a normally distributed zero mean random variable with variance σ_s^2. The received signal by user k on channel m is then given by

$$Y_{k,m} = \sum_{c=1}^{C} \mathbf{G}_{k,m}^c \mathbf{X}^c + Z_{k,m} \tag{4.4}$$

where $\mathbf{X}^c$ is the $N_t \times 1$ modulated symbol vector transmitted from the antennas of cell c. $Z_{k,m}$ is the Gaussian channel noise at user k on channel m.

4.3 Background on MIMO Broadcast Channels

Let us focus in this section on single cell case for a narrow band channel and review some important results for MIMO Broadcast Channels (BC). The generalization to multi-channel case of these results is straight-forward. Our multiuser system can be considered as a classical point-to-point MIMO system with N_t transmit antennas and K receivers with no cooperation at the receiving antennas. Let the channel gain from the N_t antennas

to the K receivers be represented by the matrix

$$\underline{\mathbf{G}} = \begin{bmatrix} \mathbf{G}_1 \\ \mathbf{G}_2 \\ \vdots \\ \mathbf{G}_K \end{bmatrix} \tag{4.5}$$

where $\mathbf{G}_k$ is the channel gain row between transmit antennas and receiver k given by (4.1). We have then the received signal vector

$$\mathbf{Y} = \underline{\mathbf{G}}\mathbf{X} + \mathbf{Z} \tag{4.6}$$

It has been shown recently in [68] that, when the transmitter perfectly knows the channel, the sum capacity of such a model is achieved using the DPC introduced by Costa in [69]. Prior to this work, authors in [70, 71] used the duality of broadcast channel with MAC to obtain an expression of the maximum sum rate given by

$$\mathcal{C}_{BC}(\underline{\mathbf{G}}, P) = \max_{\sum_{k=1}^{K} P_k \leq P} \log \det \left(I_{N_t} + \sum_{k=1}^{K} P_k \mathbf{G}_k^H \mathbf{G}_k \right) \tag{4.7}$$

This capacity can be bounded by assuming that there exist N_t users with orthogonal channel vectors all with the maximum norm $\|\mathbf{G}_{k^*}\|$ where k^* is the user with the largest channel vector norm. We have then

$$\mathcal{C}_{BC}(\underline{\mathbf{G}}, P) \leq N_t \log \left(1 + \frac{P}{N_t} \|\mathbf{G}_{k^*}\|^2 \right) \tag{4.8}$$

4.3.1 Dirty Paper Coding Principle

The received signal at a receiver k can be written as

$$Y_k = X_k + S_k + Z_k \tag{4.9}$$

where $S_k \sim \mathcal{N}(0, Q)$ represent the interferences non-causally known to the transmitter and unknown to the receiver. Rather then attempting to fight and cancel S_k, in the DPC approach the transmitter will instead use a codeword for user k in the direction of S_k. The capacity is then as if the interference were not present.

The name "Dirty Paper Coding" comes from the analogy made by Costa between sending message X_k and the situation of writing a message on a sheet of paper covered with independent dirt spots of normally distributed intensity.

Although the sum-capacity of MIMO Gaussian Broadcast Channels is achieved with DPC, this scheme however is very complicated to implement. Several works on non-linear and linear sub-optimal algorithms approaching DPC performances are proposed [72, 73, 74]. An alternative linear precoding technique called Block Diagonalization was also proposed [75]-[79]. In [48], authors proposed a suboptimal DPC strategy referred to as Zero Forcing Dirty Paper Coding (ZF-DPC) for Gaussian broadcast channel with single antenna receivers.

4.3.2 Zero Forcing Dirty Paper Coding

The scheme proposed in [48] applies for a number of users $K > 2$. For an ordered subset of users $\mathcal{K}$ let $\underline{\mathbf{G}}_{\mathcal{K}} \in \mathbb{C}^{|\mathcal{K}| \times N_t}$ be the corresponding channel matrix and let $\underline{\mathbf{G}}_{\mathcal{K}} = \underline{\mathbf{D}}\underline{\mathbf{Q}}$ be its QR decomposition using the Gram-Schmidt orthogonalization in the order given in $\mathcal{K}$. If $r = \text{rank}(\underline{\mathbf{G}}_{\mathcal{K}})$, then $\underline{\mathbf{D}} \in \mathbb{C}^{|\mathcal{K}| \times r}$ is a lower triangular matrix and $\underline{\mathbf{Q}} \in \mathbb{C}^{r \times N_t}$ has orthonormal rows. The matrix $\underline{\mathbf{Q}}^H$ is then used as precoding matrix. It was shown in [48] that the resulting sum rate is given by

$$R^{\text{ZF-DPC}} = \sum_{i=1}^{r} \log(\xi |D_i|^2) \tag{4.10}$$

where D_i is the i-th element of the diagonal of $\underline{\mathbf{D}}$ and ξ is the solution of the water filling

$$\sum_{i=1}^{r} \left[\xi - 1/|D_i|^2 \right]^+ = P \tag{4.11}$$

The maximum sum rate is then

$$R_{\text{max}}^{\text{ZF-DPC}} = \max_{\mathcal{K}} R^{\text{ZF-DPC}} \tag{4.12}$$

where the maximization is made over the ordered user sets with cardinality r. For the composite channel we have $\overline{R}_{\text{max}}^{\text{ZF-DPC}} = \mathbb{E}\left[R_{\text{max}}^{\text{ZF-DPC}}\right]$, where ξ is solution to the the short term constraint on (4.11) or the long term constraint $\mathbb{E}\left[\sum_{i=1}^{r} \left[\xi - 1/|D_i|^2\right]^+\right] = P$.

The maximization over all ordered subsets is complicated to perform especially for a large number of users. In [52, 80], authors propose a greedy algorithm for users scheduling. It consists of allocating at each iteration the user with the highest 2-norm projection on the complement space of the user already allocated. In the following, we review the pseudo code of this algorithm.

Algorithm 6 Greedy ZF-DPC algorithm description

- Step 1: Initialization

$$\mathcal{K}^* = \emptyset$$

- Step 2:

For $n = 1$ to $\min(N_t, K)$

$\gamma_k = \|\mathbf{G}_k \perp (\underline{\mathbf{G}}_{\mathcal{K}^*})\|^2, \quad k \in \{1, ..., K\} \backslash \mathcal{K}^*$

$l = \arg \max_k \gamma_k$

$\mathcal{K}^* = \mathcal{K}^* \cup \{l\}$

end

$\perp(\underline{\mathbf{X}})$ is the orthogonal projector onto the orthogonal complement of the subspace spanned by the rows of matrix $\underline{\mathbf{X}}$. This algorithm will be used in our numerical evaluation of DPC performance.

DPC combined with opportunistic scheduling (selection over the user ordered sets (4.12)) is surely the optimal way to maximize the broadcast channel ergodic capacity. But, as all strategies fully based on opportunistic scheduling, this approach is totally unfair. Motivated by the results in the previous chapter and in [19], we propose, in the following, different strategies attempting to maximize the fairness between users and evaluate the loss due to these hard fairness constraints in terms of spectral efficiency. We show that hard fairness does not necessarily introduce a high loss in system throughput.

4.4   Spatial Multiplexing Max-Min Allocation (SM-Max-Min)

The idea of SM is very simple: N_t independent data streams are transmitted in parallel at the same time from the N_t transmit antennas. In multiuser environments, each stream can be intended for a different user. This technique is then called Space Division Multiple Access (SDMA). If antenna n_t^* is assigned to user k on channel m, then its received signal on this channel can be written as

$$Y_{k,m} = \underbrace{\sqrt{\frac{P}{N_t}}G_{k,m}^1[n_t^*]X^1[n_t^*]}_{\text{Desired Signal}} + \underbrace{\sum_{n_t \neq n_t^*}^{N_t}\sqrt{\frac{P}{N_t}}G_{k,m}^1[n_t]X^1[n_t]}_{\text{Intra-cell Interference}}$$

$$+ \underbrace{\sum_{c=2}^{C}\sum_{n_t'=1}^{N_t}\sqrt{\frac{P}{N_t}}G_{k,m}^c[n_t']X^c[n_t']}_{\text{Inter-cell Interference}} + Z_{k,m} \qquad (4.13)$$

We assume that each antenna transmits with power $\frac{P}{N_t}$ in each channel, thus the total transmitted power on one channel is P. The corresponding SINR value is given by

$$\gamma_k(m, n_t) = \frac{\frac{P}{N_t}|G_{k,m}^1[n_t^*]|^2}{N_0 + \sum_{n_t \neq n_t^*}^{N_t}\frac{P}{N_t}|G_{k,m}^1[n_t]|^2 + \sum_{c=2}^{C}\sum_{n_t'=1}^{N_t}\frac{P}{N_t}|G_{k,m}^c[n_t']|^2} \qquad (4.14)$$

Each user k is assigned one channel and one antenna from which it receives its signal. We can thus accommodate up to $K = N_t.M$ users and the allocation consists of the assignment of both channel and antennas to users. Under this configuration the system can be represented by a bipartite graph as in figure 4.1 where the right hand side vertices represent the tuples (antenna, channel) to be assigned and the left hand side represents the users. The edge between vertex k and vertex (n_t, m) is weighted by the SINR achieved by user k on channel m from antenna n_t given by (4.14). Once the system corresponding graph is constructed, we use the algorithm proposed in the previous chapter, section 3.6.2, for resource allocation. This strategy guarantees that the minimum allocated SINR is the best possible among all possible allocations and thus maximizes the minimum allocated rate.

$$\pi^* = \arg\max_{\pi \in \Pi} \min_{k=0,\ldots,K-1} \gamma_k^\pi \qquad (4.15)$$

(sub-channel, antenna)   Users
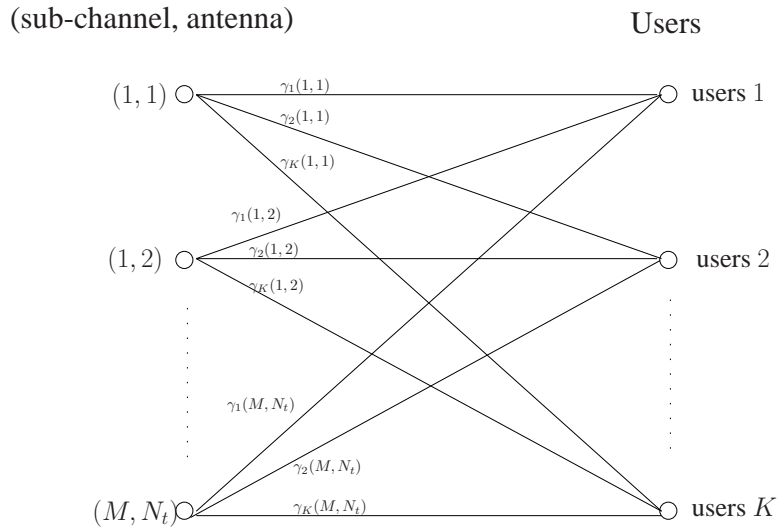
Figure 4.1: Graph representation of Spatial Multiplexing System

where Π is the set of all possible permutations and γ_k^π is the SINR of user k when the allocation according to the permutation π is performed. Permutations now concern the tuples (antenna, channel). For Gaussian signals, the achievable sum rate is given by

$$\sum_{k=1}^{K} R_k = E \left\{ \sum_{k=1}^{K} \log_2 \left(1 + \gamma_k \left(n_t^*, m^* \right) \right) \right\} \quad \text{(bits/dim)} \qquad (4.16)$$

where n_t^* and m^* are respectively, the antenna and channel assigned to user k.

4.5 Space Time Coding Max-Min allocation (STC-Max-Min)

The basic idea of STC is that the same information is transmitted on all the antenna elements, but is multiplexed in a different way on each antenna. The design of transmit diversity depends on whether or not channel gains are available at the transmitter. In the absence of this information, transmit diversity gain requires a combination of space and time diversity via a technique called the Alamouti coding [41].

When the channel gains are known to the transmitter, the same signal is transmitted from

all antennas after being multiplied by an appropriate weight vector. Only one user can be scheduled in each channel and the allocation now only concerns channels. As for spatial multiplexing case, we assume that each antenna transmits with power $\frac{P}{N_t}$. In order to be able to schedule the same number of users as in the previous scheme and thus insure a fair comparison of the two strategies, we assume that the bandwidth W of each channel is divided to N_t adjacent but disjoint sub-channels each one of a bandwidth $W' = \frac{W}{N_t}$ (i.e. FDMA in each channel) called here sub-bands to differentiate them from the original sub-channels of bandwidth W. The system now contains $N_t.M$ sub-bands. A user k experiences the same channel gain in the N_t sub-bands of the same sub-channel.

In such a configuration, the only interference is the one coming from other cells. Under the assumption that sub-band m is assigned to user k, the user's received signal is

$$Y_{k,m} = \underbrace{\sqrt{\frac{P}{N_t}}\mathbf{G}_{k,m}^1\mathbf{w}_m^1 X_m^1}_{\text{Desired Signal}} + \underbrace{\sum_{c=2}^{C}\sqrt{\frac{P}{N_t}}\mathbf{G}_{k,m}^c\mathbf{w}_m^c X_m^c}_{\text{Inter-cell Interference}} + Z_{k,m}$$

where $\mathbf{w}_m^c$ is the weight vector of dimension $N_t \times 1$ in cell c on sub-band m. The weight vector $\mathbf{w}_m^c$ must be chosen such that $\|\mathbf{w}_m^c\| = N_t$, so that the total transmit power in each sub-channel is P.

In the single receive antenna case the weight vector maximizing the SNR is given by [81]

$$\mathbf{w}_m^1 = \frac{\mathbf{G}_{k,m}^1}{\sqrt{\left\|\mathbf{G}_{k,m}^1\right\|^2}}$$

which requires the knowledge of channel gain phases. Keeping in view our objective of proposing simple schemes based only on the channel gain amplitudes, we simply choose

$$\mathbf{w}_m^1 = \begin{bmatrix} 1 \\ 1 \\ \vdots \\ 1 \end{bmatrix} \tag{4.17}$$

The SINR value for user k on sub-band m is given by

$$\gamma_{k,m} = \frac{\frac{P}{N_t}\left\|\mathbf{G}_{k,m}^1\right\|^2}{N_0 + \sum_{c=2}^{C}\frac{P}{N_t}\left\|\mathbf{G}_{k,m}^c\right\|^2} \tag{4.18}$$

Users   Sub-bands
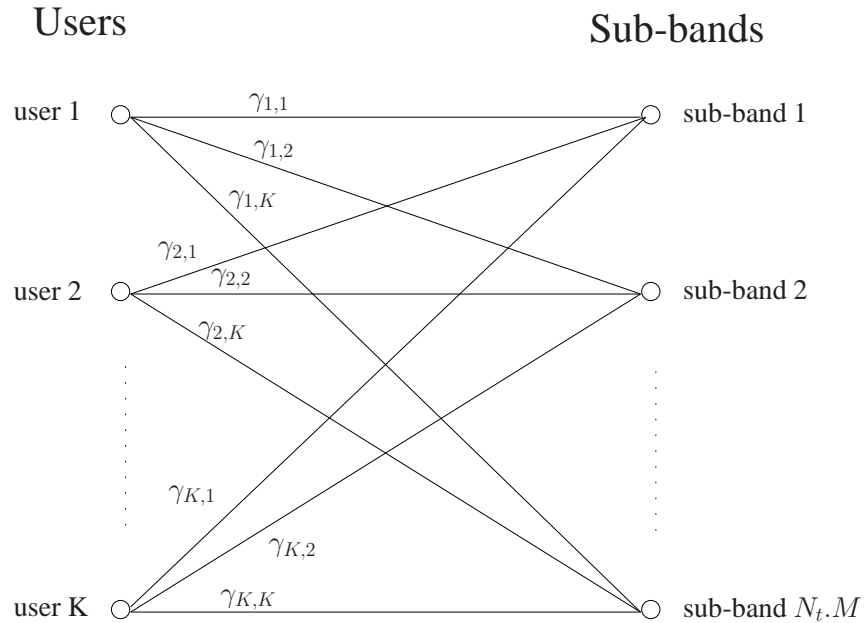
Figure 4.2: Graph representation of Space Time Coding System

This system can be represented by a bipartite graph as in figure 4.2. The right hand side of the graph represent sub-bands since no antenna selection is needed here. The weight of the edge (k, m) is set to be the SINR values $\gamma_{k,m}$. Again the algorithm in section 3.6.2 in chapter 3 is used for the allocation of sub-bands. The sum rate of this system is

$$\sum_{k=1}^{K} R_k = \mathbb{E}\left\{\sum_{k=1}^{K} \log_2\left(1 + \gamma_{k,m^*}\right)\right\} \quad \text{(bits/dim)} \tag{4.19}$$

where m^* is the sub-band assigned to user k.

4.6   Delay Limited Rate Allocation (DLR)

Here we consider the problem of channel and power allocation for the spatial multiplexing scheme where users must achieve a target rate vector independently of the channel state (delay limited rates), while minimizing the transmit power. The optimal solution is very difficult to derive and we proceed in two steps. We first assign to each user an antenna

and a sub-channel assuming equal power. We then allocate accordingly the power to achieve the desired rates. We believe that allocating resources according to the MS-Max-Min strategy described in section 4.4 tends to schedule in each sub-channel the set of users the *most orthogonal* compared to other scheduling strategies. Using this strategy for user scheduling will help minimize the power needed to meet the SINR requirement. Once each user is allocated one sub-channel and one antenna, the allocation problem is as considered in [22, 23]. The characterization of the optimal power solution (for single channel case) was first given in [22] and in the following, we review this result.

Let us consider the power allocation for the set of users scheduled in a sub-channel m. For notation simplicity let us in the remainder of this section neglect the sub-channel index. We denote $\{k_i\}_{i=1...N_t}$ the set of scheduled users on the considered channel, where k_i is the user allocated to antenna i. The SINR of user k_i can then be written as

$$SINR_{k_i} = \frac{P_{k_i}|G_{k_i}[i]|^2}{N_0 + \sum_{j\neq k} P_{k_j}|G_{k_i}[j]|^2} \tag{4.20}$$

If $\gamma_{k_i}^*$ denotes the SINR target, the rate constraint can be expressed as

$$P_{k_i} = \sum_{j\neq i} P_{k_j} \frac{|G_{k_i}[j]|^2}{|G_{k_i}[i]|^2} \gamma_{k_i}^* + \frac{N_0 \gamma_{k_i}^*}{|G_{k_i}[i]|^2} \tag{4.21}$$

If we consider $\underline{\mathbf{A}}$ the $N_t \times N_t$ matrix given by

$$A_i^j \equiv \begin{cases} 0 & j = i \\ \frac{|G_{k_i}[j]|^2}{|G_{k_i}[i]|^2} \gamma_{k_i}^* & j \neq i \end{cases} \tag{4.22}$$

and $\mathbf{B}$ the $N_t \times 1$ vector such that

$$B_i = \frac{N_0}{|G_{k_i}[i]|^2} \gamma_{k_i}^* \tag{4.23}$$

then equation (4.21) can written as

$$(\underline{\mathbf{I}} - \underline{\mathbf{A}})\,\mathbf{P} = \mathbf{B} \tag{4.24}$$

We conclude from this equation that a power allocation achieves the rate target if and only if equation (4.24) admits a positive solution in $\mathbf{P}$. $\underline{\mathbf{A}}$ is a nonnegative, primitive matrix, so that Perron-Frobenius theory guarantees the existence of a dominant, positive eigenvalue r. The following result is very well known in Perron-Frobenius theory, and enables us to characterize the existence of a solution to our problem by a constraint on the eigenvalue r.

Theorem 9 *[22] The carrier to interference equation (4.24) has a positive solution if and only if $r < 1$. If $r < 1$ then there is a unique solution P given by*

$$P = (\underline{\mathbf{I}} - \underline{\mathbf{A}})^{-1} \, \mathbf{B} \tag{4.25}$$

The existence of a solution to the power allocation depends not only on the rate target value but also on the antenna allocation and the corresponding channel gains. From where the interest on choosing an adequate antenna and channel allocation at the first step.

4.7 Single-Cell Systems

Let us first focus on single-cell systems ($\mathcal{C} = 1$) and consider symmetric users (i.e. We also neglect for the moment the large scale fading and only consider the fast variations of the channel). Thus $G_{k,m}[n_t] = H_{k,m}[n_t]$ for all k,m and n_t.

Figures 4.3 and 4.4 show the spectral efficiency as a function of the number of sub-channels M for different scheduling schemes with 4 and 2 transmit antennas respectively. Opportunistic beamforming scheme presented in [53] is also given for comparison. We have assumed for these figures that the correlation between frequency channel gains is zero. This gives an idea of the achievable rates as a function of the approximate number of degrees of freedom of the propagation environment in the available system bandwidth. We first note how all schemes profit from the multiuser diversity even for those with hard fairness constraints. The gap between the ZF-DPC scheme performance and those with fair allocations is considerable but this gap decreases with increasing number of sub-channels. The performance degradation is relatively small for $N_t = 2$. Our proposed system has the advantage of simplicity and there is no need for channel gain phase estimates at the transmitter. Also, we not that the proposed SM schemes perform almost as well as opportunistic beamforming for small to moderate number of sub-channels.

 Figure 4.5 presents the spectral efficiency as a function of the number of sub-channels for both SM-Max-Min and STC-Max-Min system with 1, 2 and 4 antennas at the transmitter and single receive antenna. We notice that SM-Max-Min transmission spectral efficiency is much higher than with STC-Max-Min transmission. This is due to the "opportunistic" spatial-multiplexing offered by multiuser-diversity as described in [21, 53].
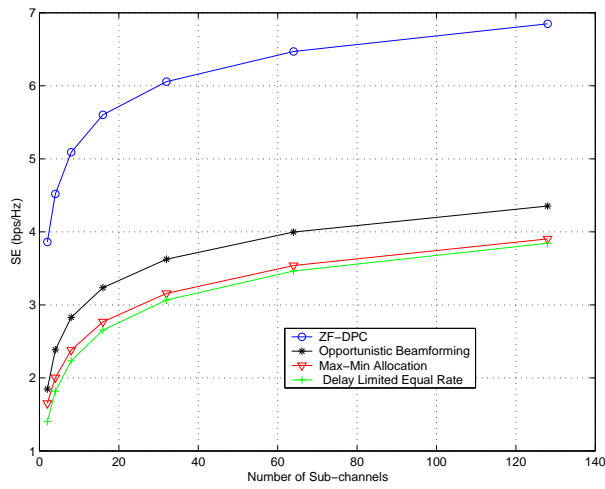
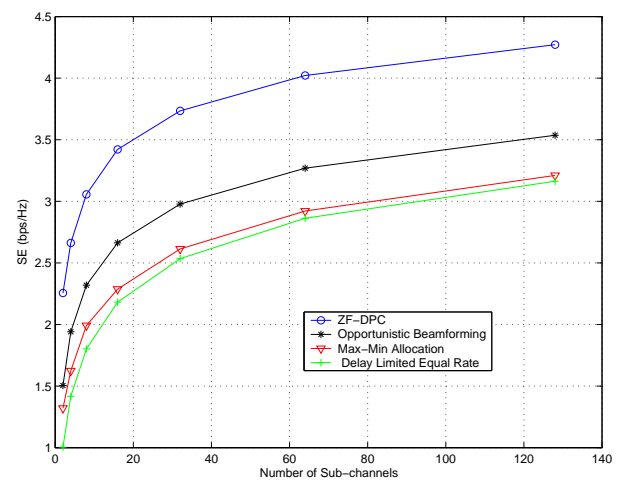Figure 4.3: Scheduling Schemes SE as a function of M for $N_t = 4$, SNR=0dB, $K = M \times N_t$

Figure 4.4: Scheduling Schemes SE as a function of M for $N_t = 2$, SNR=0dB, $K = M \times N_t$

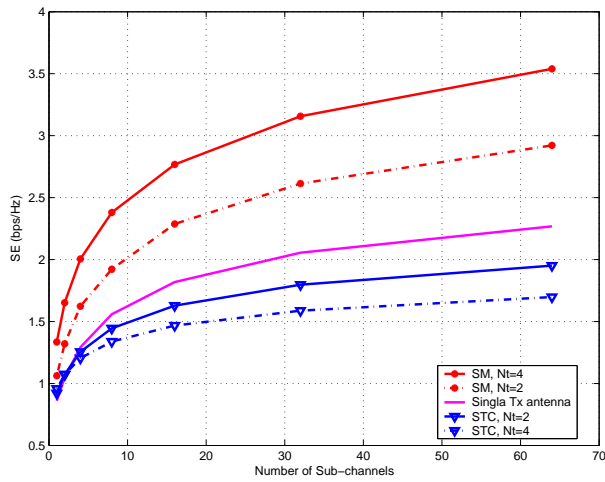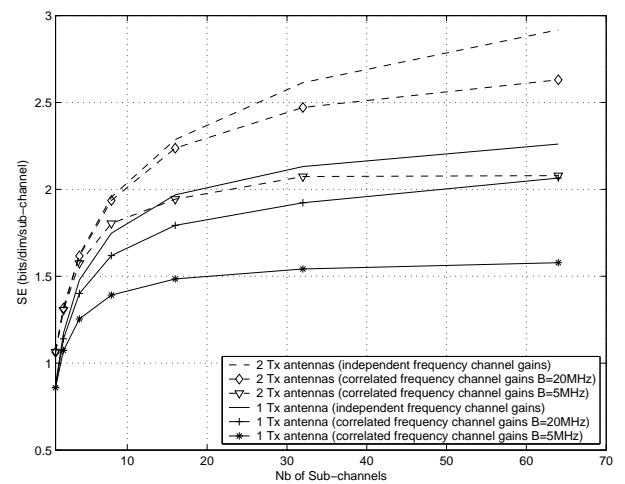Figure 4.5: SM and STC Spectral Efficiency as a function of M for different values of N_t, SNR=0dB

Figure 4.6: SM System SE for different bandwidth values for $N_t = 1, 2$, SNR=0dB

Another interesting remark is that the throughput increases with number of antennas in SM-Max-Min but decreases in STC-Max-Min which is the consequence of the reduction of channel variations due to antenna diversity (i.e. the benefits of multiuser diversity are reduced when less channel variation is present). This is known as channel hardening. Figure 4.6 plots the spectral efficiency of SM-Max-Min system on a frequency selective channel with correlated frequency channel gains for different values of the system bandwidth and with 1 and 2 transmitting antennas. We assume a maximum path delay $\tau_{max} = 2\mu s$ and an exponentially-decaying multi-path intensity profile. For a given number of sub-channels, augmenting the system bandwidth results on the increase of the sub-channels' spacing and thus diminishes the correlation between them. Channels spacing plays an important role on how much scheduling users on sub-channels can increase spectral efficiency. We note that the benefit from using multiple transmit antennas can be limited by the correlation between sub-channels. For example, for a large number of sub-channels, a single antenna 20MHz system can outperform a double antenna 5MHz system.

Multiple antennas at the receiver

In order to enhance the system performance, receive diversity can be used. Two or more antennas are placed at the receiver. The received signal is the vector given by

$$\mathbf{Y}_{k,m} = \mathbf{G}_{k,m}[n_t^*]X[n_t^*] + \sum_{n_t \neq n_t^*} \mathbf{G}_{k,m}[n_t]X[n_t] + \mathbf{Z}_{k,m} \tag{4.26}$$

where $\mathbf{G}_{k,m}[n_t]$ is the channel vector gain on channel m, from n_t-th transmit antenna to the receiving antennas of user k. $\mathbf{Z}_{k,m}$ is the Gaussian noise vector. The output of the antennas are combined to retrieve the transmitted signal. Let this weighted sum be

$$Y' = \mathbf{q}\mathbf{Y}_{k,m} \tag{4.27}$$

where $\mathbf{q}$ is a weight vector performing spatial combining. The SINR corresponding to the signal received by user k from antenna n_t^* on sub-channel m is [34]

$$\gamma_k(m, n_t^*) = \frac{\frac{P}{L} \cdot |\mathbf{q}\mathbf{G}_{k,m}[n_t^*]|^2}{\mathbf{q}\left(\sum_{n_t \neq n_t^*} \frac{P}{L}\mathbf{G}_{k,m}[n_t] \left(\mathbf{G}_{k,m}[n_t]\right)^H + N_0.\mathbf{I}\right)\mathbf{q}^H}$$

In the case of simple detection, the expression of $\mathbf{q}$ for MRC is given by $\mathbf{q} = \mathbf{G}_{k,m}[n_t^*]$. For MMSE, the filter for the detection of $X_{n_t^*}$ is given by

$$\mathbf{q} = \left(\frac{\sqrt{P/L}}{\mu_k}\Sigma_k^{-1}\mathbf{G}_{k,m}[n_t^*]\right)^H$$
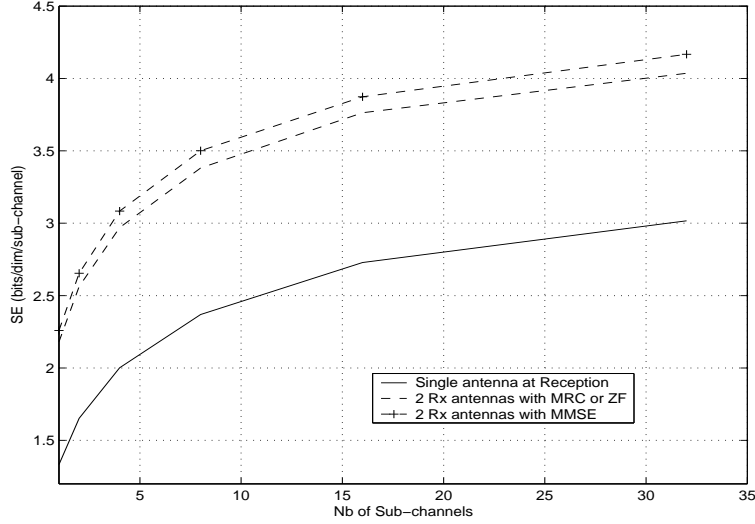
Figure 4.7: Reception techniques comparison with Max-Min allocation algorithm (4 Tx antennas, SNR=0dB, correlated frequency channel gains).

where: $\boldsymbol{\Sigma}_k^{-1} = N_0\mathbf{I} + \frac{P}{L}\sum_{n_t \neq n_t^*} \mathbf{G}_{k,m}[n_t]\left(\mathbf{G}_{k,m}[n_t]\right)^H$

and $\mu_k = \frac{P}{L}\left(\mathbf{G}_{k,m}[n_t^*]\right)^H \boldsymbol{\Sigma}_k^{-1}\mathbf{G}_{k,m}[n_t^*]$

The filter in the MMSE receiver requires the estimation of the channel gains from interfering antennas and takes advantage of this to mitigate interference.

Figure 4.7 shows the system spectral efficiency for the SM-Max-Min transmission scheme with different receivers (MMSE and MRC). We consider a system with 4 transmitting antennas at the base station and each receiver has $N_r = 2$ antennas. We assume again a frequency-selective channel with correlated frequency channel gains resulting from a maximum path delay $\tau_{max} = 2\mu s$ and an exponentially-decaying multi-path intensity profile. The system bandwidth is assumed equal to $B = 20$MHz. This figure highlights the spectral efficiency gain that can be obtained by using multiple antennas at the reception. Both schemes offer a high spectral efficiency compared to single receive antenna. Also, as expected, MMSE receiver takes advantage from the knowledge of the interferer channel gains and yields slightly better performance than MRC.

4.8 Distributed antenna multi-cellular systems: Macro-Diversity

We now consider the general case of a multi-cellular system ($C > 1$) and large scale fading effect. We assume that cells have a square shape of side distance equal to R and we only consider the first tier of eight interfering cells. Each receiver is equipped with a single antenna. In the following, we present and compare different cellular architectures depending on the placement of the transmit antennas on the cell.

4.8.1 Distributed Antenna (DAS) cellular Architecture

One interesting MIMO antenna configuration is the Distributed Antenna systems aiming for a spectral reuse 1 (i.e. all cells overlap in frequency). It is one way of increasing system capacity and benefit from the so-called "*Macro-diversity*". This is a generalization of the concept of "soft-handover" techniques employed in current 3G networks. Distributed antenna systems was first introduced to solve the problem of coverage for indoor wireless communications (also known as dead spots problem). More recent studies show that distributed antennas can bring significant power saving and a considerable increase of system capacity. The basic idea is that multiple antennas sufficiently separated in space can provide independent shadowing which is also known as Macro-Diversity. The distributed antennas within a cell are connected to a *Central Controller* (Evolution of Radio-Network Controller in UMTS) (Figure 4.8.1). Thus the system can be regarded as a macroscopic multiple antenna array. The shortened distance between users and antennas offer a considerable increase in system performance [57, 58]. Recently distributed antennas systems have received attention due to their capacity advantages. However most of the studies consider either single user case or the uplink transmissions ([59]-[62]) and only few papers have treated the multiuser downlink. Authors in [64, 65] analyze the downlink capacity in terms of multiple-antenna (MIMO) but they only consider a single-cell environment. Authors in [66] study MIMO system capacity of multi-cell with distributed antennas for the single user case. Here we consider the downlink of a multiuser multi-cell system and we study the system spectral efficiency, as well as fairness between users.
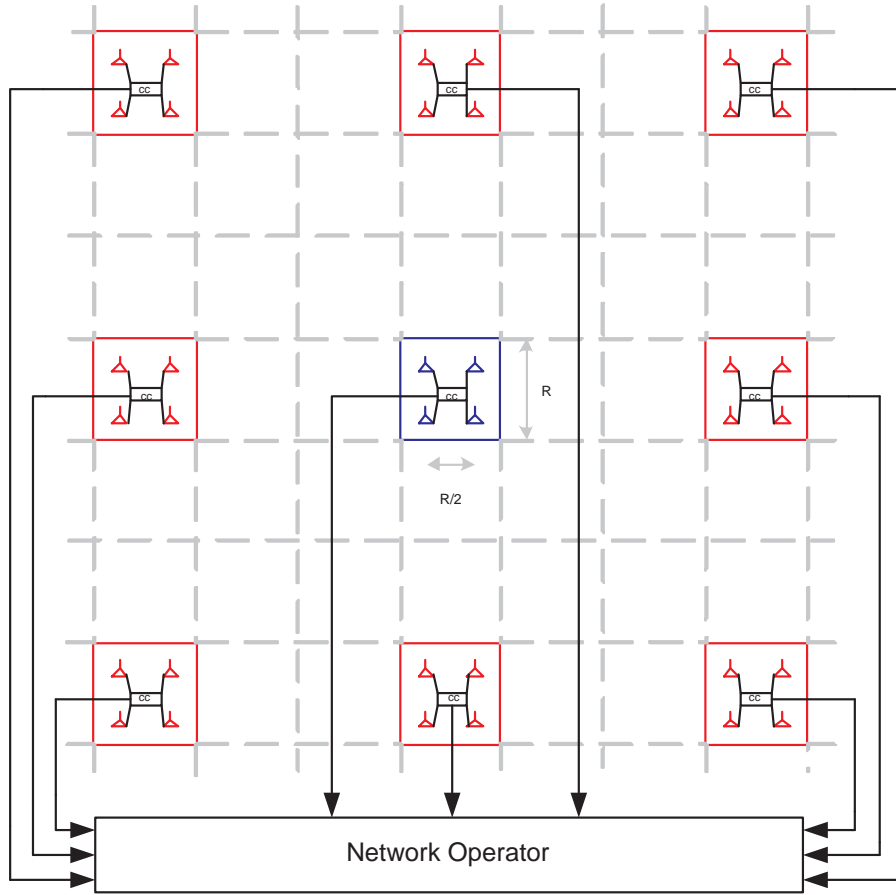
Figure 4.8: Example of Distributed Antenna Multi-Cell system for $N_t = 4$ and frequency reuse factor $F = 9$

Two variants in system architecture are possible. In the first one, the Digital Signal Processing (DSP) of signals is located at the central controller. This architecture requires the deployment of high speed links to carry raw sample data from the central controller to the transmit antennas using for example radio over fiber (RoF) technology which results in a very high deployment cost. The advantage of such an architecture is the possibility to perform distributed antennas cooperative SDMA: ZF-DPC, precoding, beamforming, ...etc, where phase information is required. The controller must also insure the synchronization of the different antennas in this case. In the second variant, the DSP is physically close to the transmit antenna side as in a modern base station. The advantage of this architecture is the lower cost compared to the previous one since moderate rate link can be deployed to carry the data from the central controller to the transmit antenna using, for instance,

WiMax technology, dedicated RF links or a wired link (Ethernet or other). The drawback of this technology is that no precoding or beamforming is possible. An other delicate issue concerns the coding of data. This arises in the case where data symbols for the same user have to be transmitted in different parts of the spectrum, from different antennas and have to be coded jointly. In this case, the FEC must be performed in a distributed manner. In both architectures, the central controller is responsible of resource allocation. We can also consider the case where central controllers of the different cells cooperate throughout the operator network.

We assume that the antennas are located in a $\sqrt{N_t} \times \sqrt{N_t}$ square grid and are equally spaced as in [57]. N_t is assumed to be a perfect square and the distance between to successive antennas is $\frac{R}{\sqrt{N_t}}$. An example of such a system is given by figures 4.8.1 for frequency reuse factor $F = 9$.We consider the use of SM-Max-Min as transmission strategy. The received signal is then given by equation (4.28).

4.8.2   Co-located Antenna systems (CAS) cellular Architecture

We assume that the N_t antennas are located in the center of the cell (figures 4.8.1). A user experiences the same large scale fading gain from all transmit antennas of the same cell. The channel vector can be simplified to

$$\mathbf{G}_{k,m}^c = \sqrt{L_k^c} \left[H_{k,m}^c [1], ..., H_{k,m}^c [N_t] \right]^T$$

where the antenna index is dropped from L_k^c

Since transmit antennas are co-located we can use either SM or STC - Max-Min based transmission. For these transmission schemes, the received signal is given respectively by

$$\mathbf{Y}_{k,m} = \underbrace{\sqrt{\frac{PL_k^1}{N_t}} H_{k,m}^1[n_t^*]X^1[n_t^*]}_{\text{Desired Signal}} + \underbrace{\sum_{n_t \neq n_t^*}^{N_t} \sqrt{\frac{PL_k^1}{N_t}} H_{k,m}^1[n_t]X^1[i]}_{\text{Intra-cell Interference}} + \underbrace{\sum_{c=2}^{C} \sum_{n_t'=1}^{N_t} \sqrt{\frac{PL_k^c}{N_t}} H_{k,m}^c[n_t']X^c[n_t']}_{\text{Inter-cell Interference}} + Z_{k,m} \quad (4.28)$$

and

$$\mathbf{Y}_{k,m} = \underbrace{\sqrt{\frac{PL_k^1}{N_t}} \mathbf{H}_{k,m}^1 X_m^1}_{\text{Desired Signal}} + \underbrace{\sum_{c=2}^{C} \sqrt{\frac{PL_k^c}{N_t}} \mathbf{H}_{k,m}^c X_m^c}_{\text{Inter-cell Interference}} + Z_{k,m}$$
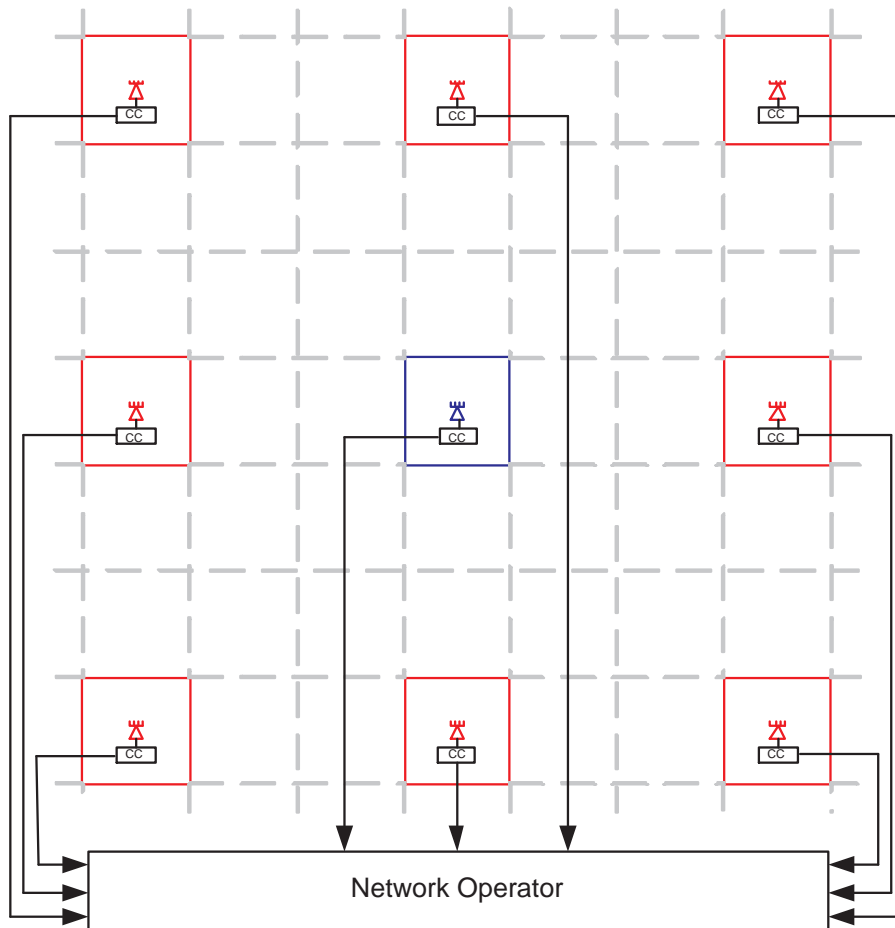
Figure 4.9: Example of Co-located Antenna Multi-Cell system for $N_t = 4$ and frequency reuse factor $F = 9$

4.8.3 Numerical Results

For all simulations we assume independent Rayleigh fading channel gains.The Shadow fading for each user is modeled as an independent log-normal random variable with standard deviation $\sigma_s = 10dB$ and the path-loss exponent α is set to 3. The considered value of P is such that a user located in the corner of the cell experiences an average SNR equal to 0dB from an antenna located at the center of the cell. We consider $K = M.N_t$ which is the maximum number of users that can be supported by the system. We consider cells of side distance $R = 100m$ and the reference distance d_0 is equal to 1m. All users are at a distance greater then d_0 from all antennas.

We first consider the case of no cooperation between central controllers of different cells. Figures 4.10 and 4.11 represent the spectral efficiency, of the three transmission schemes presented previously, as a function of the number of channels, for frequency reuse factors $F = 1$ and $F = 9$ respectively. It worth reminding that the spectral efficiency is dominated by the rates of close-in users (users close to an antenna), thus these figures can be seen as a representation of performance of this class of users. These figures confirm that distributed antennas offers a considerable gain on system performance and this even under hard fairness constraints. One other remarkable result to outline is that the system spectral efficiency decreases with the frequency reuse factor F and a system with factor $F = 1$ outperforms a system with factor $F = 9$ even if in the former, the cell of interest experiences less interferences from other cells.

Figures 4.12 and 4.13 represent the minimum allocated rate as a function of the number of sub-channels M. The minimum rate represents the performance of far-out users (extreme users). This figure shows the remarkable enhancement that distributed antennas offers on terms of fairness compared to both SM and STC in co-located antenna systems. The minimum allocated rate increases with the number of channels when distributed antennas are used whereas it converges to zeros in the case of co-located antennas. The attenuation due to path loss is very large for a far-out user which results in a small combined channel gain. In the case of collocated antennas and because of the shadowing frequency independence, far out user loose most of the diversity. In case of distributed antennas, a user in the cell corner benefits from both shortening of the distance to the nearest antennas and macro-diversity.

Figures 4.14 and 4.15 plot the spectral efficiency of cellular systems when central controllers of different cells cooperate for $F = 1$ and $F = 9$ respectively. The cooperation between the controllers induces only a slight change in system spectral efficiency, but the enhancement of the minimum allocated rate is considerable. Figure 4.16 shows this minimum allocated rate for the different schemes. In co-located antenna systems, the minimum allocated rate recovers advantage of multiuser diversity thanks to macro-diversity introduced by the cooperation between central controllers.
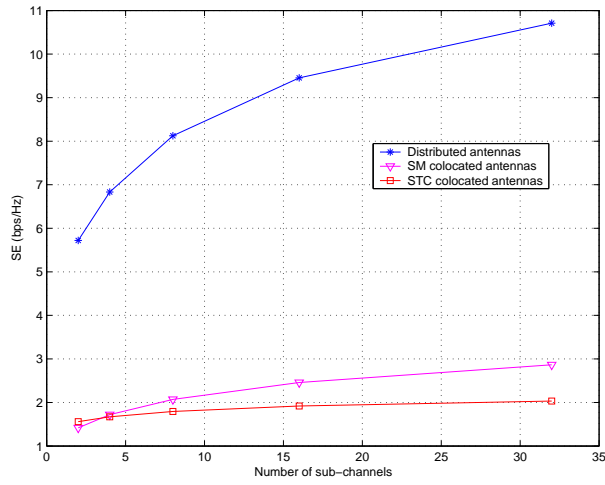
Figure 4.10: Spectral Efficiency (SE) as a function of M, for $F = 1$
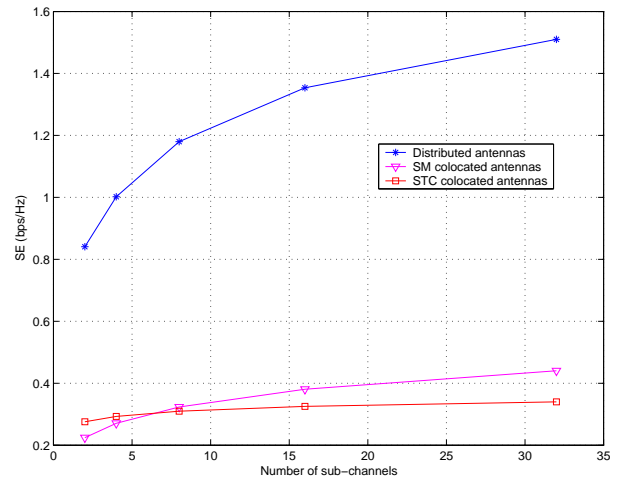
Figure 4.11: Spectral Efficiency (SE) as a function of M, for $F = 9$
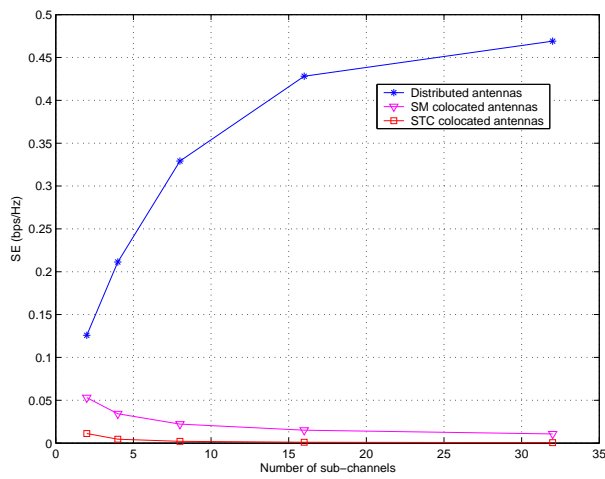
Figure 4.12: Minimum allocated rate as a function of M, for $F = 1$
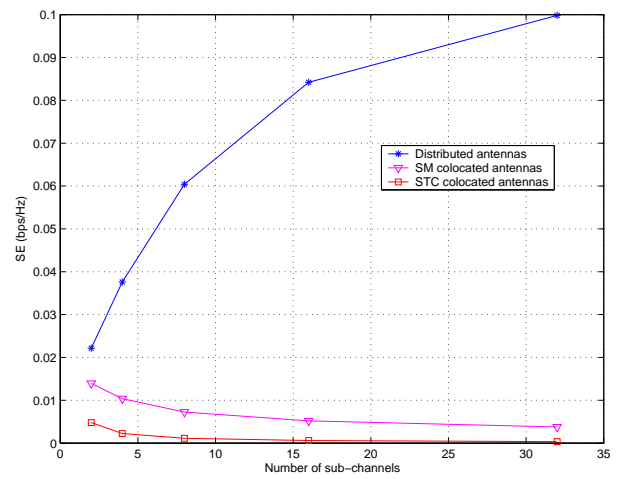
Figure 4.13: Minimum allocated rate as a function of M, for $F = 9$
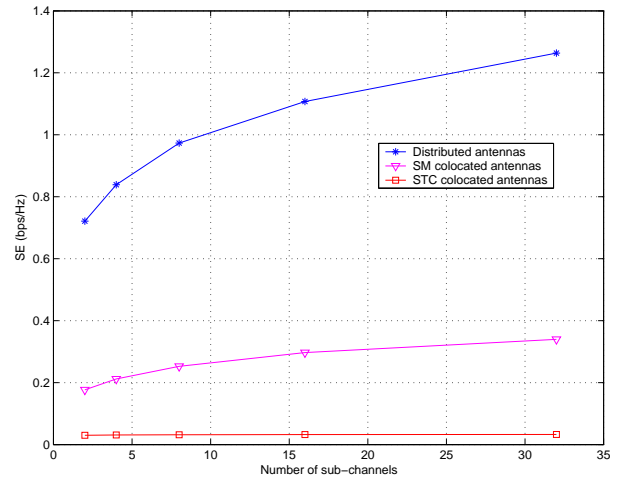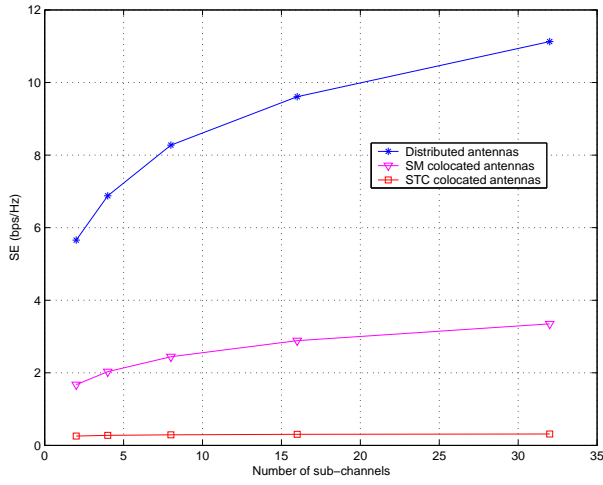
Figure 4.14: SE with Central Controllers coop-eration for $F = 1$.

Figure 4.15: SE with Central Controllers coop-eration for $F = 9$.
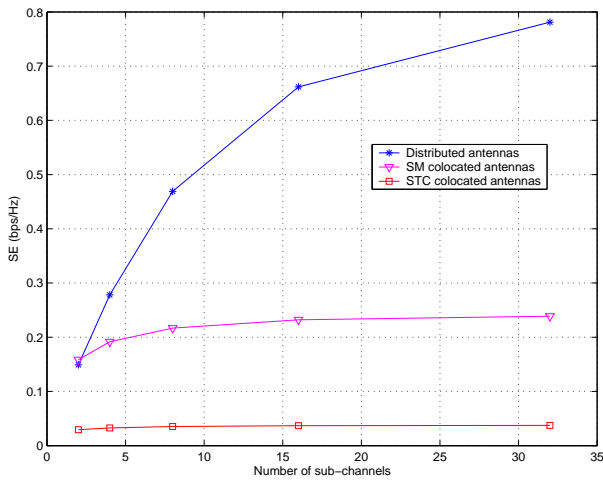
Figure 4.16: Minimum allocated rate with Central Controllers cooperation for $F = 1$.

4.9   Conclusion

In this chapter, we considered the impact of using multiple antennas on both system spectral efficiency and fairness between users for different MIMO transmission schemes. We presented different simple transmission strategies guaranteeing hard fairness by achieving a target rate or maximizing the minimum allocated SINR. This work highlights the importance of MIMO systems not only on spectral efficiency enhancement but also on increasing the fairness between users measured in terms of the minimum allocated rate. Numerical results for single cell symmetric users scenario confirms the results in the previous chapter. Hard fairness results on only a limited throughput degradation. We also show the considerable improvement in system performance when using distributed antennas compared to collocated antennas on multi-cell systems.

Chapter 5

Feedback Reduction and Power Control in Downlink MIMO-OFDMA Systems

5.1 Introduction

Current and future wireless communication systems are expected to provide a broad range of multimedia services with different delay and QoS requirements. The use of multiple antennas at both transmitter and receiver provides enhanced performance in terms of diversity and data rate without increasing the transmit power or bandwidth. A great deal of research work has been devoted to the area of combining this spatial scheme with Orthogonal Frequency Division Multiplexing (OFDM) systems. Such systems combine the advantages of both techniques, providing simultaneously increased data rate and robustness against channel delay spread.

In multiuser MIMO systems, one way to exploit the multiuser diversity gain is through opportunistic scheduling [21]. In [53], authors propose a partial feedback scheme exploiting opportunistic multiuser beamforming as a SDMA extension of the opportunistic beamforming initially introduced in [21]. Previous work on opportunistic scheduling has been mainly focused on frequency-flat fading channels. However, in an OFDMA network, only few works have utilized opportunistic schemes to enhance the system throughput. One of the major problems in employing a downlink opportunistic scheduling is the need of

accurate channel knowledge for all users at the transmitter. For MIMO-OFDMA based systems, due to the large number of sub-carriers (e.g. up to 2048 for WiMax), having accurate channel state information at the transmitter (CSIT) becomes a challenging task. Feeding back full channel state is prohibitive. Several works treated this problem. In [88, 89], a simple threshold based scheme is proposed for narrow band systems. Only users with channel gain exceeding a predefined threshold are allowed to feedback their channel quality indicator. This scheme is showed to considerably reduces the feedback load while preserving the essential of multiuser diversity gain offered by the system. In [84] authors consider the feedback reduction for MIMO-OFDMA using opportunistic beamforming based on the scheme in [21] (There is no spatial multiplexing. Only a single user is scheduled in each sub-carrier). The proposed strategy uses sub-carrier grouping (L neighboring sub-carrier are grouped on one cluster) and information on the strongest clusters is fed back to the base station. Comparison between clusters is based on the average SNR and this value with the selected clusters are fed-back to the base station. In [85], the SDMA variant of opportunistic MIMO-OFDMA is studied. The proposed scheme is also based in sub-carrier grouping. Each user feeds-back the best SINR of the central carrier of each cluster. The proposed schemes in [85, 84] could be efficient when the carriers grouping results on clusters of the order of channel coherence bandwidth. For larger grouping, these schemes may experience some limitations. The average SNR or the SINR at the central carrier are not efficient indicators on the channel quality due to large channel variations within the same group. Also using these quantities as indicators causes high outage on carriers with channel quality below the fed-back values.

In this chapter, we consider SDMA opportunistic beamforming OFDMA. The objective of our work is to propose practical feedback reduction schemes that are more efficient than the obvious extension of the narrowband strategies. In essence, our goal is to reduce the feedback rate without significantly compromising the sum rate performance. We propose different partial channel state information (CSI) schemes for MIMO-OFDMA combined with opportunistic beamforming. Our method is distinct from that of [84] as we place ourselves in an SDMA context and the best carriers within a cluster (with respect to a computed representative value) are fed back instead of feeding back the average SNR of the best clusters. In [53], it is shown that random beamforming followed by intelligent scheduling is asymptotically optimal for large number of users. However, for sparse networks (i.e. low to moderate number of users) random beamforming yields severely

degraded performance. Different power allocation strategies that shows substantial gain over standard opportunistic beamforming are presented in order to compensate this performance degradation.

The organization of this chapter is as follows: Section 5.2 presents the underlying system and channel models and formulates the problem. Section 5.3 review the MIMO-OFDMA opportunistic beamforming principles. In Section 5.4, we propose four partial feedback schemes for the MIMO-OFDMA system, which are combined with two power techniques presented in Section 5.5 and Section 5.6 concludes the chapter.

Contributions

- Frequency grouping based strategies for MIMO-OFDMA systems:

  – Proposition of an asymptotically optimal opportunistic feedback strategy.

  – Single user optimal feedback scheme.

  – Sub-optimal threshold based feedback strategy.

- Different power allocation algorithms for partial feedback MIMO-OFDMA systems.

5.2 Channel and System Models

We consider the downlink of a multiuser MIMO-OFDMA system as shown in Fig. 5.1. The base station (BS) is equipped with N_t transmit antennas and each user has a single receive antennas. The study in this chapter is valid for any number of antennas N_r. However, it is stated in [53, 87], that increasing the number of receive antennas beyond one does not substantially increase the total throughput.

Let K denote the number of users and M the number of sub-carriers. A frequency-selective channel is characterized by Π significant delayed paths. Let the multi-path

channel's time domain impulse response from transmit antenna n_t to user k be

$$h_k[n_t](t) = \sum_{p=0}^{\Pi-1} a_p \delta(t - \tau_p) \tag{5.1}$$

where a_p is the path gain following zero-mean Gaussian distribution with variance σ_p^2, τ_p is the delay corresponding to path p, and Π is the maximum channel order.

OFDM has the ability of transforming a frequency selective channel to a set of parallel flat fading channels. Let $\mathbf{H}_k^m = [H_k^m[1], ..., H_k^m[N_t]]^T$ be the $N_t \times 1$ vector of channel gains between transmit antennas and the receive antenna of user k on sub-carrier m. $H_k^m[n_t]$ denotes the channel gain from transmit antenna n_t to receiver k and is the frequency sample, at the frequency f_m corresponding to sub-carrier m, of the channel impulse response given by equation (5.1). We have that

$$H_k^m[n_t] = \sum_{p=0}^{\Pi-1} a_p e^{-j\frac{2\pi \tau_p f_m}{M}} \tag{5.2}$$

We assume that the channel is invariant during each coded block, but is allowed to vary independently from block to block.

5.3 Background: MIMO-OFDMA Opportunistic Beamforming

As in [53], SDMA random beamforming is used for transmission, i.e., N_t users can be simultaneously scheduled in each sub-carrier. The BS constructs N_t random orthonormal beams $\mathbf{q}_i \in \mathbb{C}^{N_t \times 1}$ for $i = 1, \ldots, N_t$. For each carrier m, the i-th beam vector is multiplied by s_i^m, the i-th transmit symbol of sub-carrier m. The transmit signal is then given by

$$\mathbf{x}_m = \sum_{i=1}^{N_t} \mathbf{q}_i s_i^m \tag{5.3}$$

Assuming that each user can estimate its channel with no error, in each sub-carrier m the k-th user computes the following N_t SINRs

$$\gamma_k^m[\mathbf{q}_i] = \frac{|\mathbf{H}_k^m \mathbf{q}_i|^2}{N_t/\rho + \sum_{j=1, j \neq i}^{N_t} |\mathbf{H}_k^m \mathbf{q}_j|^2} \qquad i = 1, ..., N_t \tag{5.4}$$
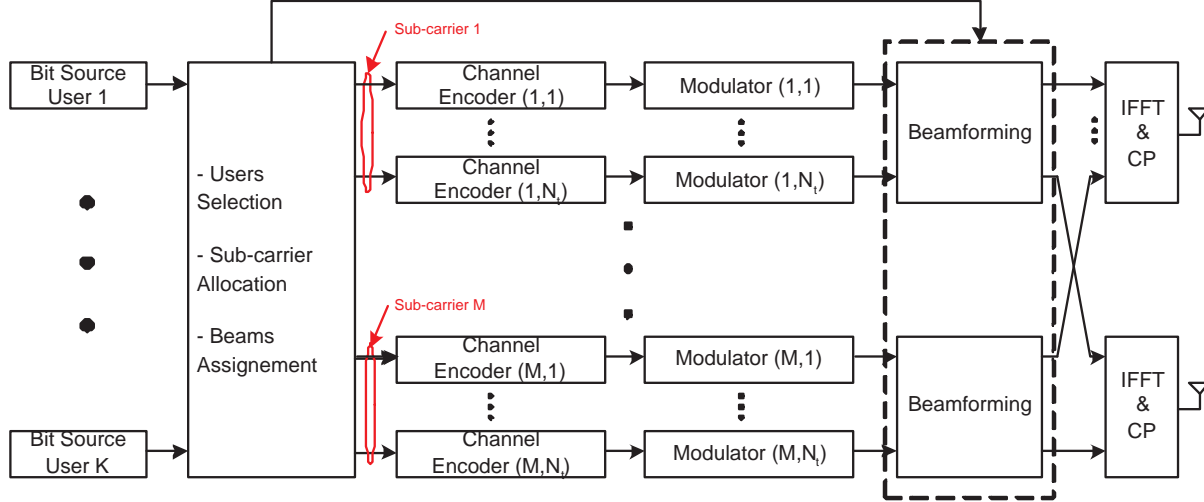
Figure 5.1: MIMO-OFDMA Transmitter model

where ρ is the SNR, assumed to be the same for all users. The SINR $\gamma_k^m[\mathbf{q}_i]$ is computed assuming that user k has been assigned the i-th beam on sub-channel m, thus $\mathbf{x}_{m,i} = \mathbf{q}_i s_i^m$ is the user's desired signal and $\mathbf{x}_{m,j} = \mathbf{q}_j s_j^m$ are interference. The achievable rate of k-th user on i-th beam and sub-carrier m is given by

$$R_k^m[\mathbf{q}_i] = \log_2\left(1 + \gamma_k^m[\mathbf{q}_i]\right) \tag{5.5}$$

Each user feed-back the best SINR value for each carrier. Based on these information, the base station performs the users selection and beams allocation. For a given carrier, each beam is assigned to the user with the highest corresponding SINR. Depending in the assignment result, data of each user are mapped into its allocated sub-carriers and bits are coded and modulated. The modulated symbols are multiplied by the user's assigned beam. The resulting streams are then transformed to time domain using IFFT and the Cyclic Prefix (CP) is added.

In the receiver (Figure 5.2) the inverse operations are performed. In each antenna the CP is removed from the received signal and a FFT block is used to transform the signal back to frequency domain. The sub-carriers allocation information fed-back from the BS is used to extract the user signal from its assigned sub-carriers. In each carrier, the signals from different antennas are then combined to retrieve the original transmitted message.
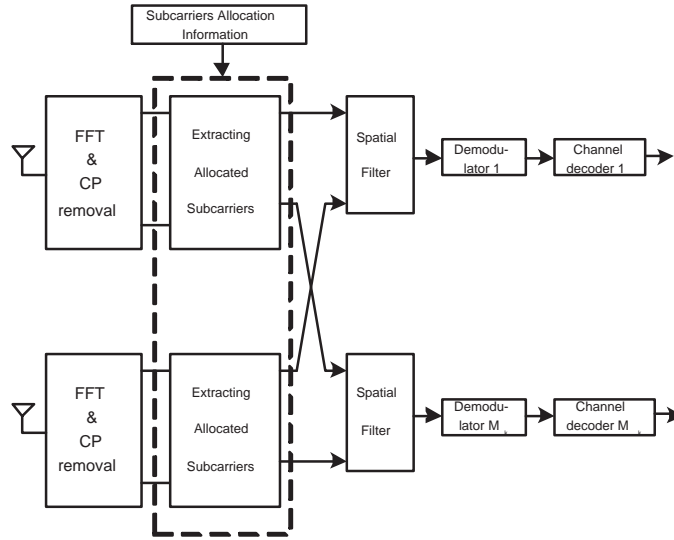
Figure 5.2: MIMO-OFDMA receiver model

It has been shown in [53], for narrowband system, that for a large number of users (asymptotic regime), this scheme achieves a sum average rate of $N_t \log \log K$ which is also the scaling law of the sum-rate capacity with perfect CSI achieved using DPC.

One of the main problems in MIMO-OFDMA systems is the large amount of feedback required for optimal joint sub-carrier/beam allocation. Since different users can be assigned on different sub-carriers, full channel state information (CSI) on each sub-carrier is needed, which leads to prohibitive feedback load. In the following section, we present different feedback strategies where each user feeds back only partial CSI for a group of neighboring sub-carriers.

5.4   Feedback Reduction and Scheduling

We assume that feedback channel is error and delay free and that each receiver has perfect CSI for all sub-carriers and antennas. However, only partial channel state information is available at the transmitter.

Our proposed strategies are based on sub-carrier grouping. We divide the set of available sub-carriers into G groups, each one containing L neighboring carriers. Without loss of

generality, we assume that M is a multiple of G so that each group has the same number of sub-carriers, i.e., $L = \frac{M}{G}$. Figure 5.3 illustrates an example of such a grouping.

Let $\{m_l^g\}_{l=1,\dots,L}$ be the set of L sub-carriers of group g and let $\gamma_k^{m_l^g}[\mathbf{q}_i]$ and $R_k^{m_l^g}[\mathbf{q}_i]$ denote the SINR and the throughput of k-th user on sub-carrier m_l^g and beam $\mathbf{q}_i$ given by (5.4) and (5.5) respectively.
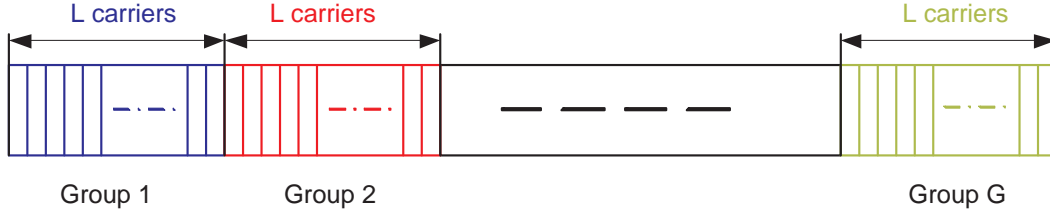
Figure 5.3: Frequency Grouping Example

5.4.1   Maximum SINR Feedback Strategy (MSFS)

The following feedback strategy is a simple extension of the scheme in [53] to multi-carrier case. For each group g, user k feeds back the maximum achieved SINR value on group g computed as

$$\overline{\gamma}_k^g = \max_{\substack{1 \le l \le L \\ 1 \le i \le N_t}} \gamma_k^{m_l^g}[\mathbf{q}_i] \tag{5.6}$$

where maximization is over all beams and all carriers of the group. The user also informs the base station of the indices i^* and m_{l*}^g, respectively the beam index and carrier index in the group corresponding to the maximum in (5.6). We have that

$$(i^*, m_{l*}^g) = \arg\max_{\substack{1 \le l \le L \\ 1 \le i \le N_t}} \gamma_k^{m_l^g}[\mathbf{q}_i] \tag{5.7}$$

Figure 5.4 shows an example of the way a user k determines the value $\overline{\gamma}_k^g$ to be fed-back.

Based on the information sent by users, the BS assigns in each carrier, a beam to the user with the highest SINR as in [53]. Since all carriers have identical channel statistics, it is clear that when the number of user is very large ($K \to \infty$), the number of users
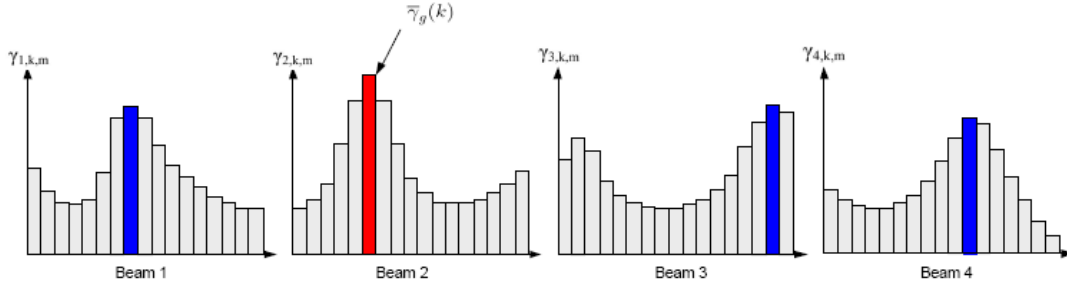
Figure 5.4: Representative value determination on MSFS

feeding-back information for a given carrier tends to $\frac{K}{L}$ which also converges to ∞. The same reasoning as in [53] can then be carried for each sub-carrier and show the asymptotic optimality of this scheme in terms of sum rate. However, for low number of users it is evident that a large number of carriers are not chosen, especially when the number of carriers per group L is large. This intuitive result calls to investigate more sophisticated feedback schemes where each user has the possibility to use efficiently a larger set of carriers at each group. For this reason, we propose the following schemes.

5.4.2 Best beam Max-Rate Representative (BMRS)

Instead of only feeding back the maximum SINR value, user k computes for each beam $\mathbf{q}_i$ a *representative value* $\overline{\gamma}_k^g[\mathbf{q}_i]$ of its channel quality on the g-th group. $\overline{\gamma}_k^g[\mathbf{q}_i]$ is representative of the SINRs in the set $\left\{\gamma_k^{m_l^g}[\mathbf{q}_i]\right\}_{l=1,\ldots,L}$ and is chosen to be the value maximizing the user sum-rate on group g assuming the following assumptions:

- Beam $\mathbf{q}_i$ is assigned to user k in all carriers of group g

- Base station transmits to the k-th user through beam $\mathbf{q}_i$ at a rate equal to $\log\left(1+\overline{\gamma}_k^g[\mathbf{q}_i]\right)$ in carriers where the user's SINR is above $\overline{\gamma}_k^g[\mathbf{q}_i]$. No transmission is scheduled on the remaining sub-carriers of the group as this will lead to an outage event

Under these assumptions, user k's achievable sum-rate with beam $\mathbf{q}_i$ on group g is

$$R_k^m[\mathbf{q}_i] = |\mathcal{A}\left(\overline{\gamma}_k^g[\mathbf{q}_i]\right)|\log\left(1+\overline{\gamma}_k^g[\mathbf{q}_i]\right) \tag{5.8}$$

where $\mathcal{A}\left(\overline{\gamma}_k^g[\mathbf{q}_i]\right)$ is the set of sub-carriers of group g where the k-th user has a SINR value on beam $\mathbf{q}_i$ greater or equal to $\overline{\gamma}_k^g[\mathbf{q}_i]$.

$\overline{\gamma}_k^g[\mathbf{q}_i]$ is then given by

$$
\begin{aligned}
\overline{\gamma}_k^g[\mathbf{q}_i] &= \arg\max R_k^m[\mathbf{q}_i] \\
&= \arg\max_{\gamma_k^{m_l^g}[\mathbf{q}_i]} \left| \mathcal{A}\left(\gamma_k^{m_l^g}[\mathbf{q}_i]\right) \right| \log\left(1 + \gamma_k^{m_l^g}[\mathbf{q}_i]\right)
\end{aligned}
$$

To find $\overline{\gamma}_k^g[\mathbf{q}_i]$, a very simple algorithm can be user. User k determines the set $\left\{\gamma_k^{m_l^g}[\mathbf{q}_i],\right\}_{l=1,...,L}$, SINRs of beam $\mathbf{q}_i$ on carriers in the g-th group, and sorts its values in decreasing order. Let $sinr_1, sinr_2,..., sinr_L$ be the sorted values. The representative is then simply given by

$$\overline{\gamma}_k^g[\mathbf{q}_i] = \arg\max_{sinr_j} \ j \ \log\left(1 + sinr_j\right) \tag{5.9}$$

For each group g, user k feeds only the representative value for its best beam (i.e., the beam with the highest sum rate over the frequencies of the group). For that, the user determines the beam vector $\mathbf{q}_{i^*}$ such that

$$i^* = \arg\max_{i=1,...,N_t} \ R_k^m[\mathbf{q}_i] \tag{5.10}$$

where $R_k^m[\mathbf{q}_i]$ is given by (5.8). The chosen representative value is then

$$\overline{\gamma}_k^g = \overline{\gamma}_k^g[\mathbf{q}_{i^*}] \tag{5.11}$$

The index i^* and the corresponding value $\overline{\gamma}_k^g$ are fed back to the transmitter. Obviously, users inform the BS about the sub-carriers that exceed their selected representative SINR. Within one group, the users may not use all sub-carriers and can ask for a different set of 'preferred' sub-carriers. Hence, the scheduling must be performed independently for each sub-carrier. Note also that for each sub-carrier, the transmitter assigns the beams to the users that support the highest SINR on these beams as in [53]. Figure 5.5 shows an example of the allocation process where three users are competing for beam $\mathbf{q}_i$ in group g.

It is clear that for a given grouping value L, this scheme is optimal when there is only one user in the system ($K = 1$). The optimality here means maximizing the system throughput for a given L, with the condition that the user can only feedback one information per group of carriers about its channel quality. The previous scheme (MSFS) is shown to be

asymptotically optimal (for $K \to \infty$). But, both strategies are clearly sub-optimal for the general case $1 < K < \infty$. Deriving an optimal schemes for any K is very difficult since the decision on the value to feedback is made in a distributed manner (the fed-back SINR is decided in the user side). In the following we propose a sub-optimal threshold based strategy inspired by the work in [88, 89].
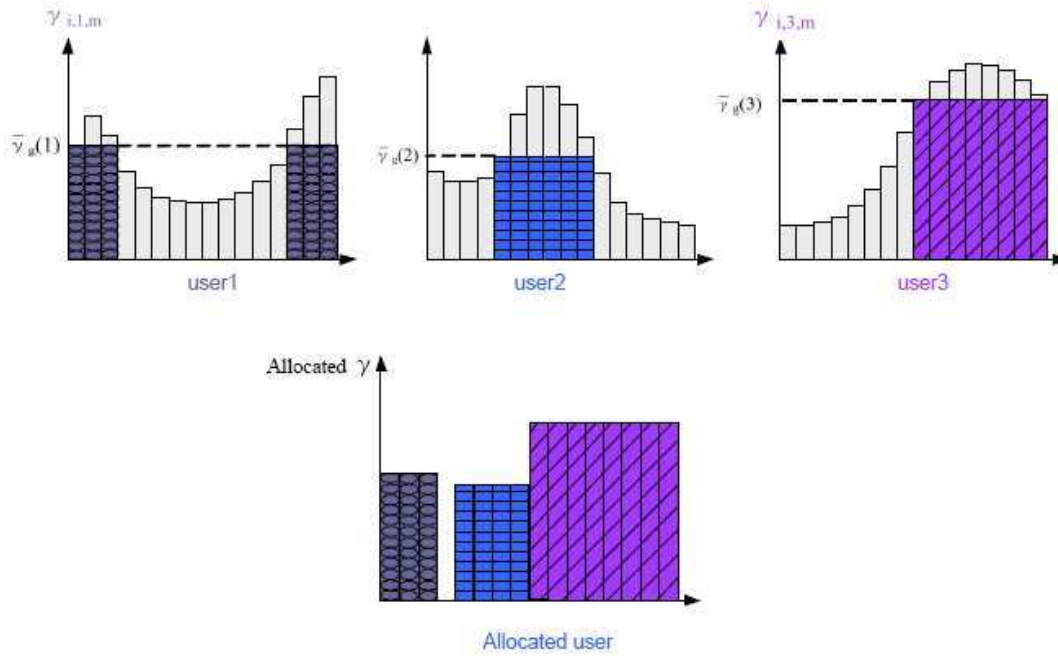
Figure 5.5: Representative based feedback strategy example

5.4.3   Threshold Based Representative Strategy (TBRS)

Gesbert and al. introduced in [88, 89] the concept of "Selective Multiuser Diversity" where users only feedback their CSI if their channel quality exceeds a given threshold. This scheme is shown to considerably reduces the feedback load while preserving the essential of the multiuser diversity. We propose in the following a feed-back reduction scheme for wideband systems inspired from the work in [88]. In our scheme, the base station determines a SINR threshold γ_{th} based on the following assumptions (These assumptions are actually not used as they are for users scheduling but only used to determine the SINR threshold.)

- For each beam $\mathbf{q}_i$ and sub-carrier m, let $\mathcal{B}_{m,i}$ be the set of users such that $\gamma_k^m[\mathbf{q}_i] \geq \gamma_{th}$.

- If $\mathcal{B}_{m,i} = \emptyset$, no user is scheduled in sub-channel m and beam $\mathbf{q}_i$.

- If $\mathcal{B}_{m,i} \neq \emptyset$, the base station schedule randomly one user from $\mathcal{B}_{m,i}$ for transmission at rate $\log(1 + \gamma_{th})$.

The base station chooses then the threshold γ_{th} maximizing the system averaged throughput under the above assumptions. The chosen value is used by users as a reference to compute there representative SINR for the different groups in a distributed manner. The achievable instantaneous throughput under the above assumptions is given by

$$R = \sum_{i=1}^{N_t} \sum_{m=1}^{M} \log\left(1 + \gamma_{i,m}^*\right) \tag{5.12}$$

$\gamma_{i,m}^*$ is the post scheduling SINR allocated in sub-channel m and beam $\mathbf{q}_i$ taking values on $\{0, \gamma_{th}\}$. The averaged throughput is

$$\mathbb{E}\{R\} = \sum_{i=1}^{N_t} \sum_{m=1}^{M} \mathbb{E}\left\{\log\left(1 + \gamma_{i,m}^*\right)\right\} = N_t M \log\left(1 + \gamma_{th}\right)\left(1 - F_\gamma(\gamma_{th})\right)^K \tag{5.13}$$

where F_γ is the cumulative density function (cdf) of the SINR γ.

The simplest probabilistic model for the channel frequency response assumes that there are a large number of statistically independent reflected and scattered paths with random amplitudes.

$$H_k^m[i] = \sum_{\gamma=0}^{\Gamma-1} \alpha_\gamma e^{-j2\pi\tau_\gamma f_m} \tag{5.14}$$

We usually assume that the path gains are independent zeromean random variables. This assumption is known as the uncorrelated scattering assumption (cf. chapter 2, section 2.1.3). Provided that the number of paths is large, which is almost always the case and that a significant number of these contribute to the total received power, it is permissible to refer to the central limit theorem and approximate $H_k^m[i]$ as a Gaussian random variable for each m. The magnitude $|H_k^m[i]|$ is then a Rayleigh random variable with density

$$f_{|H|}(\alpha) = \frac{\alpha}{\sigma^2} \exp\left(\frac{-\alpha^2}{2\sigma^2}\right), \quad \alpha > 0 \tag{5.15}$$

and the squared magnitude $|H_k^m[i]|^2$ is a chi-square distribution with two dimensions degrees of freedom having density

$$\frac{1}{\sigma^2} \exp\left(\frac{-\alpha^2}{2\sigma^2}\right), \quad \alpha > 0 \tag{5.16}$$

The SINR is given by

$$\gamma_k^m[\mathbf{q}_i] = \frac{|\mathbf{H}_k^m \mathbf{q}_i|^2}{N_t/\rho + \sum_{j=1,j\neq i}^{N_t} |\mathbf{H}_k^m \mathbf{q}_j|^2} = \frac{z}{N_t/\rho + y} \tag{5.17}$$

Since $\underline{\mathbf{Q}} = [\mathbf{q_1}, \mathbf{q_2}, ..., \mathbf{q_{N_t}}]$ is a unitary matrix, so $\mathbf{H}_k^m \underline{\mathbf{Q}}$ is a vector with i.i.d. entries. This implies that $\mathbf{H}_k^m \mathbf{q}_i$ are i.i.d. with $\chi^2(2)$ distribution. We have then $z \sim \chi^2(2)$ and $y \sim \chi^2(2N_t - 2)$. Conditioning on y, the pdf of $\gamma_k^m[\mathbf{q}_i]$, can be written as

$$\begin{aligned}
f_\gamma(\alpha) &= \int_0^\infty f_{\gamma|Y}(\alpha|y) f_Y(y) \, dy \\
&= \int_0^\infty \left(\frac{N_t}{\rho} + y\right) e^{-\left(\frac{N_t}{\rho}+y\right)\alpha} \times \frac{y^{N_t-2}e^{-y}}{(M-2)!} \, dy \\
&= \frac{e^{-\frac{N_t\alpha}{\rho}}}{(1+\alpha)^{N_t}} \left(\frac{N_t}{\rho}(1+\alpha) + N_t - 1\right)
\end{aligned} \tag{5.18}$$

and thus the cdf is given by

$$\begin{aligned}
F_\gamma(\alpha) &= \int_0^\alpha f_\gamma(\alpha) \, d\alpha \\
&= 1 - \frac{e^{-\frac{N_t\alpha}{\rho}}}{(1+\alpha)^{N_t-1}} \quad \alpha \geq 0.
\end{aligned}$$

Inserting (5.19) into (5.13) allows to find the exact expression of the average sum-rate under the base station assumptions.

$$\mathbb{E}\{R\} = \log(1 + \gamma_{th}) \left(\frac{e^{-\frac{N_t\gamma_{th}}{\rho}}}{(1+\gamma_{th})^{N_t-1}}\right)^K \tag{5.19}$$

Once the threshold value maximizing equation (5.19) is determined, this value is transmitted to the users so they can compute their representative SINR based on it as follows.

- User k determines, for each beam $\mathbf{q}_i$, the set of carriers $A_{g,i,k}(\gamma_{th})$ where the SINR is above the threshold γ_{th}. The minimum SINR in this set (i.e. the maximum SINR

supported by all carries in $A_{g,i,k}(\gamma_{th})$) is chosen as representative value for beam $\mathbf{q}_i$.

$$\overline{\gamma}_k^g[\mathbf{q}_i] = \min_{m \in A_{g,i,k}(\gamma_{th})} \gamma_k^m[\mathbf{q}_i] \tag{5.20}$$

- For each beam, user k evaluates the sum-rate on group g as if it has been allocated all sub-carriers in $A_{g,i,k}(\gamma_{th})$ for transmission with its representative value

$$R_k^m[\mathbf{q}_i] = |A_{g,i,k}(\gamma_{th})| \log(1 + \overline{\gamma}_k^g[\mathbf{q}_i]) \tag{5.21}$$

- The beam maximizing the sum-rate in (5.21) is then selected by user k. Its representative value, the beam index i^* and the set of sub-carriers in $A_{g,i^*,k}(\gamma_{th})$ are fed-back to the base station

- If none of sub-carriers has a SINR value above the threshold on none of the beams, user k choose to feed-back the over all maximum SINR value with the corresponding beam and carrier indices. The maximization is made over all beams and all carriers of the group

In the base station and as for the previous schemes, in each carrier and for each beam, the user with the best SINR value is scheduled.

5.4.4 Best Beam min-SINR Representative (B2SR)

In the previous schemes, users have to inform the BS of the indices of carriers where it can support a transmission at a rate corresponding to their fed-back representative value. This information on the desired carriers can be avoided by chosen a representative rate that can be supported in all sub-carriers of the group. The representative value for beam $\mathbf{q}_i$ is then the minimum SINR achieved by the user with this beam on group g. That is

$$\overline{\gamma}_k^g[\mathbf{q}_i] = \min_{l=1,\dots,L} \gamma_k^{m_l^g}[\mathbf{q}_i] \tag{5.22}$$

Once representative values for all beams are computed, user k performs a beam selection based on beams achievable sum-rate over carriers of group g. This sum-rate for a given beam $\mathbf{q}_i$ is given by,

$$R_k^m[\mathbf{q}_i] = L.\log\left(1 + \overline{\gamma}_k^g[\mathbf{q}_i]\right) \tag{5.23}$$

and the preferred beams is

$$i^* = \arg\max_{i=1,\dots,N_t} R_k^m[\mathbf{q}_i] \tag{5.24}$$

The beam index i^* and the corresponding value $\overline{\gamma}_k^g[\mathbf{q}_{i^*}]$ are fed-back to the BS. Feeding-back the carriers index is not needed any more since user k can support the fed-back SINR on all carriers of the group.

This alternative offers a considerable reduction in the amount of feed-back but also represents a decrease of system capacity. The complexity of the allocation process is also reduced. In fact, in the previous strategies, within the same group of carriers, different users express different "*preferred set of carriers*", which implies that the scheduling of users must be done for each carrier individually. In the last scheme, their is no preference of carriers and the user request a transmission with the same rate for all carrier of a given group. The same users scheduling is valid for all carriers of the group. The scheduling is then group based, which can considerably reduce the allocation complexity especially for a large L.

Intuitively, we can predict that for values of L such that the bandwidth of a group of sub-carriers is of the order of channel coherence bandwidth, capacity degradation should be very small. The channel variations over sub-carriers within the same group are small and thus the minimum rate in equation (5.22) is not very different from the rate in (5.9)

Remark: In all these schemes, additional feedback reduction can be achieved if each user chooses the G' best groups $(G' < G)$ and feeds back their CSI instead of feeding back information for all groups. The comparison between groups is made in terms of the users' achievable sum rate.

Figures 5.6 to 5.9 represent the system spectral efficiency , for the four feedback reduction schemes, as a function of the number of sub-carriers per group L, for different configurations. Figures 5.6 and 5.8 plot this spectral efficiency for ITU Pedestrian-B PDP (cf. tables 2.1 to 2.3) for number of carriers per group equal to $L = 16$ and $L = 64$, respectively. We assumed a system bandwidth of 2.5MHz with 256 equally spaced sub-carriers. The carrier spacing is the same as in the IEEE802.16 and 3GPP Long Term Evolution specifications. Pedestrian-B corresponds to low delay spreads i.e. large channel coherence bandwidth. We note that the opportunistic MSFS suffers in this model due to lack of frequency channel gain variations. The three other schemes on the other hand perform well and are almost the same, especially for moderate L ($L = 16$). For vehicular-B ITU

PDP (figures 5.7 and 5.9), B2SR scheme experiences very degraded performance. As we expected for highly variant channels, choosing the minimum SINR as representative value is not efficient. In this environment, the expected optimality ranges of the other strategies are highlighted. MSFS offers high performance for large number of users K and converges to the full feedback scheme. However, as expected for low to moderate K, MSFS exhibits very poor spectral efficiency. For this range of K, BMRS and TBRS perform will for low to moderate K, respectively.

Figures 5.10 and 5.12 plot the system spectral efficiency as a function of the number of carriers per group L in a Pedestrian-B ITU PDP for $K = 16$ and $K = 128$, respectively. The SE behaviors in these figures are similar. BMRS and TBRS perform almost the same and have limited spectral efficiency degradation. B2SR exhibits reasonably good performance for low to moderate L and suffers from severe degradation as L increases. Finally, MSFS suffers in performance almost everywhere. Figures 5.11 and 5.13 plot the same spectral efficiency for vehicular-B. In this case, we note that B2SR now suffer from sever performance degradation. For high number of users, MSFS is showing good performance for low to moderate L.

As we mentioned in the remark of the previous section, additional feedback reduction can be achieved if each user chooses the G' best groups ($G' < G$) and feeds back their CSI instead of feeding back information for all groups. Figure 5.14 represents the system spectral efficiency as a function of the number of users for BBS feed-back strategy for different values of G'. We remark that with a reduction of the feedback load by half there is only a very small degradation of the SE of the system. When each user feeds back the CSI for only two groups, the degradation is more severe especially for small number of users (sparse network). The probability that some carriers may not be used is high in this case. This could be solved by employing a power control over the sub-carrier.
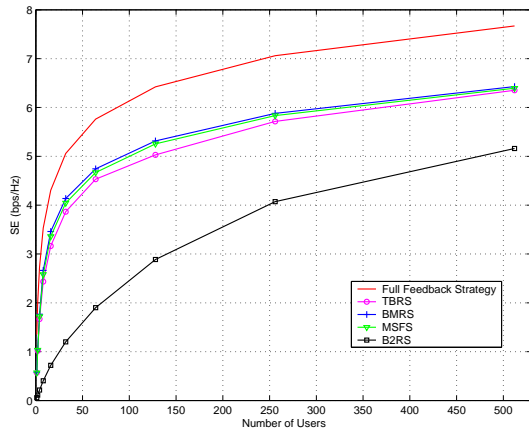
Figure 5.6: SE as a function of the number of users. (ITU Pedestrian-B PDP, SNR = 0dB and $L = 16$)
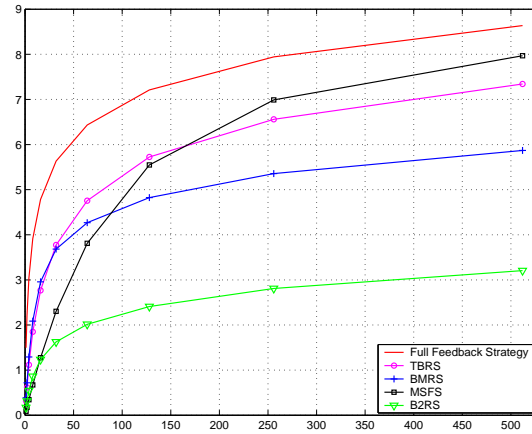
Figure 5.7: SE as a function of the number of users. (ITU Vehicular-B PDP, SNR = 0dB and $L = 16$)
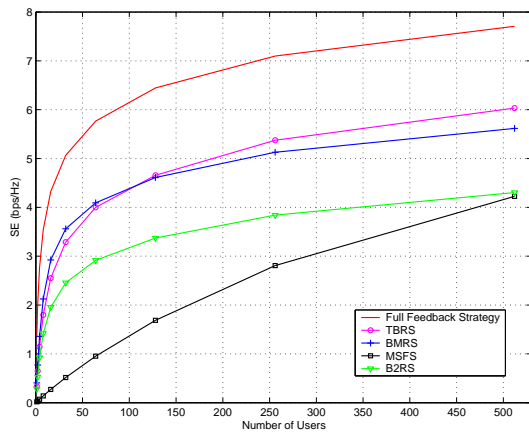
Figure 5.8: SE as a function of the number of users. (ITU Pedestrian-B PDP, SNR = 0dB and $L = 64$)
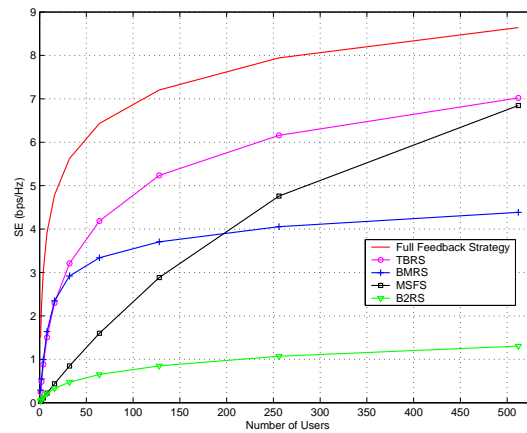
Figure 5.9: SE as a function of the number of users. (ITU Vehicular-B PDP, SNR = 0dB and $L = 64$)
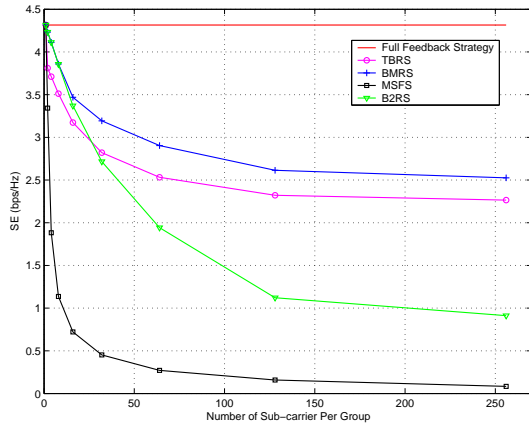
Figure 5.10: SE as a function of L. (ITU Pedestrian-B PDP, SNR = 0dB, Nb of users = 16.)
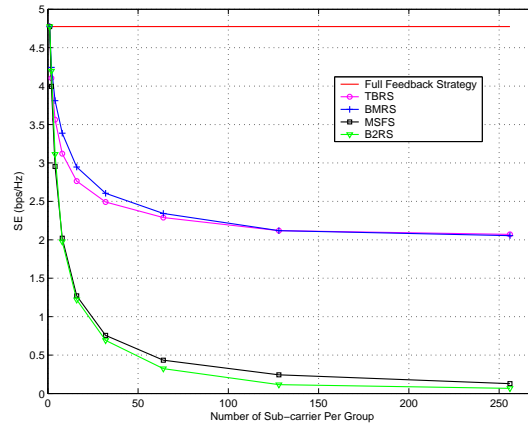
Figure 5.11: SE as a function of L. (ITU Vehicular-B PDP, SNR = 0dB, Nb of users = 16.)
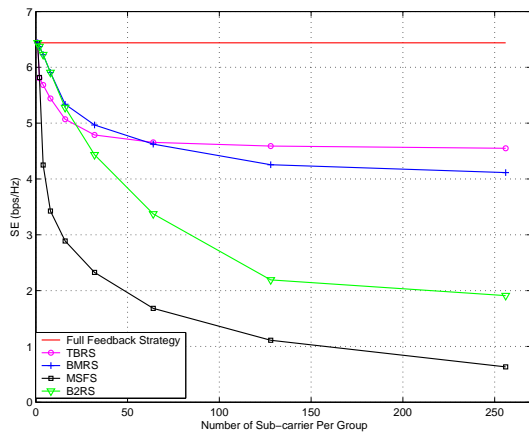
Figure 5.12: SE as a function of L. ITU Pedestrian-B PDP, SNR = 0dB, Nb of users = 128.)
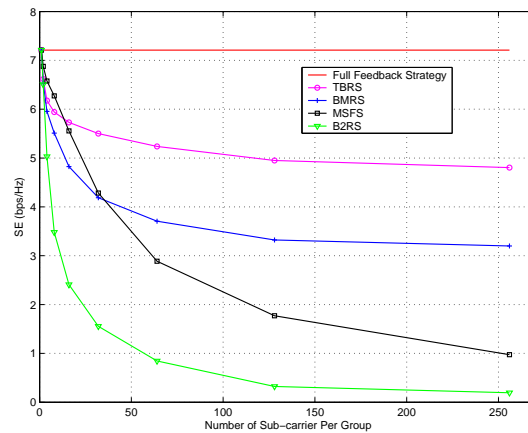
Figure 5.13: SE as a function of L. (ITU Vehicular-B PDP, SNR = 0dB, Nb of users = 128.)
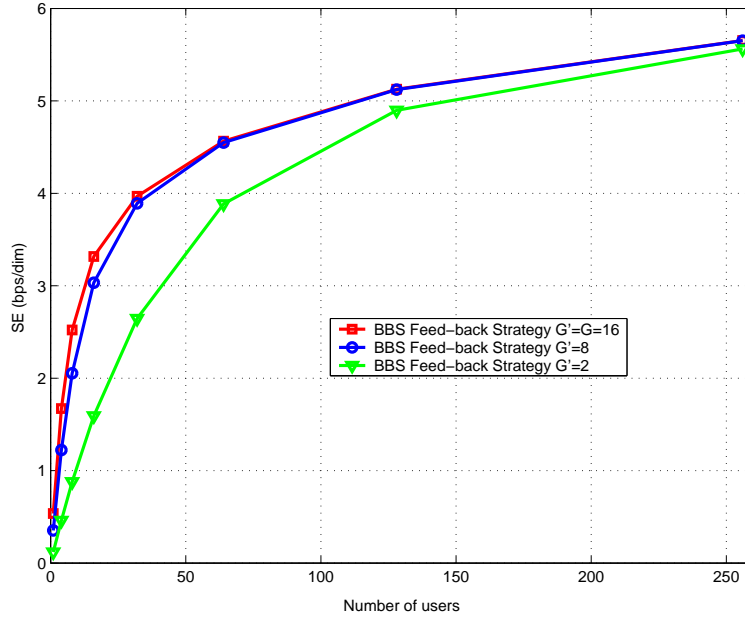
Figure 5.14: SE as a function of the number of users. ($\tau_{\max} = 10\mu s$, SNR = 0dB and $L = 16$)

5.5 Power Allocation based on Partial CSIT

In this section, we present two general classes of power allocation algorithms for sum rate maximization on each sub-carrier. Our objective is to optimize the sum rate of scheduled users based on their partial CSIT subject to a fixed amount of power available at the transmitter.

Let us denote $\mathcal{S}_m$ the scheduling set containing the indices of users selected via the above mentioned schemes on the m-th sub-carrier ($|\mathcal{S}_m| \leq N_t$). On each sub-carrier m, once the group of scheduled user is defined, the transmitter allocates different power levels to the randomly generated beams to improve the system overall performance.

Let $\mathbf{P^m} = [P_1^m, ..., P_{N_t}^m]$ denote the set of transmission powers of beams $\{\mathbf{q}_i\}_{i=1}^{N_t}$ on sub-carrier m. The SINR of k-th user is given by

$$\gamma_k^m[\mathbf{q}_i] = \frac{P_i^m |\mathbf{H}_{k,m}\mathbf{q}_i|^2}{N_t/\rho + \displaystyle\sum_{j=1,j\neq i}^{N_t} P_j^m |\mathbf{H}_{k,m}\mathbf{q}_j|^2} \tag{5.25}$$

The optimization problem of the power vectors $\mathbf{P^m}$ that maximizes the throughput can be formulated as

$$\max_{\{\mathbf{P^m}\}_{m=1,\ldots M}} \sum_{m=1}^{M} \sum_{\substack{i=1,\ldots,N_t \\ k \in \mathcal{S}_m}} \log\left(1 + \gamma_k^m[\mathbf{q}_i]\right)$$

$$\text{subject to } \sum_{m=1}^{M} \sum_{i=1}^{N_t} P_i^m = M \times P$$

The intuition behind the beam power allocation is the fact that for low - yet practical - number of users, it becomes more and more unlikely that N_t randomly generated equipowered beams will match well the channels of any set of N_t users in the network. This performance degradation can be compensated by redistributing the power to the beams. Two power allocation methods for multiuser opportunistic beamforming based on different amount of feedback have been proposed [86]. Below we provide a brief description of the extension of these methods to the OFDMA case.

5.5.1 SIR-based power allocation (SPA)

We consider the Maximum SINR Feedback Strategy (MSFS) where for each group, each user feeds back the maximum SINR and the indices of the corresponding carrier and beam. Based on this information, the BS determines the set $\mathcal{S}_m$ of scheduled user on each carrier m. We call active those carriers for which at least one user had fed-back a representative value (i.e. carriers such that $|\mathcal{S}_m| > 0$). In order to improve performance a second step where additional CSIT feedback is provided, yet involving the scheduled users. Each user feeds back for the carrier it had been assigned the values of, what we will call in this paper, *effective channel gain* $\mathcal{H}_k^m[\mathbf{q}_i] = |\mathbf{H}_k^m \mathbf{q}_i|^2$. The total power is equally divided between active carriers and power allocation is performed in each carrier depending on the number of scheduled users:

- For $|\mathcal{S}_m| > 2$, the power is allocated using the iterative power allocation proposed in [86].

- For $|\mathcal{S}_m| = 2$, the power is allocated according the optimal closed-form solution as in [86].

- For $|\mathcal{S}_m| = 1$, all power is allocated to the scheduled user.

5.5.2 Greedy power allocation (GPA)

Here we consider the case where only one user is assigned power in each carrier, i.e., only one beam per carrier is turned on. In such a scheme, users feed back the *effective channel gain* values $\mathcal{H}_k^m[\mathbf{q}_i] = |\mathbf{H}_k^m \mathbf{q}_i|^2$.

Opportunistic Greedy Power Allocation

For each group g, user k feeds back the highest $\mathcal{H}_k^{m_{l^*}^g}[\mathbf{q}_{i^*}]$, given by

$$\mathcal{H}_k^{m_{l^*}^g}[\mathbf{q}_{i^*}] = \max_{\substack{1 \leq l \leq L \\ 1 \leq i \leq N_t}} \mathcal{H}_k^{m_l^g}[\mathbf{q}_i] \tag{5.26}$$

Each carrier is then allocated to the user with the highest *effective channel gain* and water filling power allocation is performed over the frequencies. The power allocated to sub-carrier m is given by:

$$P_m = \left[\frac{1}{\lambda} - \frac{1}{\rho \mathcal{H}_m} \right]^+ \tag{5.27}$$

where $\mathcal{H}_m$ is the *effective channel gain* fed back by the selected user for sub-carrier m and λ satisfies $\sum_{i=1}^{M} P_m = M \cdot P$

Representative Greedy Power Allocation

Here each user computes a representative value for each beam as follows

$$\overline{\mathcal{H}}_k^g[\mathbf{q}_i] = \arg \max \left| \mathcal{A} \left(\mathcal{H}_k^{m_l^g}[\mathbf{q}_i] \right) \right| \log(1 + \rho \mathcal{H}_k^{m_l^g}[\mathbf{q}_i]) \tag{5.28}$$

The user feeds back the representative value and the index of the beam where the user achieves the maximum sum rate over the frequencies of group g. The user also informs the BS of the carriers in the group with an *effective channel gain* on the selected beam higher than the representative value. As in the previous scheme, each carrier is assigned to the user with the highest corresponding *effective channel gain*. The power is allocated using a frequency water filling algorithm.

We assume a system bandwidth of 1.25MHz with 128 equally spaced sub-carriers. We also consider a multi-path channel model with ITU Vehicular B power delay profile. This channel model is the one with the smallest coherence bandwidth among all ITU channel models and thus is the one where we have the highest performance degradation in frequency grouping based algorithms. The plots are obtained through Monte-Carlo simulations.

Figure 5.15 shows the system spectral efficiency for the three proposed power allocation techniques as a function of the number of users for $N_t = 4$, $L = 16$ and SNR = 0dB. For low number of users, the greedy power allocation algorithm have the best performance exhibiting gain of more than 1bps/Hz and 2bps/Hz compared to SPA and MSFS strategies respectively. This gain however vanishes for moderate and large number of users as it cannot exploit the multiplexing gain available in the channel. Note also that SPA converges to MSFS for large number of users as equal power allocation is asymptotically optimal.

5.6 Conclusions

The important issue of feedback reduction in MIMO-OFDMA networks using opportunistic beamforming was addressed here. We proposed and evaluated different practical low rate feedback schemes that allow significant reduction on the amount of required CSIT with little loss on throughput. We also proposed different power allocation algorithm compatible with feed-back reduction for MIMO-OFDMA.
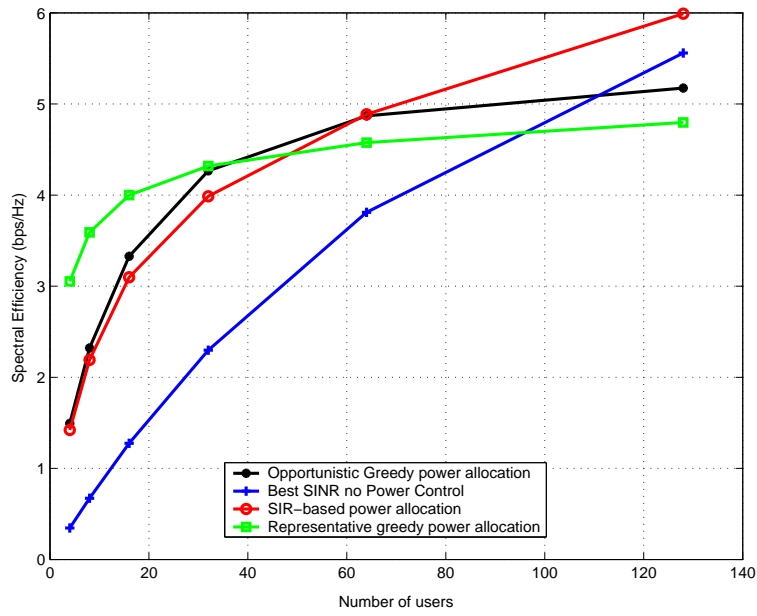
Figure 5.15: Spectral efficiency as a function of the number of users for different feedback reduction/power allocation schemes, $N_t = 4$ and $L = 16$

Chapter 6

Conclusions and perspectives

Conclusions

In this thesis we have tackled the problem of resource allocation for multiuser wideband systems under hard fairness and delay rate constraints. We considered both single and multiple antennas. Thus in chapter 3, we provided a Lagrangian characterization of rate vectors in the boundary of delay limited capacity region. We then proposed an iterative algorithm minimizing the transmit power while allowing each user to achieve its desired rate. We next considered resource allocation for orthogonal signaling systems. We proposed different practical algorithm delay resource allocation to achieve delay limited rate while minimizing the transmit power or maximum fairness between users when no power control is allowed. We extended our study to the downlink of multiple antenna systems in chapter 4. Extensions of the fair allocation algorithm for multiple antenna systems had been proposed. We showed that even with simple transmit schemes (no need for channel gain phases), and under hard fairness schemes a wideband system can offer capacity approaching that of Zero-Forcing Dirty Paper Coding (ZF-DPC) scheme. Results in chapters 3 and 4 shows the yet believed idea that guarantying Quality of Service for user comes at the cost of high capacity degradation is not necessarily true in wideband systems. This result may encourage research for other applicable and simple resource allocation and users scheduling algorithm achieving maximum fairness between users for

future cellular broadband systems. We also investigated the use of distributed multiple antennas in cellular wideband systems in chapter 4. We highlighted their benefit for both spectral efficiency and fairness enhancement. In chapter 5, we addressed the feed-back load for MIMO-OFDMA systems. We proposed different strategies designed to considerably reduce the feed-back load while preserving channel information allowing an efficient scheduling and thus a high system performance. We also provide simple power allocation algorithms for MIMO-OFDMA systems.

Areas for further research

As, we outlined previously, the results in this thesis, call for research attention on applicable and simple resource allocation algorithm with maximum fairness and for delay limited systems. Such algorithm are possible without a high sacrifice of the system total capacity. A study of algorithm taking into account the traffic load of different users, as in [54, 35], should be carrier out.

Power control for partial feedback MIMO-OFDMA has to be investigated, and algorithm more efficient than the simple ones proposed in chapter 5 could be proposed.

Bibliography

[1] T.S. Rappaport, "Wireless Communications - Principles and Practice," 2nd Edition, Prentice Hall, 2001.

[2] T. Okumura, E. Ohmori, and K. Fukuda, "Field strength and its variability in VHF and UHF land mobile service," Review Electrical Communication Laboratory, Vol. 16, No. 9-10, pp. 825873, Sept.-Oct. 1968.

[3] R.H. Clarke. "A Statistical Theory of Mobile Radio Reception," Bell Systems Technical Journal, 47:9571000, 1968.

[4] W.C. Jakes, "Microwave Mobile Communications," John Wiley and Sons, New York, 1974.

[5] R.S. Kennedy, "Fading Dispersive Communication Channels," Wiley-Interscience, New York, 1969.

[6] P. Billingsley, "Probability and Measure," Wiley , New York, 1986.

[7] D. Tse and P. Viswanath, "Fundamentals of Wireless Communication," Cambridge University Press.

[8] H. Hashemi, "Impulse response modeling of indoor radio propagation channel," IEEE j. Select Areas Commun., Vol. SAC-11, pp967-978, Sept. 1993

[9] G.L. Turin & al, "A statistical Model of urban multipath propagation," IEEE Trans. Vej. Technol., Vol. VT21, Feb.1972

[10] JG Proakis, "Digital Communications," McGraw-Hill, Third Edition, 1995

[11] R. Knopp and P. A. Humblet, "Information capacity and power control in single-cell multiuser communications" *In Proc. IEEE ICC'95, Seattle, WA.*, June 1995.

[12] R. Knopp, "Coding and multiple-access over fading channels," PhD. Thesis

[13] R. Knopp and P. A. Humblet, "Multiple-Accessing over Frequency-Selective Fading Channels," *In Proc. IEEE PIMRC'95, Toronto, Ont.*, Sept. 1995.

[14] D. N. C. Tse and S. D. Hanly, "Multiaccess fading channels. I: Polymatroid structure, optimal resource allocation and throughput capacities" *IEEE Transactions on Information Theory,* Vol. 44, pp. 2796-2815, Nov. 1998.

[15] S. D. Hanly and D. N. C. Tse, "Multiaccess fading channels. II: Delay-limited capacities" *IEEE Transactions on Information Theory,* Vol. 44, pp. 2816-2831, Nov. 1998.

[16] L. Li and A. J. Goldsmith, "Capacity and Optimal Resource Allocation for Fading Broadcast Channels - Part I: Ergodic Capacity" *IEEE Transactions on Information Theory,* Vol. 47, NO. 3, March 2001.

[17] L. Li and A. J. Goldsmith, "Capacity and Optimal Resource Allocation for Fading Broadcast Channels - Part II: Outage Capacity" *IEEE Transactions on Information Theory,* Vol. 47, NO. 3, March 2001.

[18] R. Müller, G. Caire and R. Knopp, "Multiuser Diversity in Delay Limited Cellular Wedeband Systems" *IEEE ......,* Vol.

[19] G. Caire, R. Müller and R. Knopp, "Multiuser Diversity in Wireless Systems: Delay-Limited vs. scheduling" *Submitted to IEEE Transactions on Information Theory*.

[20] D. N. C. Tse, "Transmitter directed, multiple receiver system using path diversity to equitably maximize throughput," patent filed, May 24, 1999

[21] P. Viswanath; D. N. C. Tse and R. Laroia, "Opportunistic beamforming using dumb antennas," *IEEE Transactions on Information Theory*, Vol. 48, pp. 1277 -1294, June 2002.

[22] S. D. Hanly, "An algorithm for combined cell-site selection and power control to maximize cellular spread spectrum capacity" *IEEE J. Select. Areas Commun.,* Vol. 13, pp. 1332-1340, Sept. 1995.

[23] R. Yates and C. Y. Huang,"Integrated power control and base station assignment," *IEEE Trans. Vehicul. Technol.*, Vol. 44, pp. 638 -644, Aug. 1995.

[24] R. Yates, "A framework for uplink power control in cellular radio systems," *IEEE J. Select. Areas Commun.,* Vol. 13, pp. 1341, Sept. 1995.

[25] M. Realp, R. Knopp and A. I. Prez-Neira, "Resource Allocation in Wideband Wireless Systems", IEEE Personal, Indoor and Mobile Radio Communications (PIMRC) 2005, September 2005

[26] M. Ergen; S. Coleri and P. Varaiya, "QoS Aware Adaptive Resource Allocation Techniques for Fair Scheduling in OFDMA based BWA Systems," *IEEE Trans. Broadcasting,* December 2003.

[27] Knopp, R. ,"Achieving Multiuser Diversity under hard Fairness Constraints," *Proceedings. 2002 IEEE International Symposium on Information Theory*, 2002, p. 451.

[28] G. Caire, G. Taricco and E. Biglieri, "Optimal power control for minimum outage rate in wireless communications," Proc. of IEEE ICC '98, Atlanta, GA, June 1998.

[29] Nihar Jindal, Sriram Vishwanath, and Andrea Goldsmith, "On the Duality of Gaussian Multiple-Access and Broadcast Channels," IEEE Transactions on Information Theory, vol. 50, no. 5, pp. 768783, May 2004.

[30] "Feasibility Study For OFDM for UTRAN enhancement" 3GPP TR 25.892 V1.1.0 (2004-03)

[31] C. Berge, "Two theorems in graph theory" *Proc. Natl. Acad. Sci. 43, pages 842-844, 1957*

[32] Ahuja, R. K. , Magnanti, T. L. , Orlin, J. B. "Network Flows," Prentice Hall, 1993.

[33] D. Gesbert et *al*, "From Theory to Practice: An Overview of MIMO Space-Time Coded Wireless Systems" *IEEE Journal Selected Areas in Communications,* Volume: 21 , Issue: 3 , April 2003 pp. 281 - 302

[34] Y. Akyildiz and B.D. Rao, "Maximum Ratio Combining Performance with Imperfect Channel Estimates" *in Proc. IEEE ICASSP 2002*, Volume: 3 , pp. 2485-2488

[35] E.M. Yeh, "An Inter-layer View of multiaccess communications," *Proc. IEEE ISIT 2002*.

[36] R. Knopp and P. Hamblet "Multiuser Diversity" Research Report.

[37] R. Cheng and S. Verdu "Gaussian Multiaccess Channels with Capacity Region and Multiuser Water-Filling," *IEEE Transactions on Information Theory,* Vol. 39, May 1993.

[38] E. Telatar, "Capacity of multiantenna Gaussian channels," *AT&T Bell Laboratories, Tech. Memo.,* June 1995.

[39] G.J. Foschini and M.J. Gans, "On limits of wireless communications in a fading environment when using multiple antennas," *Wireless Pers. Commun.,* vol. 6, pp. 311-335, Mar. 1998.

[40] V. Tarokh, N. Seshadri and AR Calderbank, "Space-Time codes for high data rate wireless communication: performance criterion and code construction," *IEEE Trans. on Inform. Theory,* Vol. 44, No. 2, pp. 744-765,, March 1998.

[41] S. Alamouti, "Space block coding: A simple transmitter diversity technique for wireless communications," *IEEE J. Select. Areas. Commun.*, vol. 16, pp. 14511458, Oct. 1998.

[42] G. J. Foschini, G. D. Golden, P. W. Wolniansky, and R. A. Valenzuela, "Simplified processing for wireless communication at high spectral efficiency," IEEE J. Select. Areas Commun.Wireless Commun. Series, vol. 17, pp. 18411852, 1999.

[43] W. Choi, K. Cheong, and J. Cioffi, "Iterative soft interference cancellation for multiple antenna systems," in Proc. Wireless Communications and Networking Conf., Chicago, IL, 2000, pp. 304309.

[44] A. Lozano and C. Papadias, "Layered space time receivers for frequency selective wireless channels," IEEE Trans. Commun., vol. 50, pp. 6573, Jan. 2002.

[45] G. J. Foschini, "Some basic layered space time architectures and their performance," IEEE J. Select. Areas Commun.Special Issue on MIMO Systems, to be published.

[46] M. Kobayashi; D. Gesbert and G. Caire, "Antenna diversity versus multi-user diversity: Quantifying the trade-offs," ISITA 2004, International Symposium on Information Theory and its Applications, October 10-13, 2004, Parma, Italy

[47] L. Zheng and D. N. C. Tse, "Diversity and multiplexing: A fundamental tradeoff in multiple antenna channels," IEEE Trans. Inform. Theory, vol. 49, pp. 1073-1296, May 2003.

[48] G. Caire and S. Shamai, "On the achievable throughput of a multi-antenna Gaussian broadcast channel" *IEEE Trans. on Inform. Theory,* Vol. 49, No. 7, pp. 1691–1706, July 2003.

[49] P. Viswanath, D. N. C. Tse, and R. Laroia, "Opportunistic beamforming using dumb antennas," IEEE Trans. Infor. Theory, vol. 48, pp. 1277- 1294, Jun. 2002.

[50] A. G. Kogiantis, N. Joshi, and O. Sunay, "On transmit diversity and scheduling in wireless packet data," IEEE Intl. Conf. on Commun., vol. 8, pp. 2433-2437, Jun. 2001.

[51] R. W. Heath Jr., M. Airy, and A. J. Paulraj, "Multiuser diversity for MIMO wireless systems with linear receivers," in IEEE Proc. Asilomar Conf. Signals, Systems, amd Computers, Pacific Grove, CA, pp. 1194- 1199, Nov. 2001.

[52] Z. Tu and R. S. Blum, "Multiuser diversity for a dirty paper approach," IEEE Commun. Lett., vol. 7, pp. 370-372, Aug. 2003.

[53] M. Sharif and B. Hassibi, "On the Capacity of MIMO Broadcast Channel with Partial Side Information," *IEEE Trans. Inf. Theory,* volume: 51, no.2, pp. 506-522, Feb. 2005.

[54] H. Boche; A. Jorswieck and T. Haustein, "Channel Aware Scheduling for Multiple Antenna Multiple Access Channels" *Proc. 2003 The Thrity-Seventh Asilomar Conference,* Volume: 1 , Nov. 2003 pp. 992 - 996

[55] V. K. N. Lau and Y-K. Kwok, "Performance analysis of SIMO space-time scheduling with convex utility function: zero-forcing linear processing," IEEE Trans. Veh. Technol., vol. 53, pp. 339-350, Mar. 2004.

[56] V. K. N. Lau, Y. Liu, and T. A. Chen, "The role of transmit dviersity on wireless communications reverse link analysis with partial feedback," IEEE Trans. Commun., vol. 50, pp. 2082-2090, Dec. 2002.

[57] K. J. Kerpez, "A Radio Access System with Distributed Antennas," *IEEE Transactions on Vehicular Technology,* May 1996, vol 45, pages 265-275.

[58] P. Chow, A. Karim, V. Fung, and C. Dietrich, "Performance Advantages of Distributed Antennas in Indoor Wireless Communication Systems," *Proc. 44th IEEE Vehicular Technology Conference,* June 1994, vol. 3, pages 1522-1526.

[59] M. V. Clark and et al., "Distributed versus centralized antenna arrays in broadband wireless networks," *in Proc., IEEE Veh. Technology Conf.*, May 2001, vol. 1, pages 33-37.

[60] L. Dai, S. Zhou, and Y. Yao, "Capacity with MRC-based macrodiversity in CDMA distributed antenna systems," *in Proc., IEEE Globecom,* Nov. 2002, vol. 1, pages 987-991.

[61] W. Roh and A. Paulraj, "Outage performance of the distributed antenna systems in a composite fading channel," *in Proc., IEEE Veh. Technology Conf.*, Sept. 2002, Vol. 2, pages 1520-1524.

[62] A. Obaid and H. Yanikomeroglu, "Reverse-link power control in CDMA distributed antenna systems," *in Proc., IEEE Wireless Communications and Networking Conf.*, Sept. 2000, Vol. 2 pages 608-612.

[63] R. E. Schuh and M. Sommer, "WCDMA coverage and capacity analysis for active and passive distributed antenna systems," *in Proc., IEEE Veh. Technology Conf.*, May 2002, vol. 1, pages 434-438.

[64] H. Zhuang, L. Dai, L. Xiao, and Y. Yao, "Spectral efficiency of distributed antenna systems with random antenna layout," *Electronics Letters*, Mars 2003, vol. 39, pages 495-496.

[65] L. Xiao, L. Dai, H. Zhuang, S. Zhou, and Y. Yao, "Information-theoretic capacity analysis in MIMO distributed antenna systems," *Proc., IEEE Veh. Technology Conf.*, Apr. 2003, vol. 1, pages 779-782.

[66] W. Choi and J. G. Andrews, "Downlink Performance and Capacity of Distributed Antenna Systems in a Multicell Environment", *submitted to IEEE Trans. on Wireless Comm.*, Nov. 2004.

[67] Wake, D.; Webster, M.; Wimpenny, G.; Beacham, K.; Crawford, L., "Radio over fiber for mobile communications," *IEEE International Topical Meeting on Microwave Photonics 2004. MWP'04*. Oct.2004. Pages:157-160

[68] H.Weingarten, Y. Steinberg, and S. Shamai, "The capacity region of the Gaussian-MIMO broadcast channel," in Proceedings of Conference on Information Sciences and Systems, March 2004.

[69] M. Costa, "Writing on dirty paper, IEEE Trans. Inform. Theory, vol. 29, no. 3, pp. 439441, May 1983.

[70] S. Vishwanath, N. Jindal, and A. Goldsmith, "Duality, achievable rates, and sum-rate capacity of MIMO broadcast channels, IEEE Trans. Inform. Theory, vol. 49, no. 10, pp. 26582668, Oct. 2003.

[71] P. Viswanath and D. N. Tse, "Sum capacity of the vector Gaussian broadcast channel and uplink-downlink duality," IEEE Trans. Inform. Theory, vol. 49, no. 8, pp. 19121921, Aug. 2003.

[72] M. Airy, A. Forenza, R. W. Heath Jr., and S. Shakkottai, "Practical costa precoding for the multiple antenna broadcast channel," in Proc. IEEE Globecom, Dec. 2004, vol. 6, pp. 39423946.

[73] R. Zamir, S. Shamai, and U. Erez, "Nested linear/lattice codes for structured multi-terminal binning," IEEE Trans. on Info. Theory, vol. 48, no. 6, pp. 12501276, Jun. 2002.

[74] M. Stojnic, H. Vikalo, and B. Hassibi, "Rate maximization in multi-antenna broadcast channels with linear preprocessing," in IEEE Globecom, Dec. 2004, vol. 6, pp. 39573961.

[75] Q. H. Spencer, A. L. Swindlehurst, and M. Haardt, "Zero-forcing methods for down-link spatial multiplexing in multiuser MIMO channels," IEEE Trans. on Signal Processing, vol. 52, no. 2, pp. 461471, Feb. 2004.

[76] Z. Pan, K. K. Wong, and T. S. Ng, "Generalized multiuser orthogonal space-division multiplexing," IEEE Trans. on Wireless Communications, vol. 3, no. 6, pp. 19691973, Nov. 2004.

[77] K. K. Wong, R. D. Murch, and K. B. Letaief, "A joint-channel diagonalization for multiuser MIMO antenna systems," IEEE Trans. on Wireless Communications, vol. 2, no. 4, pp. 773786, Jul. 2003.

[78] L. U. Choi and R. D. Murch, "A transmit preprocessing technique for multiuser MIMO systems using a decomposition approach," IEEE Trans. on Wireless Communications, vol. 3, no. 1, pp. 2024, Jan. 2004.

[79] Z. Shen, R. Chen, J. G. Andrews, R. W. Heath Jr., and B. L Evans, "Sum capacity of multiuser MIMO broadcast channels with block diagonalization," Accepted to IEEE Trans. on Wireless Commnunications.

[80] J. Jiang, R.M. Buehrer, W.H. Tranter, "Greedy scheduling performance for a zero-forcing dirty-paper coded system," IEEE Trans. on Wireless Comm. Vol. 54, pp. 789- 793, May 2006

[81] A. Paulraj, R. Nabar, and D. Gore. "Introduction to Space-Time Wireless Communications," Cambridge University Press, 2003.

[82] I. Toufik and R. Knopp, "Channel Allocation Algorithms For Multi-carrier Systems," *IEEE VTC Fall 2004, Los Angeles, USA* pp. 1129 - 1133, vol. 2, Sept. 2004.

[83] I. Toufik and R. Knopp, "Multiuser Channel Allocation Algorithms Achieving Hard Fairness," *IEEE GLOBECOM 2004, Dallas, USA* pp. 146 - 150, vol.1. 29 Nov.-3 Dec. 2004.

[84] P. Svedman, S. K. Wilson, L. Cimini, and B. Ottersten, "A simplified feedback and scheduling scheme for OFDM," *in Proc. IEEE Veh. Tech. Conf. (VTC 2004)*, Milan, Italy, May 2004.

[85] M. Fakhereddin, M. Sharif and B. Hassibi, "Throughput Analysis inWideband MIMO Broadcast Channels With Partial Feedback," IEEE Workshop on Signal Proc. for Wireless Comm., June 2005.

[86] M. Kountouris and D. Gesbert, "Robust multi-user opportunistic beamforming for sparse networks," *Proc. IEEE Int. Work. on Sig. Proc. Adv. on Wirel. Comm. (SPAWC)*, New York, U.S.A, June 2005.

[87] M. Sharif and B. Hassibi, "Scaling laws of sum rate using time-sharing, DPC, and beamforming for MIMO broadcast channels," in Proc. IEEE Int. Symp. Information Theory, Chicago, IL, Jun./Jul. 2004, p. 175.

[88] D. Gesbert, M. Slim Alouini, "How much feedback is multi-user diversity really worth? ", In Proceedings of IEEE Intern. Conf. On Communications (ICC), 2004.

[89] V. Hassel, D. Gesbert, M. Slim-Alouini, G. Oien, "A threshold based feedback algorithm for exploiting multiuser diversity," Submitted to IEEE Trans. on Wireless Communications, 2005.

Introduction

Une des matières les plus attrayantes et les plus actives de la recherche dans le domaine des communications pendant les dernières décennies a été la technologie sans fil. Cette attention est la conséquence du grand succès des téléphones cellulaires et la demande croissante de nouveaux services sans fil. Avoir une connectivité permanente offre aux personnes la flexibilité, le sentiment de sécurité et les rend plus productifs. L'internet aussi bien que l'intranet deviennent de plus en plus basées sur des connections sans fil et il est inévitable que la demande de débits élevés, de fiabilité et de qualité du service (QoS) devienne égale aux exigences actuelles pour les systèmes filaires. Tout au long de l'histoire, les systèmes cellulaires ont constamment accompagné ces changements dans les besoins du marché et ont évolué pour satisfaire la demande des clients. Les réseaux sans fil de première génération ont été destinés aux communications de voix et de données à des débits très bas utilisant des techniques de modulation analogues. Récemment, nous avons vu l'évolution des systèmes de deuxième et de troisième-génération offrant plus de débits et ainsi un large éventail de services sans fil basés sur des technologies numériques. L'évolution continue vers un système éliminant les incompatibilités entre les technologies précédentes et devenant réellement un système global (A global system).
Cette évolution des systèmes mobiles est le fruit d'un développement et de recherche permanents de nouvelles technologies de plus en plus efficaces.
Un problème fondamental dans les systèmes de communications sans fil est l'allocation des ressources limitées aux utilisateurs actifs. L'approche traditionnelle optimise chaque couche indépendamment des autres. Ceci peut mener à une conception du réseau largement sous-optimale. Traditionnellement dans les communications sans fil multi-utilisateurs, lors de la conception de la couche physique, les utilisateurs sont considérés comme symétriques, ayant les mêmes quantités de données à transmettre et les mêmes contraintes de retard et de latence. L'objective étant de maximiser la capacité du canal, cela peut résulter d'un système fortement injuste. De l'autre cote, l'attribution de ressource au niveau des couches plus élevées (MAC et couches réseau) considère les liaisons physiques comme des pipelines avec des débits fixes. Récemment plusieurs études ont considéré une approche inter-couche et ont prouvé que ceci peut sensiblement améliorer les performances globales du système.

Dans cette thèse, Nous considérons le problème d'allocation du canal avec des contraintes dures d'équitabilité pour les systèmes multi-utilisateurs à bande large. La motivation derrière le choix de ce type de systèmes vient de la convergence des réseaux mobiles futurs vers une solution basée sur OFDMA ou MIMO-OFDMA.

Il peut paraître évident que garantir une Qualité de Service pour l'ensemble des utilisateurs s'accompagne systématiquement d'une dégradation importante des performances du système. Nous démonterons que, pour les systèmes à large bande avec les ressources intelligemment allouées, cette dégradation est minime. Nous considérons premièrement une system multi-utilisateurs avec une seule antenne et nous donnons une définition de la Capacité limitée par le délai (Delay limited Capacity) avec une caractérisation lagrangienne de sa surface de frontière. On propose un algorithme itératif pour trouver l'allocation de ressources permettant à un ensemble d'utilisateurs d'atteindre leur vecteur de débits cibles avec un minimum de puissance. Nous proposons également différents algorithmes pour l'allocation de ressource avec une signalisation orthogonale et avec différentes contraintes dures d'équitabilité. On montre par des résultats numériques que ces algorithmes justes, pour accès multiple orthogonal, réalisent des performances approchant celles de l'allocation optimale. Nous étendons par la suite notre étude

au cas multicellulaire avec des antennes multiples. Nous montrons comment la dimension spatiale affecte les performances du système en termes d'efficacité spectrale et du débit minimum alloué. Nous proposons différentes techniques d'attribution et de transmission basées sur le Codage Spatio-Temporel (STC) et Multiplexage Spatial (SM) avec une extension de l'étude aux antennes distribuées. Dans la dernière partie de cette thèse, nous abordons un autre problème très important pour les futurs systèmes de communication sans fil: la réduction du feed-back. Ainsi nous proposons différents schémas de feedback des informations sur la qualité du canal pour les systèmes de MIMO-OFDMA avec beamforming opportuniste.

Ce travail de thèse a donné lieu à plusieurs publications :

- Issam TOUFIK and Raymond KNOPP,"Channel Allocation Algorithms For Multi-Carrier Multiple-antenna Systems," EURASIPs Signal Processing Journal, Volume 86 N8, August 2006 , pp 1864-1878.

- Issam TOUFIK and Raymond KNOPP, "Multiuser Channel Allocation Algorithms Achieving Hard Fairness," Globecom 2004, 47th annual IEEE Global Telecommunications Conference, November 29th-December 3rd, 2004, Dallas, USA.

- Issam TOUFIK and Raymond KNOPP, "Channel Allocation Algorithms For Multicarrier Systems," VTC Fall 2004, IEEE Vehicular Technology Conference, September 26-29, 2004, Los Angeles, USA.

- Issam TOUFIK and Hojin KIM, "MIMO-OFDMA Opportunistic Beamforming with Partial Channel State Information," IEEE Intern. Conf. on Communications (ICC), 2006.

- Issam TOUFIK and Marios Kountouris, "Power Allocation and Feedback Reduction for MIMO-OFDMA Opportunistic Beamforming," IEEE Vehicular Technology Conference,

- Issam TOUFIK and Raymond KNOPP, "Wideband Channel Allocation In Distributed Antenna Systems" VTC Fall 2006, IEEE 64th Vehicular Technology Conference, 25-28 September 2006, Montreal, Canada.

Allocation Dynamique juste du canal dans les system Large-bande

L'analyse dans ce chapitre est dans le même esprit que [19] puisque nous étudions également la Capacité limitée par le délai pour les systèmes cellulaires à large bande mais en se focalisant plutôt sur des scénarios pratiques (nombre d'utilisateurs limités). On considère généralement que l'équitabilité vient au coût d'une dégradation significative de la capacité et des performances du système. Dans ce chapitre, nous démontrons que, pour les systèmes à large bande, d'importants gains de diversité multi-utilisateurs (Multi-User Diversity) peuvent être atteints même sous des contraintes dures d'équitabilité, et ainsi des débits globaux élevés peuvent être assurés. Nous montrons également que l'efficacité spectrale, des schémas avec contraintes de délai, approchent celles des stratégies totalement injustes, dans lesquelles le seul objectif est de maximiser la somme des débits. Ces résultats sont conformes à ceux dans [19], où les auteurs montrent que pour les systèmes à large bande, une allocation avec délais limités, la signalisation optimale ne souffrent pas de perte significative par rapport à une allocation selon le principe d'allocation à équitabilité proportionnelle (Proportional Fairness Scheduling (PFS)) pour des valeurs de SNR élevées.

Nous explorons également des algorithmes pratiques pour les cas d'accès multiple orthogonaux (systèmes Du Type OFDMA). Nous prouvons que même avec une telle signalisation sous-optimale, le système ne souffre pas d'une diminution importante de la capacité.

Systèmes avec une antenne simple.

Modèle du system et du canal :
Nous considérons la liaison ascendante d'un système unicellulaire ou K utilisateurs équipés d'une seule antenne chacun transmettent à une station de base équipée à son tour d'une seule antenne de réception. On note par W, la largeur de bande totale et par K l'ensemble d'utilisateurs. La bande W est divisée en M sous-canaux parallèles et de largeur de bande égales. Nous supposons que les données sont codées en blocs de durée T, et que T est plus court que la période de cohérence du canal de sorte que le canal peut être considéré stationnaire pour la durée de transmission d'un bloc, mais puisse changer de bloc en bloc. Nous supposons également que le gain du canal d'un utilisateur est constant sur un sous-canal mais peut changer d'un sous-canal à l'autre (c.-à-d. W/M est plus petite que la largeur de la bande de cohérence du canal). Notons par $\mathcal{H}$ l'ensemble des états possibles du canal. L'état du canal à l'instant n peut être représenté par la matrice de gain

$$\underline{\mathbf{H}}(n) = \begin{bmatrix} H_1^1(n) & H_1^2(n) & \cdots & H_1^M(n) \\ H_2^1(n) & \ddots & & \vdots \\ \vdots & & \ddots & \vdots \\ H_K^1(n) & \cdots & \cdots & H_K^M(n) \end{bmatrix}$$

où $H_k^m(n)$ est le gain du canal de l'utilisateur k sur le sous-canal m. Le signal reçu sur le sous-canal m, à l'instant n peut s'écrire :

$$Y^m(n) = \sum_{k=1}^{K} \sqrt{P_k^m(n)} H_k^m(n) X_k^m(n) + Z^m(n)$$

où $X_k^m(n)$ and $P_k^m(n)$ sont respectivement le signal et la puissance transmis de l'utilisateur k sur le sous-canal m. $Z^m(n)$ est le bruit gaussien. Nous supposons que les gains du canal sont parfaitement connus par les utilisateurs et la station de base ainsi la puissance de transmission peut être adaptée aux variations du canal. Nous appellerons allocation de puissance la fonction associant un état du canal $\underline{\mathbf{H}}$, une matrice de puissance

$$
\underline{\mathcal{P}}(\underline{\mathbf{H}}) = \begin{bmatrix} \mathcal{P}_1^1(\underline{\mathbf{H}}) & \mathcal{P}_1^2(\underline{\mathbf{H}}) & \cdots & \mathcal{P}_1^M(\underline{\mathbf{H}}) \\ \mathcal{P}_2^1(\underline{\mathbf{H}})_2^1 & \ddots & & \vdots \\ \vdots & & \ddots & \vdots \\ \mathcal{P}_K^1(\underline{\mathbf{H}}) & \cdots & \cdots & \mathcal{P}_K^M(\underline{\mathbf{H}}) \end{bmatrix}
$$

où $\mathcal{P}_k^m(\underline{\mathbf{H}})$ est la puissance allouée à l'utilisateur k sur le sous-canal m (pour la simplicité de la notation, nous allons utiliserons $\underline{\mathcal{P}}(n)$ à la place de $\underline{\mathcal{P}}(\underline{\mathbf{H}}(n))$ pour noter l'allocation de puissance correspondant à l'état du canal à l'instant n). Une allocation de puissance est dites faisable s'elle vérifie

$$
\mathbb{E}\left[\sum_{m=1}^{M} \mathcal{P}_k^m(n) \right] \leq \overline{P}_k
$$

Capacité ergodique

Nous rappelons ici que la capacité ergodique (aussi connue sous le nom de capacité de Shannon) est définie comme étant l'ensemble des débits de données qui peuvent être envoyés sur le canal avec une petite probabilité d'erreur moyennés sur le processus d'évanouissement du canal (Channel fading). Dans le cas de signaux gaussiens, cette capacité est donnée par :

$$
\mathcal{C}_g(\underline{\mathbf{P}}, \underline{\mathbf{H}}) = \left\{ \mathbf{R} : \sum_{m=1}^{M} \sum_{k \in S} R_k^m \leq \sum_{m=1}^{M} \log\left(1 + \frac{\sum_{k \in S} P_k^m |H_k^m|^2}{N_0} \right), \quad \forall S \subset \mathcal{K} \right\}
$$

Il a été montré que le point de la région de cette capacité correspondant au maximum du débit total est atteint avec l'allocation de puissance :

$$
\mathcal{P}_k^m(n) = \begin{cases} \left[\frac{1}{\lambda_k} - \frac{N_0}{|H_k^m(n)|^2} \right]^+ & \text{if } |H_k^m(n)|^2 \geq \frac{\lambda_k}{\lambda_{k'}} |H_{k'}^m(n)|^2 \\ 0 & \text{otherwise} \end{cases}
$$

(1)

Ce point est le point de transmission optimal pour les communications non-temps-réel. Quand les utilisateurs ont des contraintes de délais, cette capacité n'est plus optimale et on parle alors de la Capacité limitée par le délai (Delay limited Capacity).

Capacité limitée par le délai

La Capacité limitée par le délai est définie comme étant l'ensemble des débits de transmission qui peuvent être garantis dans tous les états du canal sous des contraintes de puissance. Contrairement à la capacité ergodique, où la puissance et l'information mutuelle entre l'émetteur et le récepteur peuvent changer selon l'état du canal afin de maximiser les débits moyens, dans le cas de la Capacité limitée par le délai, les puissances sont coordonnées entre les utilisateurs et les sous-canaux avec l'objectif de maintenir une information mutuel constante indépendamment de l'état du canal. Dans le cas d'un canal à évanouissement plat (flat fading channel) à accès multiple (MAC), la Capacité limitée par le délai est étudiée d'une manière élégante dans [15] et explicitement caractérisée en exploitant la structure Polymatroid de la région de capacité. Cette structure n'est pas valide pour des systèmes à large bande et seulement une caractérisation lagrangienne implicite est possible. Cette capacité est également étudiée pour les systèmes à large bande dans [19] où les auteurs ont considéré le cas d'utilisateurs asymétriques. Ils montrent que pour un très grand nombre d'utilisateurs et pour des SNR élevés, garantir des débits sans retard résulte en seulement une petite diminution des débits.

La Capacité limitée par le délai est définie pour les systèmes à bande large comme :

$$
\begin{aligned}
\mathcal{C}_d(\overline{\mathbf{P}}) &\equiv \bigcup_{\substack{\underline{\mathcal{P}}:\mathbb{E}\left[\sum_m \mathcal{P}_k^m\right]\leq \overline{P}_k \\ k=1,\ldots,K}} \bigcap_{\underline{\mathbf{H}}\in\mathcal{H}} \mathcal{C}_g(\underline{\mathcal{P}},\underline{\mathbf{H}}) \\
&\equiv \bigcup_{\substack{\underline{\mathcal{P}}:\mathbb{E}\left[\sum_m \mathcal{P}_k^m\right]\leq \overline{P}_k \\ k=1,\ldots,K}} \bigcap_{\underline{\mathbf{H}}\in\mathcal{H}} \left\{ \mathbf{R} : \sum_{k\in S} R_k \leq \sum_{m=1}^{M} \log\left(1 + \frac{\sum_{k\in S}\mathcal{P}_k^m |H_k^m|^2}{N_0}\right), \quad \forall S \subset \mathcal{K} \right\}
\end{aligned}
$$

Le théorème suivant donne une caractérisation lagrangienne de la frontière de région de cette capacité. La preuve du théorème est donnée dans l'annexe A du manuscrit de la thèse en anglais. Cette preuve est inspirée par le raisonnement dans [14, 15].

Théorème :

Pour un vecteur, de contrainte de puissance, donné $\overline{P}$, la surface de frontière de $\mathcal{C}_d(\overline{\mathbf{P}})$ est l'ensemble des vecteurs de débits R^* tels qu'il existe λ et pour chaque instant n, il existe une matrice d'allocation de puissance $\underline{\mathcal{P}}(\cdot)$, une matrice d'allocation de débit $\underline{\mathcal{R}}(\cdot)$ et un vecteur $\alpha(n)\in\mathfrak{R}^K$ de récompense de débit (rate rewards), où pour chaque sous-canal m, $(\mathcal{R}^m(n), \mathcal{P}^m(n))$ est une solution au problème d'optimisation

$$
\max_{\mathbf{r},\mathbf{p}} \sum_{k=1}^{K} \alpha_k(n) r_k - \lambda_k p_k
$$

$$
subject\ to \quad \sum_{k\in S} r_k \leq \log\left(1 + \frac{\sum_{k\in S} p_k |H_k^m(n)|^2}{\sigma^2}\right)
$$

Et

$$\sum_{m=1}^{M} \mathcal{R}_k^m(n) = R_k^* \quad , \quad \mathbb{E}\left[\sum_{m=1}^{M} \mathcal{P}_k^m(n)\right] = \overline{P}_k \quad \forall k \in \mathcal{K}$$

$\mathcal{R}^m(n)$ et $\mathcal{P}^m(n)$ sont le vecteur de débits et le vecteur de puissances allouées aux utilisateurs a l'instant n pour le sous-canal m.

Apres quelques simplification, nous trouvons que les débits et puissances optimal sont données respectivement par :

$$
\begin{aligned}
\mathcal{R}_k^m(n) &= \int_{A_k^m} \frac{1}{N_0 + z} \, dz \\
&= \int_0^\infty \frac{1}{N_0 + z} \mathcal{I}\left\{u_k^m(z) > u_{k'}^m(z), \forall k' \neq k \ \text{ and } \ u_k^m(z) > 0\right\} dz
\end{aligned}
$$

(2)

Et

$$
\begin{aligned}
\mathcal{P}_k^m(n) &= \frac{1}{|H_k^m(n)|^2} |A_k^m| \\
&= \frac{1}{|H_k^m(n)|^2} \int_0^\infty \mathcal{I}\left\{u_k^m(z) > u_{k'}^m(z), \forall k' \neq k \ \text{ and } \ u_k^m(z) > 0\right\} dz
\end{aligned}
$$

(2)

Atteindre un vecteur de débits cibles $\mathbf{R}^*$ avec un minimum de puissance

L'objectif de cette section est de trouver, pou tout état du canal $\underline{\mathbf{H}}(n)$, les allocations de puissances $\underline{\mathcal{P}}(n)$ et de débits $\underline{\mathcal{R}}(n)$, permettant d'atteindre un vecteur de débit $\mathbf{R}^*$ tout en minimisant le total de la puissance transmise.

On note par $\mathbf{R}^*$ le vecteur de débit à atteindre. L'objectif annoncé peut être écrit d'une manière mathématique comme

$$\min_{\mathbf{p}} \sum_{k=1}^{K} p_k$$

Tel que

$$\mathbf{R}^* \in \mathcal{C}_d(\mathbf{p})$$

Un vecteur de puissances $\mathbf{P}^*$ est solution au problème ci-dessus si et seulement si pour chaque bloc n, il existe une allocation de débits $\underline{\mathcal{R}}(n)$, une allocation de puissances $\underline{\mathcal{P}}(n)$ et un vecteur $\alpha(n) \in \mathfrak{R}^K$, tels que pour chaque sous-canal m, $(\mathcal{R}^m(n), \mathcal{P}^m(n))$ est une solution à

$$\max_{\mathbf{r},\mathbf{p}} \sum_k \alpha_k(n) r_k - p_k$$

$$\text{subject to} \quad \sum_{k \in S} r_k \leq \log_2\left(1 + \frac{\sum_{k \in S} p_k |H_k^m(n)|^2}{N_0}\right) \quad \forall S \subset \mathcal{K})$$

$$\text{and } \sum_{m=1}^{M} \mathcal{R}_k^m(n) = R_k^*, \qquad \mathbb{E}\left\{\sum_{m=1}^{M} \mathcal{P}_k^m(n)\right\} = P_k^*, \quad \forall k \in \mathcal{K}.$$

Pour un alpha donné, les allocations de puissances et de débits optimales sont données par les équations (2) et (3) respectivement, avec $\lambda_k = 1 \quad \forall k$. Pour trouver le vecteur $\alpha(n)$ permettant d'attendre les débits souhaités, un algorithme itératif peut être utilisé. Soit $\alpha^{(0)}(n)$ un vecteur de départ quelconque. A chaque itération i et pour chaque k, on calcule $\alpha_k^{(i)}(n)$ comme étant la solution unique à l'équation

$$\sum_{m=1}^{M} \mathfrak{R}_k^{m*}(n) = R_k^*$$

en supposant que pour les autres utilisateurs, les « *récompenses de débits* » (rate rewards) sont fixés au valeur de l'itération précédente. Cet algorithme converge à la solution optimale.
Une approche similaire est proposée dans [19].

Accès Orthogonal :

Il a été montré dans la section précédente que pour atteindre la Capacité limitée par le délai la stratégie optimale consiste à multiplexer plusieurs utilisateurs dans un même sous-canal avec un décodage successif en réception. Une telle approche a des inconvénients tels la propagation d'erreur dans le décodage successif ainsi que la complexité du récepteur. Ceci motive la recherche de stratégies à accès multiple orthogonal, mais qui ne dégradent pas les performances du système. Pour cela, Nous imposons dans notre système qu'il y a seulement un seul utilisateur occupant chaque sous-canal. Chaque utilisateur est garanti d'être alloué un sous-canal à n'importe quel instant pour transmettre. Sous ces contraintes, le system peut supporter jusqu'à K=M utilisateurs simultanément, et nous considérons ce cas extrême dans les sections suivantes. Rappelons que pour un nombre fixe de sous-canaux M et sous la contrainte K<M, imposer K=M offre une diversité-multiutilisateurs maximale dans le cas où on souhaite maximiser le débit totale ergodique, alors que la capacité limitée par le délai souffre de cette condition puisqu'il y a un plus grand nombre de contraintes de débit à satisfaire.
Le system avec K utilisateurs et K sous-canaux peut être représenté par un graphe bipartite pondéré $G = (X, Y, E)$ où l'ensemble de gauche X représente les sous-canaux et l'ensemble de droite Y représente les utilisateurs et E est l'ensemble des arêtes du graphe (voir Figure 1).

Sub-Channels   Users
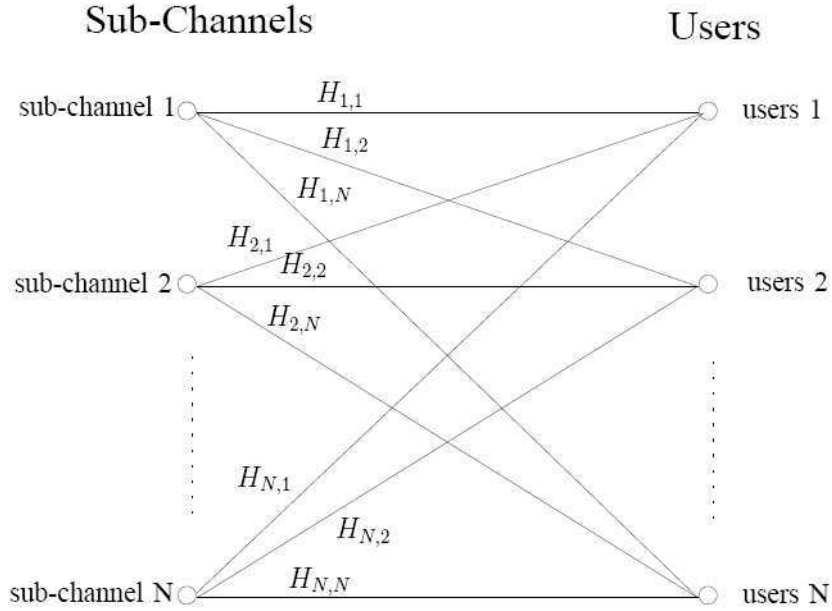
Figure 1: Représentation du système par un graphe

Pour la simplicité de notation, on dénote l'arête entre le sommet $x \in X$ et le sommet $y \in Y$ par le couple (x, y). Chaque arête (x, y) est pondérée par le débit atteignable par l'utilisateur x sur le sous-canal y i.e. $w(x, y) = R_{x,y} = \log\left(1 + \dfrac{P|H_{x,y}|^2}{N_0}\right)$

Définition : Dans un graphe $G = (X, Y, E)$, un *couplage parfait C* est un sous-ensemble de E qui relie chaque sommet de X avec un et seulement un sommet de Y.

Un couplage parfait dans G est de cardinalité $|C| = K$.

Une allocation de sous-canaux aux utilisateurs est équivalente à un couplage parfait dans le graphe G. Il existe $K!$ allocations possibles chacune peut être représentée par un couplage parfait C_i avec $i = 1, ..., N!$. Notons $A_i = (a_i(1), a_i(2), ..., a_i(N))$ le vecteur représentant l'allocation correspondante au couplage parfait C_i tel que $a_i(n)$ est l'indice du sous-canal alloué à l'utilisateur n quand l'allocation C_i est choisie.

L'allocation Max-Min

Cette allocation consiste à trouver le couplage parfait C_{i^*} tel que

$$i^* = \arg \min_{i=1,...,N!} \min_{n=0,...,N-1} H_{a_i(n),n} = \arg \min_{i=1,...,N!} \min_{n=0,...,N-1} R_{a_i(n),n}$$

Cette allocation garantie qu'à chaque instant le gain de canal minimum alloué est le meilleur sur toutes les allocations possibles et donc cette stratégie maximise le minimum de tous les débits.

On propose un algorithme qui permet d'atteindre ce critère d'allocation en un temps polynomial.

Description d'algorithme :

a) Construire le graphe $G = (X, Y, E)$ correspondant au système.
b) Trouver dans E l'arête (x^*, y^*) avec le poids minimum.
c) Enlever (x^*, y^*) de E, i.e. $E = E - (x^*, y^*)$
d) Vérifier si le nouveau graphe admet un couplage parfait :
   - Si oui aller à (b)
   - Sinon aller à (e)
e) Allouer y^* à x^* et enlever les deux soumet x^* et y^* de G ainsi que toutes les arêtes incidentes de ces deux sommet.
f) Si tous les utilisateurs sont assignés un sous-canal, alors finir l'algorithme, sinon aller a (b).

Pour vérifier l'existence d'un couplage parfait dans un graphe, le lecteur peut se référer à [16].

L'allocation FRA (Fixed rate allocation)

Dans cette stratégie, l'objective est de trouver l'allocation (couplage) permettant au utilisateur d'atteindre un vecteur de débits souhaités $R = (R_1, R_2, ..., R_N)$ tout en minimisant la puissance totale transmise (où R_i est le débit souhaité par l'utilisateur i).

Le « Hungarian Algorithm » permet de trouver cette allocation, mais avec le poids de l'arête entre un utilisateur x et un sous-canal y égale à l'opposé de la puissance nécessaire à x pour atteindre son débit sur y

$$w(x, y) = -\frac{\gamma_x N_0}{H_{x,y}}$$

où γ_x est le SNR nécessaire à x pour atteindre son débit.

Résultats numériques

Les figures 2 et 3 représentent respectivement la pdf et la cdf du plut petit débit alloué (worst allocated rate) en utilisant l'allocation Max-Min pour différentes valeurs du nombre de sous-canaux M. Ces figures montrent l'impacte de la diversité multiutilisateurs caractérisée par l'amélioration considérable dans la moyenne du débit minimum alloué et la diminution de sa variance.

De plus, pour un nombre grand d'utilisateur dans le system, la pente de la CDF du plus petit débit alloué est extrêmement raide (près de la moyenne). Cela suggère qu'une allocation de puissance ne devrait pas apporter beaucoup d'avantage. D'un point de vue architecture de system, c'est une caractéristique très attrayante.
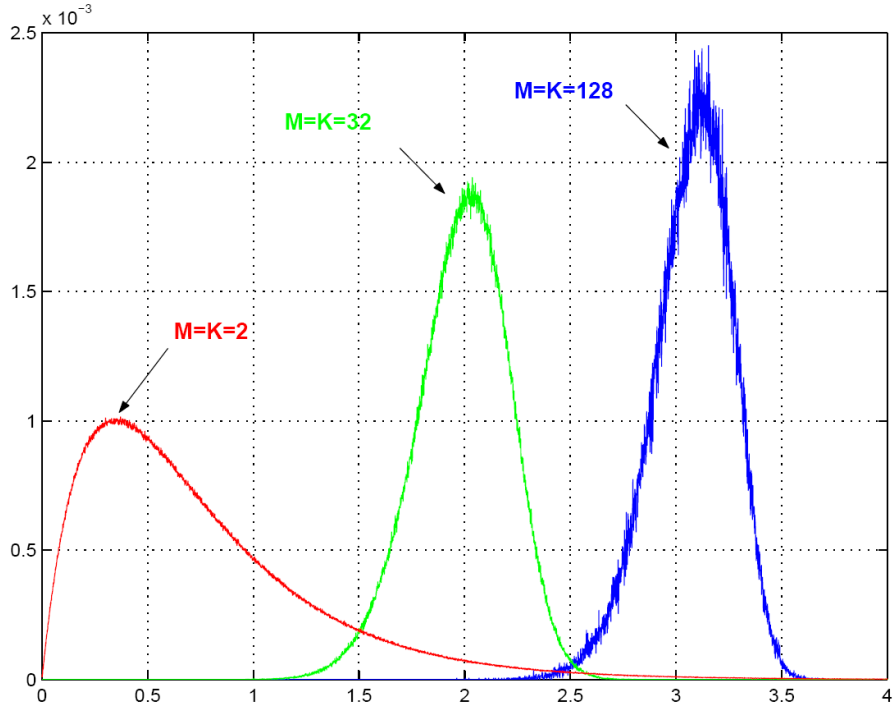
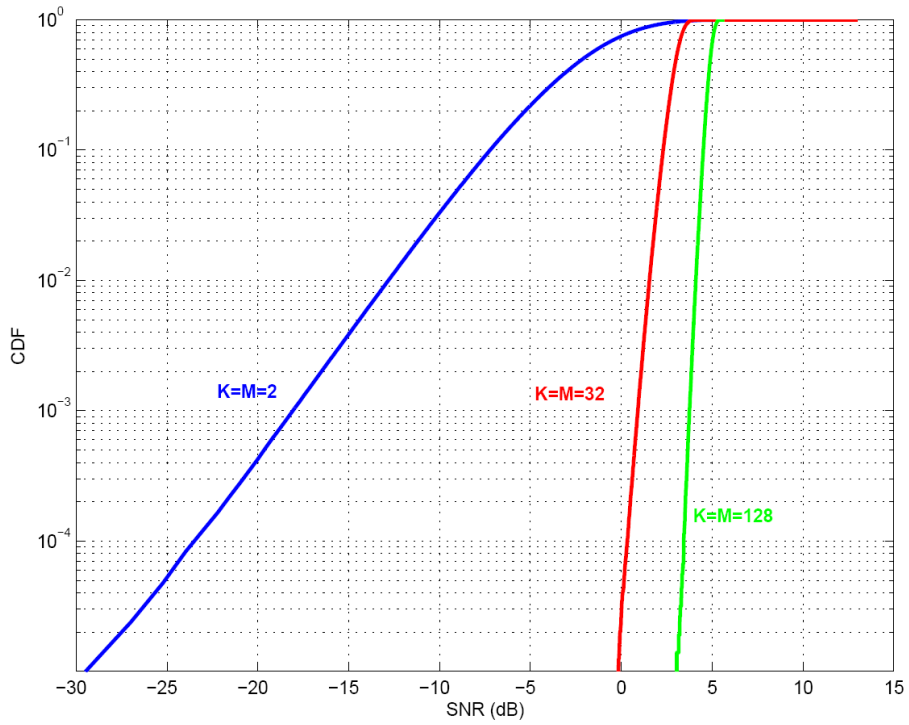**Figure 2: La pdf du plut petit débit alloué**

Figure 3: La cdf du plut petit débit alloué

Figure 4 représente l'efficacité spectrale du système (égale aussi au débit moyen par utilisateur) en fonction du nombre d'utilisateurs dans le system avec les allocations équitables présentées précédemment que l'on compare au débit maximum ergodique obtenu en allouant dans chaque sous-canal l'utilisateur avec les meilleurs conditions de canal et ou la puissance est allouée selon l'équation (1). Les courbes "*Optimal delay limited rates*" et "*orthogonal delay limited rates*" représentent le débit commun (débit égal pour tous les utilisateurs) avec accès multiple optimal et orthogonal respectivement. Ce débit n'est pas le point optimal sur la frontière de la région de la Capacité limitée par le délai puisqu'il ne correspond pas forcement au point maximisant le débit total. Nous considérons un canal Rayleigh et des gains de canaux non-corrélés et un SNR moyen de 0dB. La première chose à noter sur cette figure est que dans tout les cas il y a une augmentation de l'efficacité spectrale avec le nombre d'utilisateur ce qui montre que même en cas de contraintes dure d'équitabilité en peut toujours tirer profit de la diversité d'utilisateur. On peut également noter qu'avec des contraintes dures d'équitabilité on peut toujours avoir des performances très proches de celles du cas non-équitable.
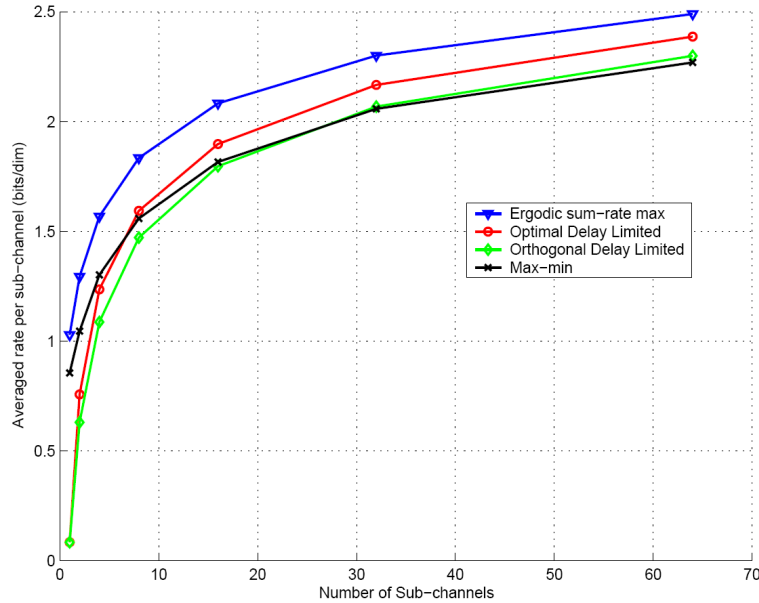
Figure 4: Débit moyen par utilisateur (SNR = 0 dB)-gains indépendants

Figure 5 représente l'efficacité spectrale du system en fonction du nombre d'utilisateurs avec l'allocation Max-Min dans un canal sélectif en fréquence avec des gains sur différents sous-canaux corrélés. Le nombre de fréquence est fixé à 64 et chaque utilisateur est alloué le même nombre de sous-canaux égal à $\dfrac{M}{N}$, en utilisant l'allocation Max-Min. La largeur de bande de chaque sous-canal est constante et seulement l'espacement entre les porteuses change. La performance de l'algorithme dans le cas de gains indépendants est donnée pour comparaison. Comme il peut être prévu, la largeur de bande joue un rôle très important sur l'efficacité spectral du système. On note que lorsque la largeur de bande est choisie proprement l'efficacité spectrale peut être augmentée par un facteur supérieur à 2 même quand une allocation avec contrainte dure d'équitabilité est appliquée. Pour une largeur de bande de $50MHz$, les performances du system approchent de celles du cas indépendants. Un autre résultat intéressant est celui donné par la

courbe d'en bas ($5MHz$): Pour un nombre d'utilisateurs dans le system supérieur au nombre de bandes de cohérence, augmenter le nombre d'utilisateur permet seulement une très faible amélioration de l'efficacité spectrale.
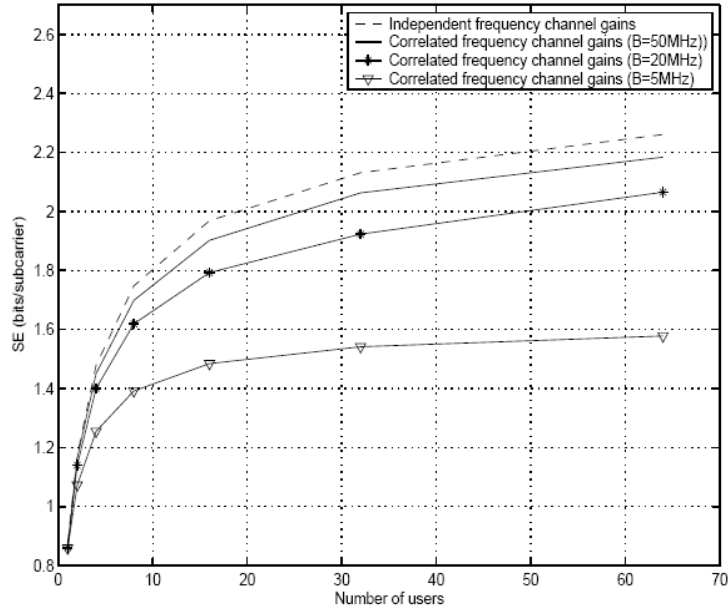

Figure 4: Efficacité Spectral en fonction du nombre d'utilisateurs (alloc. Max-Min)

Système avec antennes multiples.

Dans cette section on considère le cas général d'un système multi-cellular avec C cellules avec une facture de réutilisation de fréquence F. Nous considérons que la cellule d'intérêt est la cellule $c = 1$ et que les autres sont les cellules interférentes. Chaque cellule est équipée de N_t antennes de transmission. La bande totale du système est W divisée en M sous-canaux parallèles. Chaque utilisateur est équipé d'une seule antenne réceptrice. Le canal entre les antennes de la cellule c et l'utilisateur k peut être représenté par le vecteur de dimension $1 \times N$

$$\mathbf{G}_{k,m}^{c} = \left[G_{k,m}^{c}[1], G_{k,m}^{c}[2], ..., G_{k,m}^{c}[N_t] \right]$$

où $G_{k,m}^{c}[i]$ est donné par

$$G_{k,m}^{c}[i] = \sqrt{L_{k}^{c}[i]} H_{k,m}^{c}[i]$$

$H_{k,m}^{c}[n_t]$ est la gain du canal de l'antenne n_t vers l'utilisateur k sur le sous-canal m. Le canal est considéré stationnaire pour la durée de transmission d'un block mais peut varier d'un block à un autre. $\sqrt{L_{k}^{c}[n_t]}$ correspond à l'évanouissement du canal à grande échelle (large scale fading)

et qui englobe l'affaiblissement de parcours (path loss) et l'atténuation due aux effets de masques (shadowing). Le signal reçu par l'utilisateur k sur le sous-canal m s'écrit

$$Y_{k,m} = \sum_{c=1}^{C} \mathbf{G}_{k,m}^{c} \mathbf{X}^{c} + Z_{k,m}$$

où $\mathbf{X}^c$ est le vecteur des symboles transmis par les antennes de la cellules c et $Z_{k,m}$ et le bruit gaussien de l'utilisateur k sur le sous-canal m.

Pour les transmissions Broadcast MIMO, il a été montre que le DPC (Dirty paper coding) combiné avec une sélection optimale des utilisateurs est la stratégie optimale pour maximiser le débit moyen total du system, mais cela résulte en un system totalement inéquitable. Ceci combiner avec les résultats trouvés dans le chapitre précédent motive notre travail pour la recherche de nouvelles techniques essayant de maximiser l'équitabilité entre les utilisateurs tout en garantissant des débits moyen de system élevés.

1) *Allocation Max-Min avec multiplexage spatial*

N_t flux de données indépendants sont transmit en même temps sur chaque même sous-canal à partir des N_t antenne de transmission. Dans un contexte multi-utilisateurs, chaque flux peut être destiné à un utilisateur différent. Si l'antenne n_t^* est assignée à l'utilisateur k sur le sous-canal m, alors le signal reçu sur ce même sous-canal peut être écris

$$Y_{k,m} = \underbrace{\sqrt{\frac{P}{N_t}} G_{k,m}^{1}[n_t^*] X^1[n_t^*]}_{\text{Desired Signal}} + \underbrace{\sum_{n_t \neq n_t^*}^{N_t} \sqrt{\frac{P}{N_t}} G_{k,m}^{1}[n_t] X^1[n_t]}_{\text{Intra-cell Interference}}$$
$$+ \underbrace{\sum_{c=2}^{C} \sum_{n_t'=1}^{N_t} \sqrt{\frac{P}{N_t}} G_{k,m}^{c}[n_t'] X^c[n_t']}_{\text{Inter-cell Interference}} + Z_{k,m}$$

On suppose que la puissance transmise par chaque antenne est égale à $\dfrac{P}{N_t}$ ainsi la puissance transmise par sous-canal est P. La value du SINR est alors donnée par

$$\gamma_n(l,m) = \frac{\dfrac{P}{L}\left|H_{l,m,n}\right|^2}{N_0 + \sum_{l' \neq l}\dfrac{P}{L}\left|H_{l',m,n}\right|^2} \quad (4)$$

Chaque utilisateur est alloué un sous-canal et une antenne de laquelle il reçoit son signal. Dans ce system on peut accommoder jusqu'à $N = L.M$ utilisateurs est l'allocation ce fait sur les sous-canaux et les antennes. Ici encore, on peut représenter le system par un graphe (Figure 5). Dans ce cas le côté gauche du graphe représente les paires (antenne, sous-canal). Le poids d'une arête

entre une paire (antenne, sous-canal)=(l,m) et un utilisateur n est égal au SINR donne par l'équation (4).
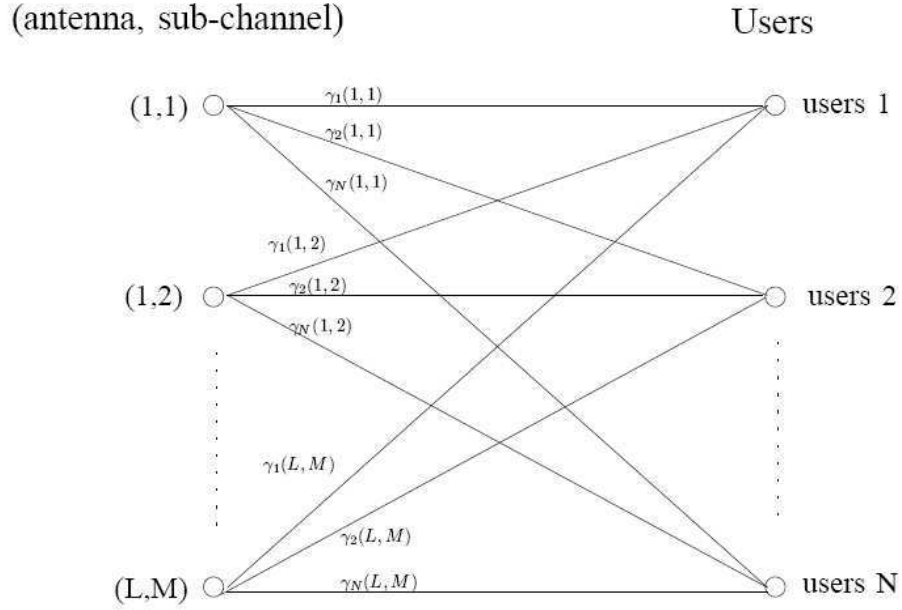
Figure 5: Représentation par un graph du system *avec multiplexage spatial*

Une fois le graph correspondant au system est construit, l'algorithme présenté dans le chapitre précédent peut être utilisé pour exécuter l'allocation. Cette stratégie garantie que le SINR minimum alloué et le meilleur possible parmi toutes les allocations possibles.

2) *Allocation Max-Min avec codage spatio-temporel*

Dans ce system, chaque utilisateur reçoit sont signal sur un sous-canal mais de toutes les antennes avec un accès orthogonal (un seul utilisateur par sous-canal). Ce system est similaire au cas avec une seule antenne. Chaque sous-canal peut être vu comme un canal avec un gain égal à $\dfrac{\sum_{l=1}^{L} H_{l,m,n}}{L}$ et le SINR de l'utilisateur k sur le sous-canal m est donnée par

$$\gamma_{k,m} = \frac{\frac{P}{N_t}\left\|\mathbf{G}_{k,m}^1\right\|^2}{N_0 + \sum_{c=2}^{C}\frac{P}{N_t}\left\|\mathbf{G}_{k,m}^c\right\|^2}$$

L'allocation se fait de la même manière dans le cas avec une seule antenne.

3) *Débit limité par le délai (Delay limite Rate Allocation(DLR))*

Dans ce cas, nous considérons le problème d'allocation de canal et de puissance pour le cas de multiplexage spatial ou les utilisateurs doivent atteindre un vecteur de débits cibles indépendamment de l'état du canal (delay limited rate), tout en minimisant la puissance total

transmise. La solution optimale est très difficile à atteindre et nous procédons en deux étapes. Nous allouons d'abord un sous-canal et une antenne à chaque utilisateur en assumant une puissance égale transmise de toutes les antennes. Une fois l'allocation terminée, nous assignons alors en conséquence la puissance afin d'atteindre les débits souhaités. Allouer les ressources selon la stratégie MS-Max-Min tend à mettre dans chaque sous-canal les utilisateurs les *plus orthogonaux*. Cette stratégie aiderait donc à minimiser la puissance nécessaire pour permettre aux utilisateurs d'atteindre leurs débits souhaités.

L'allocation des puissances dans chaque sous-canal est alors similaire au problème considéré dans [Hanly].

Soit $\{k_i\}_{i=1\ldots N_t}$ l'ensemble d'utilisateur alloués au sous-canal m, ou k_i est l'utilisateur assigné à l'antenne i. le SINR pour l'utilisateur k_i peut être écris

$$SINR_{k_i} = \frac{P_{k_i}|G_{k_i}[i]|^2}{N_0 + \sum_{j \neq k} P_{k_j}|G_{k_i}[j]|^2}$$

Si $\gamma_{k_i}^*$ est le SINR cible, la contrainte de débit peut être exprimée par

$$P_{k_i} = \sum_{j \neq i} P_{k_j} \frac{|G_{k_i}[j]|^2}{|G_{k_i}[i]|^2} \gamma_{k_i}^* + \frac{N_0 \gamma_{k_i}^*}{|G_{k_i}[i]|^2} \tag{5}$$

Notons par $\underline{A}$ la matrice $N_t \times N_t$ donnée par

$$A_i^j \equiv \begin{cases} 0 & j = i \\ \frac{|G_{k_i}[j]|^2}{|G_{k_i}[i]|^2} \gamma_{k_i}^* & j \neq i \end{cases}$$

et par B le vecteur $N_t \times 1$ tel que

$$B_i = \frac{N_0}{|G_{k_i}[i]|^2} \gamma_{k_i}^*$$

L'équation (5) peut s'écrire

$$(\underline{I} - \underline{A}) P = B \tag{6}$$

$\underline{A}$ est une matrice non-négative primitive. La théorie de Perron-Frobenius garanti alors l'existence d'une valeur propre positive dominante r. le résultat suivant et bien connu dans la théorie de Perron-Frobenius, et nous permet de caractériser l'existence d'une solution à notre problème par une contrainte sur la valeur propre r.

Théorème : l'équation (6) a une solution positive si et seulement si r<1. Si r<1 alors il y a une solution unique P donnée par

$$P = (\underline{I} - \underline{A})^{-1} B$$

4) *Résultat numérique pour le cas unicellulaire et utilisateurs symétriques*

Nous considérons ici le cas d'une seule cellule et que les utilisateurs sont symétriques (on considère uniquement l'évanouissement rapide du canal sans le path loss).

Les figures 6 et 7 représentent l'efficacité spectrale du système pour les différents schémas présentés précédemment en fonction du nombre de sous-canaux M pour différentes valeur de N_t ($N_t = 4$ et $N_t = 2$ respectivement). Le schéma de beamforming opportuniste aléatoire introduit dans [53] est donné pour comparaison. Nous avons considéré pour ces figures que la corrélation entre les gains des sous-canaux est égale à zéro. Cela donne une idée sur les débits atteignables en fonction des degrés de liberté du système. Notons d'abord que tous les schémas jouissent de la diversité multi-utilisateurs même pour les schémas avec contraintes dure d'équitabilité. Le gap entre ZF-DPC et les allocations équitable est considérable, mais il diminue avec le nombre croissant des utilisateurs. La dégradation est relativement petite pour $N_t = 2$. Les schémas proposés ont l'avantage de simplicité et de ne pas nécessiter de connaissance de phase. Les schémas proposés ont des performances comparable a celle du schéma classique basé sur du beamforming opportuniste aléatoire.

Figure 8 représente l'efficacité spectral des deux system, SM-Max-Min et STC-Max-Min, en fonction du nombre d'utilisateurs avec 1, 2 et 4 antenne de transmission à la station de base. On note premièrement que l'efficacité spectrale augmente avec le nombre d'utilisateurs dans les deux cas (diversité d'utilisateurs). Dans le SM-Max-Min, l'efficacité spectrale augmente avec le nombre d'antenne ; Ceci étant dû au multiplexage spatial opportuniste décrit dans [6] et [16]. L'efficacité spectrale dans le cas du STC-Max-Min diminue avec le nombre d'antenne et ceci est dû au durcissement du canal (Channel hardening) qui peut s'expliquer par la réduction de la variation du canal par l'augmentation du nombre d'antennes.
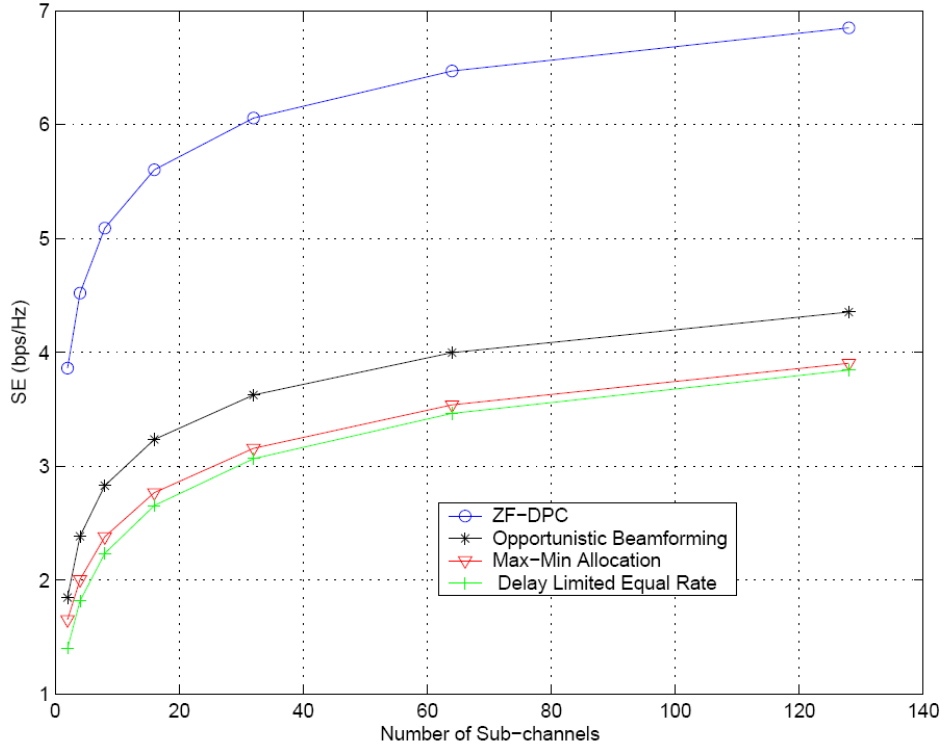
Figure 6: Efficacité spectrale du système en fonction de M ($N_t = 4$)
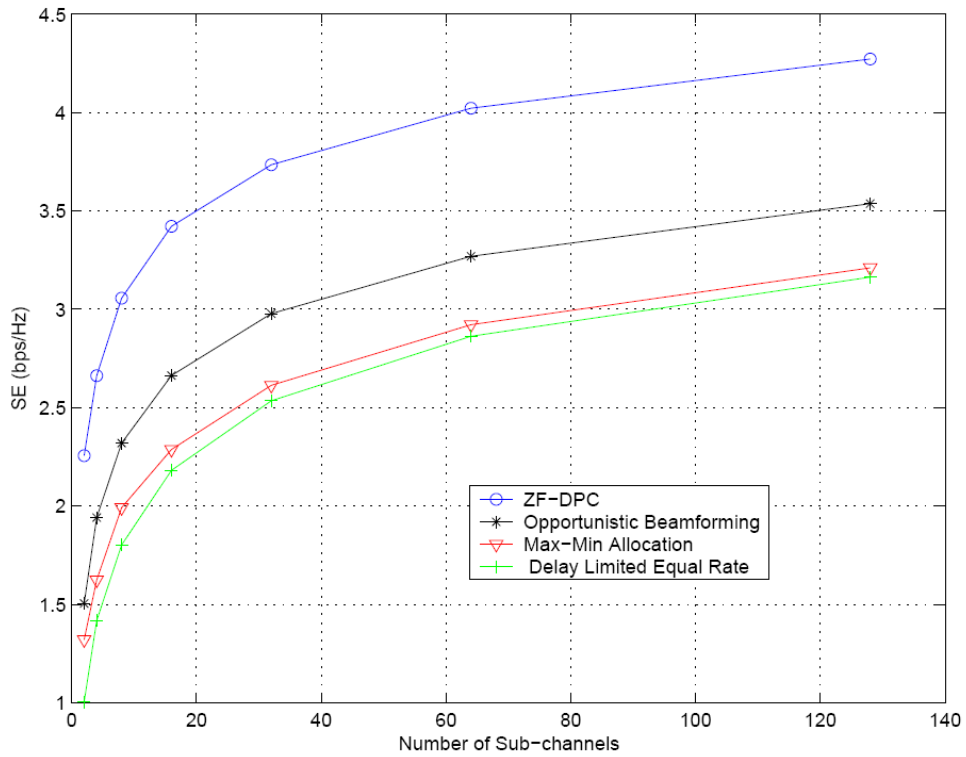
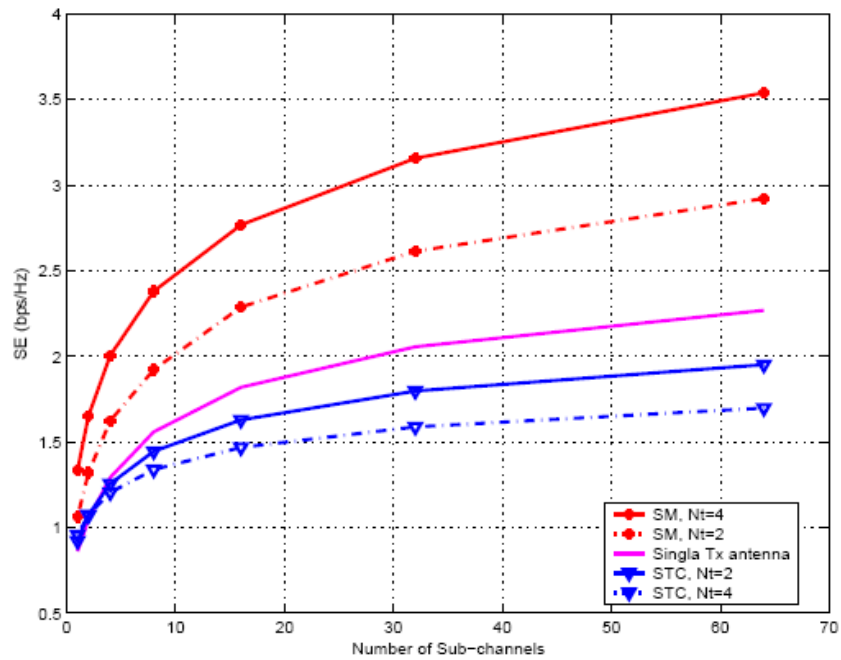**Figure 7: Efficacité spectrale du système en fonction de M ($N_t = 2$)**

Figure 8: Efficacité spectral en fct. de K ($N_t = 1,2,4$)

I-   **Conclusion**

Dans ce rapport, on a étudié l'effet d'une contrainte dure d'équitabilité sur la diversité d'utilisateur et sur l'efficacité spectrale et on a monté qu'une telle contrainte n'a que peu d'effet si l'allocation est proprement faite et que les performances restent très proches de celles d'un système totalement inéquitable et qui a seulement pour objectif la maximisation de la capacité du système. On a également proposé des algorithmes permettant l'allocation des ressources (sous-canaux et antennes) avec différents critères d'optimisation pour les cas avec une ou plusieurs antennes du côté de la station de base.

Réduction du Feedback pour les systèmes MIMO-OFDMA

Dans ce chapitre, nous considérons un system MIMO-OFDMA utilisant le beamforming opportuniste. L'objectif de notre travail est de proposer les schémas pratiques de réduction du feedback qui sont plus efficaces que la prolongation évidente des stratégies proposées pour les systèmes a bande étroite. Essentiellement, notre but est de réduire le débit du feedback sans compromettre de manière significative les performances du system. Nous proposons différents schémas avec informations partielles sur l'état du canal (CSI) pour MIMO-OFDMA combiné avec beamforming opportuniste. Notre méthode est distincte de celle de [84] car nous nous plaçons dans un contexte de SDMA (Space Division Multiple-Access) et les informations concernant les meilleurs porteuses dans un certain group de porteuses (par rapport a une valeur représentative du groupe) sont renvoyées la station de base au lieu de renvoyer le SNR moyen des meilleurs groupe. Dans [53], il est montré qu'un beamforming aléatoire suivi d'une allocation intelligente est asymptotiquement optimal (c.a.d pour un grand nombre d'utilisateurs). Cependant, pour un nombre d'utilisateurs modéré ou bas), le beamforming aléatoire offre des performances sévèrement dégradées. Plusieurs stratégies d'allocation de puissance qui montre un gain substantiel par-rapport au beamforming opportuniste standard sont présentées afin de compenser cette dégradation de performances.

Modèle du system et du canal

On considère le canal descendant d'un system MIMO-OFDMA multi-utilisateur. La station de base est équipée de N_t antennes de transmission et chaque utilisateur est doté d'une seule antenne de réception. Le nombre d'utilisateurs présents dans le system étant K et M est le nombre de sous-porteuse.
$\mathbf{H}_k^m = [H_k^m[1], ..., H_k^m[N_t]]^T$ représente le vecteur des gains de canaux entre les antennes de transmission et les récepteur k dans la sous-porteuse m. Comme dans [hassibi], SDMA basé sur du beamforming aléatoire est utilisé en transmission. La station de base construit N_t beams aléatoires et orthogonaux $\mathbf{q}_i \in \mathbb{C}^{N_t \times 1}$, $i = 1, ..., N_t$. La station de base, basée sur les informations rétroagies par les utilisateurs, alloue les beams et les sous-porteuses. Le SINR (signal to interference and noise ratio) de l'utilisateur k sur la sous-porteuse m avec le beam q_i est donné par

$$\gamma_k^m[\mathbf{q}_i] = \frac{|\mathbf{H}_k^m \mathbf{q}_i|^2}{N_t/\rho + \sum_{j=1, j \neq i}^{N_t} |\mathbf{H}_k^m \mathbf{q}_j|^2} \qquad i = 1, ..., N_t$$

Ou ρ est le SNR et que nous supposons être le même pour tout les utilisateurs. Le débit atteignable par l'utilisateur k sur la sous-porteuse m avec le beam q_i est

$$R_k^m[\mathbf{q}_i] = \log_2\left(1 + \gamma_k^m[\mathbf{q}_i]\right)$$

Réduction du feedback et allocation

Nous supposons que le canal de rétroaction est sans erreurs ou délai. Le récepteur a une connaissance complète de l'état du canal pour toutes les sous-porteuses et de toutes les antennes, mais seulement une information partial est renvoyé au transmetteur.

Les stratégies proposées sont basées sur le regroupage des sous-porteuses voisines (sub-carriers clustering). L'ensemble des sous-porteuse est divisé en G groupes chacun contenant L sous-porteuses voisines. La figure suivante illustre un exemple ce regroupage.
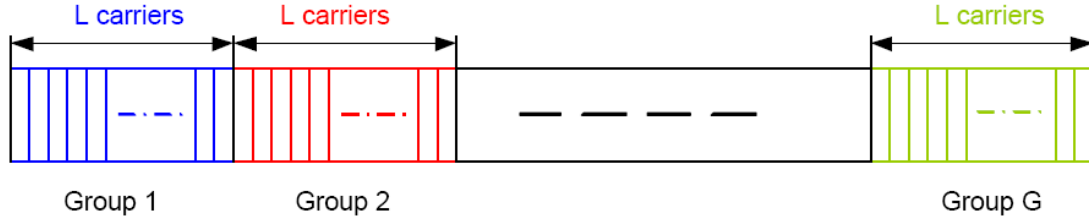

Figure 9: Example de regroupage des sous-porteuses

Soit $\{m_l^g\}_{l=1,...,L}$ l'ensemble des L sous-porteuses du groupe g et soit $\gamma_k^{m_l^g}[\mathbf{q}_i]$ et $R_k^{m_l^g}[\mathbf{q}_i]$ respectivement le SINR et le débit atteignables par l'utilisateur k sur sous-porteuse m_l^g avec le beam q_i.

SINR maximum (MSFS)

Cette stratégie est l'extension du schéma dans [53] au cas multi-porteuse. Pour chaque groupe g, l'utilisateur k renvois au transmetteur la valeur du SINR maximum sur tout le groupe g. La maximisation est faite sur toutes les sous-porteuses du groupe g et tous les beams. La valeur renvoyée par l'utilisateur est alors

$$\overline{\gamma}_k^g = \max_{\substack{1 \leq l \leq L \\ 1 \leq i \leq N_t}} \gamma_k^{m_l^g}[\mathbf{q}_i]$$

L'utilisateur renvois également l'indice de la sous-porteuse et du beam choisis. On peut facilement montrer que schéma est asymptotiquement optimal (pour $K \rightarrow \infty$). Pour un nombre d'utilisateurs modéré ou petit, cependant ce schéma peut montrer des performances limitées.

Représentatif de Débit Maximum (BMRS)

Au lieu de seulement renvoyer la valeur maximale su SINR, l'utilisateur k calcule pour chaque beam q_i une valeur représentative $\overline{\gamma}_k^g[\mathbf{q}_i]$ de sa qualité de canal sur le groupe de sous-

porteuses g. $\overline{\gamma}_k^g[\mathbf{q}_i]$ est choisi comme étant la valeur du SINR maximisant le débit total atteint par l'utilisateur k sur le group g avec les hypothèses suivantes

- le beam $\mathbf{q}_i$ est alloué a l'utilisateur k sur toutes les sous-porteuses du groupe g.

- la station de base transmit a l'utilisateur k par le beam $\mathbf{q}_i$ a un débit égale a $\log\left(1 + \overline{\gamma}_k^g[\mathbf{q}_i]\right)$ dans les sous-porteuse avec un SINR meilleur que $\overline{\gamma}_k^g[\mathbf{q}_i]$ et aucune transmission n'a lieu dans les autres sous-porteuse.

Sous ces hypothèses, le débit atteignable par l'utilisateur k avec le beam $\mathbf{q}_i$ sur le group g est donné par

$$R_k^m[\mathbf{q}_i] = |\mathcal{A}\left(\overline{\gamma}_k^g[\mathbf{q}_i]\right)| \log\left(1 + \overline{\gamma}_k^g[\mathbf{q}_i]\right)$$

Ou $\mathcal{A}\left(\overline{\gamma}_k^g[\mathbf{q}_i]\right)$ est l'ensemble de sous-porteuse ayant un SINR meilleur a $\overline{\gamma}_k^g[\mathbf{q}_i]$. La valeur représentative du beam $\mathbf{q}_i$ sur le group g est

$$\begin{aligned}
\overline{\gamma}_k^g[\mathbf{q}_i] &= \arg\max R_k^m[\mathbf{q}_i] \\
&= \arg\max_{\gamma_k^{m_l^g}[\mathbf{q}_i]} \left|\mathcal{A}\left(\gamma_k^{m_l^g}[\mathbf{q}_i]\right)\right| \log\left(1 + \gamma_k^{m_l^g}[\mathbf{q}_i]\right)
\end{aligned}$$

Le beam offrant le meilleur débit avec sa valeur représentative est choisi. Ainsi la valeur représentative ainsi que l'indice du beam correspondants sont renvoyé au transmetteur. Le récepteur porte également à la connaissance de la station de base l'ensemble de sous-porteuse capable de supporter une transmission au débit choisi (les sous-porteuse du groupe g ayant une valeur de SINR plus grande que le valeur rapportée).

Pour une valeur L donné, ce schéma est clairement optimal lorsqu'il y a un seul utilisateur ($K=1$). L'optimalité ici veut dire maximiser le débit total du système avec la condition que chaque utilisateur rapporte une seule information par groupe de L sous-porteuses.

Représentatif basé sur un seuil (TBRS)

Jusqu'à la nous avons présenté deux schémas de réduction du feed-back, l'un est optimal pour un ayant un seul utilisateur et l'autre est optimal dans le cas asymptotique, mais tout deux clairement sous-optimaux dans le cas général $1 < k < \infty$. Dériver une stratégie optimale pour le cas général est très difficile puisque la décision sur la valeur rétractée est prise d'une façon distribuée. Dans ce qui suis nous présentons une stratégie inspirer par le concept de ''Diversité-multiutilisateurs sélective'' présenté dans [davG]. Ainsi la station de base détermine une valeur seuil de SINR γ_{th} basé sur les hypothèses suivantes :

- Pour chaque beam q_i et sous-porteuse m, soit $\mathcal{B}_{m.i}$ l'ensemble des utilisateurs tel que \$....\$ $\gamma_k^m[\mathbf{q}_i] \geq \gamma_{th}$
- Si $\mathcal{B}_{m.i} = \emptyset$, aucune transmission n'a lieu sur le beam q_i et la porteuse m
- Sinon, la station de base choisi aléatoirement un utilisateur parmi $\mathcal{B}_{m.i}$ et lui transmit a un débit $\log\left(1 + \gamma_{th}\right)$.

(L'allocation et la transmission n'ont pas lieu ainsi, mais ces hypothèses sont seulement utilisées pour le calcul de γ_{th}).

La station de base calcule la valeur de γ_{th} maximisant le débit total du système pour un nombre d'utilisateur donné K. Dans le cas d'un canal Rayleigh, \$\gamma_th\$ est la valeur maximisant

$$\mathbb{E}\{R\} = \log\left(1 + \gamma_{th}\right)\left(\frac{e^{-\frac{N_t \gamma_{th}}{\rho}}}{\left(1 + \gamma_{th}\right)^{N_t - 1}}\right)^K$$

Une fois cette valeur déterminée et portée a la connaissance des utilisateurs, ces derniers calculent leur valeur SINR représentative comme suit
k sur la sous-porteuse m

- l'utilisateur k détermine, pour chaque beam q_i, l'ensemble de sous-porteuses $A_{q,i,k}(\gamma_{th})$ ayant une valeur de SINR supérieure a γ_{th}. Le SINR minimum dans cet ensemble est choisi comme valeur représentative pour le beam q_i

$$\overline{\gamma}_k^g[\mathbf{q}_i] = \min_{m \in A_{q,i,k}(\gamma_{th})} \gamma_k^m[\mathbf{q}_i]$$

- Pour chaque beam, l'utilisateur k évalue le débit total sur le groupe g comme s'il était allouée toute les sous-porteuses dans $A_{q,i,k}(\gamma_{th})$
- Le beam maximisant ce débit total est alors choisi par l'utilisateur k. Sa valeur représentative et son indice ainsi que l'ensemble sont portés à la connaissance du transmetteur.
- Si $A_{q,i,k}(\gamma_{th}) = \emptyset$ pour tout les beam, alors l'utilisateur k renvois au transmetteur la valeur du valeur de SINR maximale a l'instar de schéma MSF.

Représentatif Min-SINR (B2SR)

Dans tout les schémas précédents, l'utilisateur dois informer la station de base des indices de sous-porteuse sur les quelle uns transmission avec le débit choisi est possible. Cette charge de feedback supplémentaire peut être évitée en choisissant de renvoyer au

transmetteur une valeur supportable sur toutes les sous-porteuses. Pour un beam q_i, cette valeur est le SINR minimum atteint sur les sous-porteuse du groupe g. le beam offrant le plus grand SINR minimum est ainsi choisi par l'utilisateur.

Résultat numérique

Les figures 10 a 13 représentent l'efficacité spectral du system, pour les quatre schémas de réduction du feedback présentés, en fonction du nombre du nombre d'utilisateur. Pour les figures 10 et 12 on considère un canal de propagations selon le modèle ITU Pedestrian-B et avec un nombre de sub-carriers L est gale a 16 et 64 respectivement alors que pour les figures 11 et 13 on considère un modèle ITU Vehicular-B.
Lors de ces simulations nous avons considère un une largeur de band de 2.5MHz avec 256 sous-porteuse uniformément espacées (l'espacement entre les sous-porteuses est le même qu'en IEEE802.16 et dans les spécifications du 3GPP Long Term Evolution). Pedestrian-B correspond un petit retard de diffusion (delay spreads) i.e. une large bande de cohérence. Nous remarquons dans cet environnent, le MSFS opportuniste souffre du manqué de variation des gains de canal en fréquence. Les trois autres schémas ont en revanche de bonne et presque les mêmes performances, et cela et encore plus vrai pour L = 16. Pour ITU Vehicular-B, B2SR a de très mauvaises performances. Comme prévu pour des canaux avec d'importantes variations en fréquence, choisir le SINR minimum n'est pas efficace. Dans cet environnement, les performances des différents schémas de feedback correspondent aux intervalles d'optimalité annoncés précédemment.
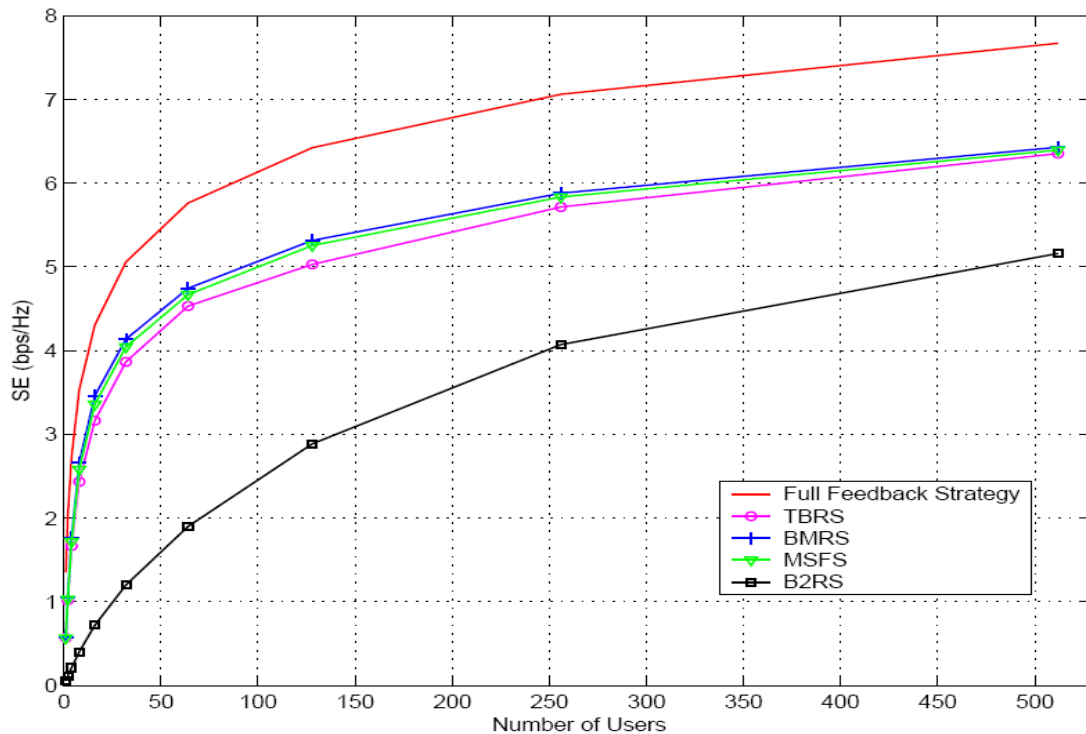

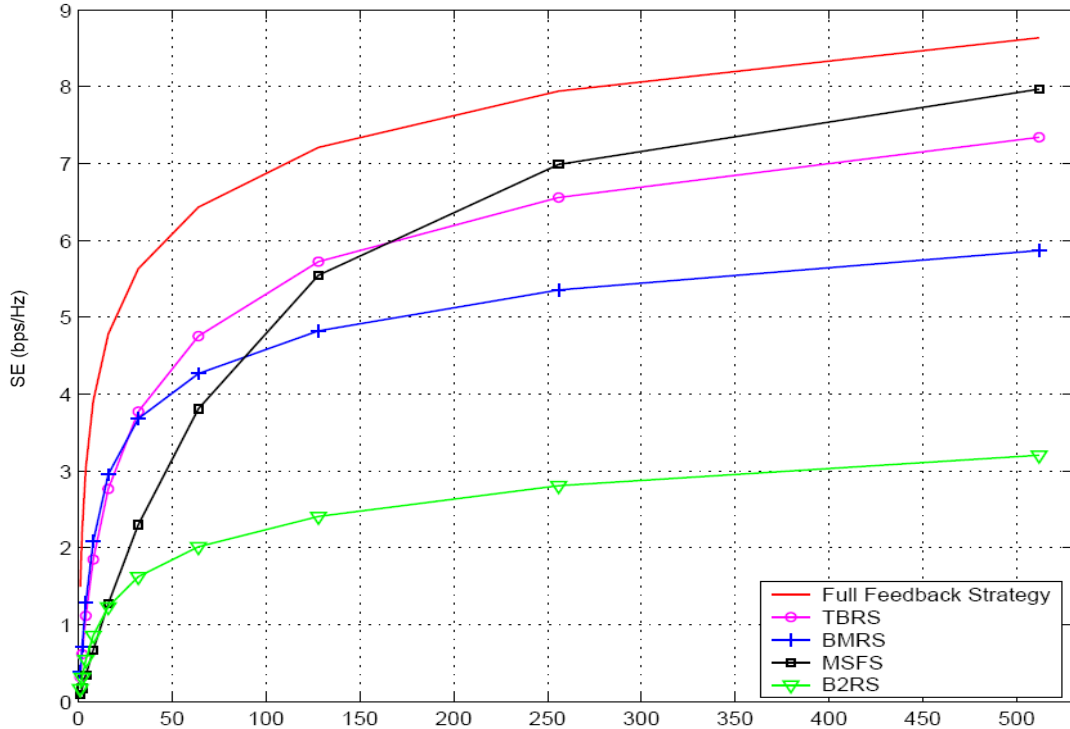**Figure 10: Efficacité spectrale en fonction de K (ITU Pedestrian-B, SNR = 0dB and L = 16)**

Figure 11: Efficacité spectrale en fonction de K (ITU Vehicular-B, SNR = 0dB and L = 16)
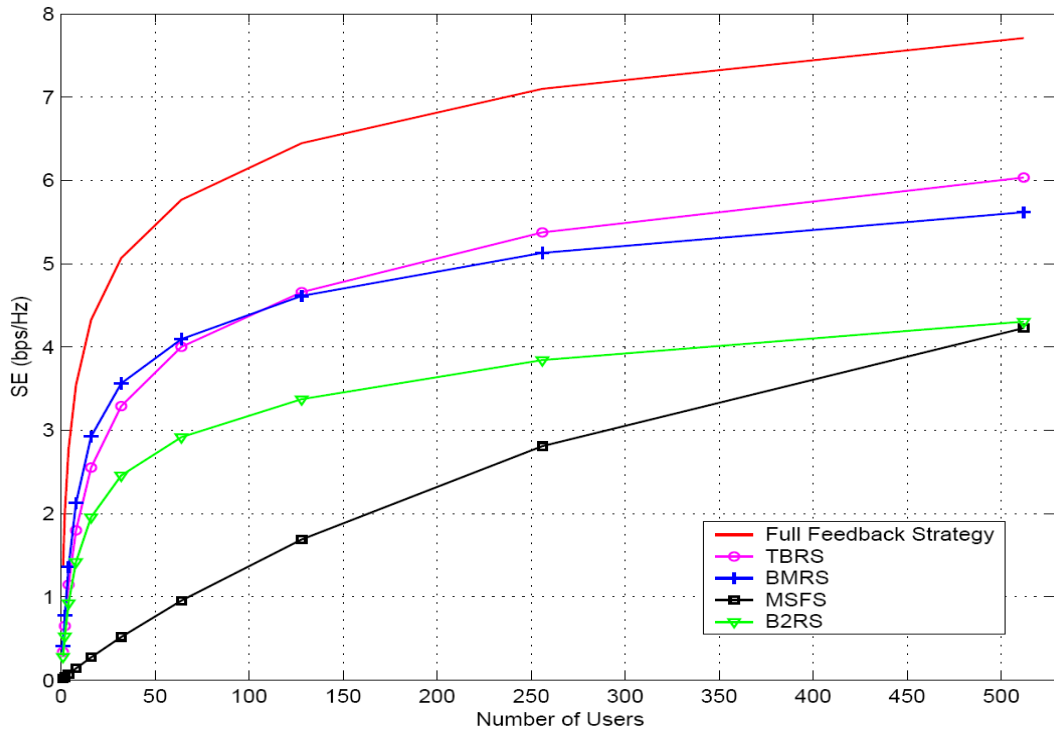

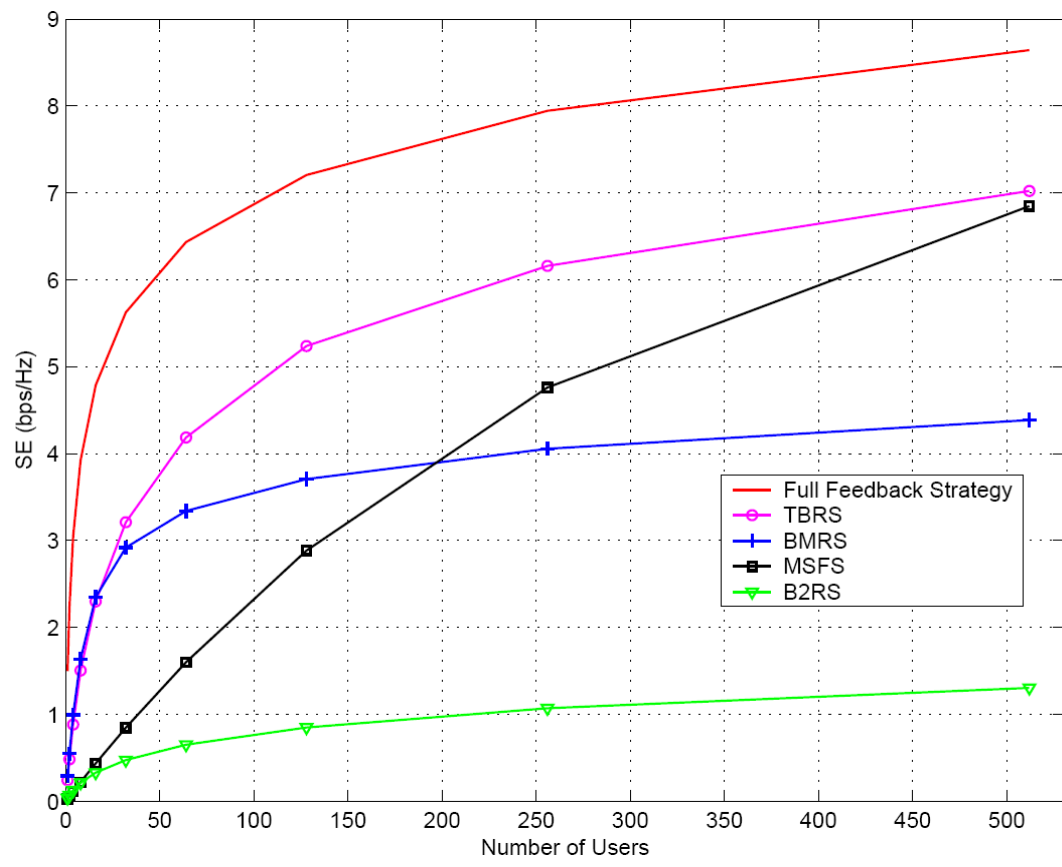**Figure 12: Efficacité spectrale en fonction de K (ITU Pedestrian-B, SNR = 0dB and L = 64)**

Figure 13: Efficacité spectrale en fonction de K (ITU Vehicular-B, SNR = 0dB and L = 64)